An exergy-based framework for efficiency improvement for integrated oxy-fuel power generation systems with CO_2 capture

by

Ahmed Shafeen

A thesis
presented to the University of Waterloo
in fulfillment of the
thesis requirement for the degree of
Doctor of Philosophy
in
Chemical Engineering

Waterloo, Ontario, Canada, 2014

AUTHOR'S DECLARATION

I hereby declare that I am the sole author of this thesis. This is a true copy of the thesis, including any required final revisions, as accepted by my examiners.

I understand that my thesis may be made electronically available to the public.

Abstract

The global energy and electricity demand is increasing rapidly along with the consumption of fossil fuels, more specifically coal and natural gas. This results in accelerated growth of anthropogenic emissions of greenhouse gases (GHG), in particular CO_2, into the atmosphere which is assumed to be the main cause of global warming. In order to mitigate CO_2 emissions while sustaining the growth in power generation, it is necessary to develop advanced energy efficient technologies for power generation. Power generation systems based on fossil fuel combustion technologies will maintain their dominant position in the global energy infrastructure for decades to come. However, in order to sustain power generation in a carbon constraint environment, the fossil fuel based combustion systems need to be more energy efficient and emit significantly less pollutants (in particular CO_2) to the atmosphere. Oxy-fuel power generation technology is a promising and novel technology pathway for power generation which provides high efficiency and near zero emission opportunities with CO_2 capture. The Oxy-fuel combustion has been widely used in steel and glass industries for many decades; however its potential use in power generation is relatively new. Hence, extensive research and development (R&D) as well as process simulation and modeling work are required to develop and validate the technology.

The CO_2 capture processes are inherently energy intensive and associated with high capital investment and increased operating cost, along with significant efficiency loss. Efficiency loss in any industrial process including power plants is also due to the waste heat from different unit operations. However, in order to reduce waste heat and improve efficiency, these plants require better heat integration, the first step of which is to identify point sources for heat loss and calculate the available amount of heat that can be utilized. This can be done by performing an exergy analysis on the overall plant and incorporate the efficiency improvement measures based on the exergy analysis results. In order to make tangible improvement in efficiency and emission control, existing fossil fuel power plants and, even more so, new plants based on the next generation technologies that are yet to be implemented, require extensive process modeling to validate and optimize the design

concepts before their implementation. These efforts will make the technology more competitive or to comply with environmental regulations in support of Carbon Capture and Storage (CCS), which is considered to be a key transitional technology solution to the issue of climate change and continuous utilization of fossil fuel resources in the next few decades.

Using a systematic exergy-based approach, the present study aims at developping an efficient integrated oxy-fuel power generation system process model with air separation and CO_2 capture and compression modules. The integrated model was developed in HYSYS process simulation software package. The overall model consists of four major modules/subsections, namely, 1) oxy-fuel boiler & combustion loop, 2) balance of plant (BOP), 3) air separation unit (ASU), and 4) CO_2 capture and compression unit (CO_2CCU) also known as $CanCO_2$ (a patented process). The single reheat BOP steam cycle condition is 242 bar/593°C/622°C Rankine cycle, where the main steam and reheat steam are at 593°C and 622°C, respectively. Each subsection is modeled in detail to work as an independent model in separate flow sheets and then combined together in a main flow sheet to generate the integrated model. This model is a fuel agnostic model and a typical lignite coal was used for this study. Detailed exergy analysis for various process streams were carried out as an exergy analysis tool was implemented in the model to automate the exergy analysis calculation with an exergy reference condition at 25°C and 1 atmosphere. This automated exergy analysis tool allows generating data at various process conditions with single change of a process parameter in the overall model. Accordingly exergy efficiency improvement potentials were identified for different unit operations. This identification allowed incorporating process improvement measures which ultimately increased the overall efficiency of the plant. A sequential approach was undertaken for this model improvement. The final outcome of this exercise was an improved integrated oxy-fuel model with higher net power efficiency. The model was developed for a 786 MWgross power plant (521.25 MW net in the base model) integrated with CO_2 capture and air separation unit (ASU). The O_2 generated from the ASU has a purity of ~95% (% mol). The performance result, based on exergy analysis, indicates an efficiency improvement of approximately 0.6 percentage point based on high heating value (HHV) and a net power gain of approximately 2.14% compared to a base model. In specific cases, the

gain in HHV efficiency and net power can increase up to 1.15 percentage point and 4.12%, respectively. The captured CO_2 has a purity and recovery rate of 95.78% (% mol) and 92.55%, respectively, at pipeline transport conditions (110 bar, 43°C).

This unique model is a first step to develop an integrated high efficiency oxy-fuel plant with CO_2 capture, which is considered to be a sustainable technology for future deployment for near-zero emission power generation plants. This model is unique in nature in the context that it provides a flexible platform to develop simultaneously a process model of an integrated oxy-fuel power plant and perform exergy analysis for the same model where the power generation capacity of the model could be of any range as defined by the user (> 0 MW ~ no upper limit in MW number). The major process parameters also can be manipulated relatively easily by changing them in a single location and the ripple effect of which recalculates and builds a new overall model automatically (including exergy calculations).

This research work establishes a unique approach to improve the performance of integrated oxy-fuel power generation systems. It can be extended by including cost analysis tool and generate techno-economic data. Moreover, similar to exergy analysis tool, a detailed optimization analysis can also be implemented in the overall model which could be a separate study of its own. However, this current analysis will be very useful for technology demonstration and commercialization of the oxy-fuel technology in power generation application and reduce CO_2 emission to the atmosphere from these plants.

Acknowledgements

I would like to take this opportuninty to convey my sincere thanks and gratitude to a number of people for their guidance and support.

Table of Contents

List of Figures

xiii

List of Tables

Nomenclature

ASU = air separation unit

BOP = balance of plant

BFW = boiler feed water

CEA = Canadian electricity association

CO_2CCU = CO_2 capture and compression unit

CCW = closed cooling water

C_p = heat capacity of substance at constant pressure

C_v = heat capacity of substance at constant volume

CPU = CO_2 processing unit

CV = control volume

CW = cooling water

DOE = department of energy (United States of America)

E^{PH} = physical exergy

E^{KN} = kinetic exergy

E^{PT} = potential exergy

E^{CH} = chemical exergy

E = total exergy

$\dot{E}_j$ = exergy flow rate

EES = engineering equation solver

EOS = equation of state

EXP = expander

ESRL = earth system research laboratory (Hawaii, USA)

e = specific exergy

e^{KN} = kinetic exergy

e^{PH} = specific physical exergy

e^{PT} = potential exergy

e^{CH} = chemical exergy

ε^M	=	specific molar exergy of mixing
FDF	=	forced draft fan
FGD	=	flue gas desulfurization
FWH	=	feed water heater
h	=	specific enthalpy
h^M	=	enthalpy of mixing
HP	=	high pressure
HTS	=	high temperature steam
HHV	=	higher heating value
$\overline{HHV}$	=	higher heating value (mole basis)
i	=	Inlet
$\dot{I}$	=	rate of exergy destruction
IP	=	intermediate pressure
IEA	=	international energy agency
ITM	=	ion transport membrane
IGCC	=	integrated gasification combined cycle
LP	=	low pressure
LNG	=	liquefied natural gas (exchanger)
LHV	=	lower heating value
$\overline{LHV}$	=	lower heating value (mole basis)
$\dot{m}$	=	mass flow rate
MP	=	medium pressure
MW	=	mega watt
NEB	=	national energy board
OCW	=	open cooling water
PAPH	=	primary air pre-heater
PAF	=	primary air fan
PCCW	=	partially closed cooling water
PG Cooler	=	process gas cooler
Q	=	thermal energy

$\dot{Q}$ = Heat transfer rate to the system

RAPH = recycle air pre-heater

S = entropy of substance at temperature T

S_0 = entropy of substance at temperature T_0

S^M = entropy of mixing

SAF = secondary air fan

SAPH = secondary air pre-heater

VPSA = vapour pressure swing adsorption

W_{rev} = reversible work

λ = efficiency

ω_i = acentric factor

ψ = exergy efficiency

Chapter 1
Introduction

1.1 Introduction

Since the Industrial Revolution in the 19th century, anthropogenic carbon dioxide (CO_2) emissions to the atmosphere have increased rapidly. This is due to excessive burning of fossil fuels, such as natural gas, oil and coal which generate large quantities of CO_2 and are believed to be the major cause of global warming. The concentration of CO_2 further increased in the atmosphere as the deforestation over the following decades continued unabatedly. In 2005, global atmospheric concentrations of CO_2 (379 ppmv) were 35% higher than what they were before the Industrial Revolution during the mid-1800s. Since the pre-industrial revolution the amount of emissions increased from near zero to 29 Gt CO_2 in 2009. The fastest growth was observed in the last decade between 1995 and 2005, which was 1.9 ppmv/year (IEA, 2011a). Recent atmospheric data recorded by the Mauna Loa Observatory (MLO) in Hawaii (ESRL, 2014), indicates that the global CO_2 concentration in the atmosphere has reached up to 400 ppm level. The growing energy demand from fossil fuels has played a major role in the upward trend of CO_2 emissions. The distribution of current world CO_2 emissions indicates that the electricity and heat generation sectors are the major producers of anthropogenic CO_2, having the largest share of about 41% of total emissions (IEA, 2011a). In 2009, about 43% of CO_2 emissions from fossil fuel combustion were generated from coal, 37% from oil and 20% from natural gas (IEA, 2011a). Also, according to current statistics, the proven coal reserve will last for another 133 years with the current rate of coal production and consumption (NEB, 2013b). These clearly indicates that coal will remain as a major player in power generation and will contribute significantly to the atmospheric CO_2 emissions in the years to come. The world energy demand is increasing rapidly with a projected forecast of 75 percent increase in electricity demand by 2035 (IEA, 2011b; NEB, 2013b) along with the emissions of CO_2 and other greenhouse gases (GHG). Apart from CO_2, power plants also emit other pollutants such as nitrogen oxides (NO_x), sulphur oxides (SO_x), mercury (Hg) and other trace metals. It is necessary to stabilize the GHG emissions to an agreed level and for that, large reduction of CO_2 emissions is needed.

The current electricity generation capacity in Canada is roughly about 134 GW and nearly 9% of this electricity is generated from coal (NEB, 2013a; NEB, 2013b). Canada is blessed with abundant natural resources, and coal is among one of the prominent resources that is supplying a significant portion of our energy need. It is a relatively cheap and easily accessible resource that has been used for several decades in power generation. However for ensuring a secure and sustainable fossil energy resource in the future, the use of fossil fuels in power generation must be done sensibly and efficiently. Novel technologies must be adopted and significant efforts must be made to improve efficiency and emissions reduction.

Oxy-fuel combustion in power generation is a relatively novel concept. This concept has been widely used in steel and glass industries for many decades; however its use in power generation is relatively new. It uses pure oxygen, instead of air, for fuel combustion and recycles a major portion of the combustion flue gas into the boiler to moderate the flame temperature. As pure O_2 is used in the combustion process, the resulting combustion flue gas contains high concentration of CO_2 and H_2O, which can be relatively easily separated with less energy penalty. However, on the other hand, O_2 production consumes energy and reduces the overall plant efficiency. Various studies have indicated that oxy-fuel power generation with CO_2 capture is competitive (Adams & Davidson, 2007; Kanniche et al., 2010; Rubin et al., 2012) and potentially even better than the conventional air fired power generation processes coupled with post-combustion CO_2 capture. According to a detailed study undertaken by DOE, it indicates that oxy-combustion with super critical steam condition for the BOP has a higher net thermal efficiency (approximately 1%) and a lower LCOE (approximately 0.8 cents/kWh) than an air-fired amine based system. Also amine scrubbing for CO2 capture in an air-fired power plant causes to increase the levelized cost of electricity (LCOE) by nearly 75% compared to 63% for the oxy-combustion case (for both cases the cost is excluding the cost of CO_2 transport, storage, and monitoring). Also oxy-combustion has the lowest cost of CO_2 capture as well as the cost of CO_2 avoided (DOE /NETL 2008). Moreover, a separate study undertaken by a consortium of industries and Canadian Clean Power Coalition (CCPC) on 'Future CO_2 Capture Technology Options for the Canadian Market' also revealed the better performance of oxy-combustion process.

According to this study thermal efficiency of an optimized oxy-fuel power plant is approximately 1% point higher than that of the amine based CO_2 capture power plant. In addition, the oxy-fuel option has lower levelized cost than the amine scrubbing option (BERR 2007). Some of the major benefits for oxy-combustion technology with CO_2 capture, compared to the conventional air combustion technology, include reduced CO_2 emissions, 60-70% reduction in NO_x, potential for higher Hg removal in bag house, and the technology can readily be applicable to new coal fired power plants (DOE 2008; BERR, 2007). The oxy-fuel power generation systems are currently being experimented at pilot-scale level and only a few small scale pre-commercial demonstration plants are being operated (Wall et al., 2009; Wall et al., 2011; CALLIDE, 2014; Levasseur et al., 2009; Strömberg et al., 2009). The largest of these demonstration plants has a capacity of only 30 $MW_{thermal}$, whereas a single unit for standard conventional power plant is usually 500 MW_{net} capacity in size. There are lots of opportunities to improve the efficiency of oxy-fuel combustion based power plants if all the components of the overall oxy-fuel plant are integrated and if the waste heat is reduced from the integrated plant. These opportunities need to be explored further through detailed process modelling and thermodynamic analysis (exergy analysis) including all the four major sections of an oxy-fuel plant i.e. the boiler and flue gas section, the balance of plant (BOP) also known as steam cycle, the CO_2 capture and compression unit (CO_2CCU) also identified here as $CanCO_2$, and the air separation unit (ASU). An exergy analysis in each section for the major components can determine the exergy destruction rates, the point sources for exergy destruction and the exergy efficiency of the individual unit operations. Based on these results appropriate process improvement measures can be proposed to reduce the overall heat loss and improve the efficiency of the integrated process.

1.2 Research objective

The main goal of this research work is to develop an integrated and improved process model of an oxy-fuel combustion power plant with CO_2 capture by reducing waste heat through an exergy analysis. This thesis aims - at developing an integrated model including all four major sections of the overall process i.e. the boiler and flue gas section, the balance of plant (BOP) also known as steam cycle, the CO_2 capture and compression unit (CO_2CCU) also

3

identified here as $CanCO_2$, and the air separation unit (ASU). It also aims at identifying and quantifying the exergy destruction rates for various unit operations in the integrated model and proposes and implements the improvement measures to increase the overall plant efficiency. Moreover, various process conditions have been taken into consideration to observe their impact on the performance of the overall process. The following tasks have been considered to achieve the research goal:

- Develop an integrated process model of an oxy-fuel power generation system incorporating all four major sections i.e. combustion boiler and flue gas section, BOP, ASU and $CanCO_2$.

- Incorporate exergy analysis calculation equations for the process streams in all four sections of the model.

- Verify the steady state process model and exergy analysis data with reported data in the open literature.

- Identify the quantity and location of exergy loss at major unit operations in each section of the integrated plant.

- Improve the integrated process model by increasing the exergy efficiency and utilizing waste heat; and perform a sensitivity analysis.

1.3 Scope of work

The integrated model of the oxy-fuel power generation system with a capacity of 786 MW_{gross} was developed in the state-of-the-art HYSYS process simulation and modeling software platform (Aspen HYSYS). The 786 MW_{gross} plant capacity was chosen as it resembles a standard single unit utility boiler and also sufficient data are available in the open literature for a representative similar size of existing conventional air fired power plant (DOE 2008). The boiler and flue gas section model was developed based on the experience gained over the years from the existing pilot scale oxy-fuel combustion boiler (0.3 $MW_{thermal}$) at CanmetENERGY in Ottawa and available literature in the public domain, as there is no commercial unit available. The combustion section was modelled based on the required heat input to the BOP section to generate 786 MW_{gross} electricity. The BOP model was developed

based on the process parameters and model layout published by DOE for a 786 MW$_{gross}$ oxy-fuel power plant (DOE 2008). The ASU model was developed based on the process parameters and model layout published by the International Energy Agency (IEA) in their report 2005/9 (IEA, 2005). The ASU size was determined by the O$_2$ requirement for the overall plant. The CO$_2$ capture and compression unit model (CanCO$_2$) was developed by scaling up (~6250 times) of an existing novel pilot-scale CO$_2$ capture model which was earlier co-developed by the author (patent ref: WIPO, 2014). This capture model is successfully being demonstrated at a pilot-scale level as a standalone trailer mounted CO$_2$ capture unit located at CanmetENERGY in Ottawa. It is currently being extensively used to generate valuable data for CO$_2$ capture from oxy-fuel combustion systems. Details of this unit can be found in different publications (Zanganeh et al., 2010; 2009a; 2009b; 2008a; 2008b; 2008c; 2006; Chansomwong et al., 2013a; 2013b; 2011; Shafeen et al., 2010). The exergy analysis concept and equations were included in the model based on published literature (Bejan et al., 1988; Dincer et al., 2007; Cengel et al., 2006)

1.4 Research contribution

The oxy-fuel combustion process is a promising technology for developing near zero emission power plants. There are few studies available related to the process models of individual sections for the oxy-fuel plants. However, there are only two, to the best of the author's knowledge, integrated process configuration of an oxy-coal plant including Boiler, BOP, ASU and CO$_2$ capture unit available in the open literature (Fu and Gundersen, 2013; Hagi et. al., 2013). Fu and Gundersen published a process model for 792 MW$_{gross}$ plant. The process configuration with exergy analysis, modelled in Aspen Plus, however did not elaborate the details of the model development methodology and the exergy equations. Moreover, the process models of three individual sections (boiler and flue gas section, ASU and CO$_2$ capture unit) therein is different than the process models presented in this thesis. Only the BOP configuration might be similar as the reference is same (DOE, 2008) for both studies. However, the modeling approach is quite different as the BOP model, as well as all section models, in this thesis were developed in an automated fashion to float around different plant capacity ranges. Hagi et al. published a process model for 1000 MW$_{gross}$ oxy-

pulverized coal power plant including exergy analysis developed in Aspen Plus. The process improvement approach suggested in this study is based on heuristic rules. This published process model and the approach for its improvement is completely different than the models and approach used in this study. The capacity range in this study is flexible and user defined, which is very unique and characterizes a significant deviation from the published processes (Fu and Gundersen, 2013; Hagi et. al., 2013). This flexibility is introduced by incorporating ratios (ratios derived from a base flow rate) instead of fixed flow rates for the process streams. This flexibility allows generating detailed process models and process design parameters, including complete exergy analysis data, for oxy-fuel power generation systems at different capacity ranges instantaneously. The published studies do not appear to be flexible and only generate data for a fixed capacity plants (e.g. 792 MW and 1000 MW).

This thesis further looks into the oxy-fuel power generation technology in an equation oriented sequential approach in which the temperature, pressure, flow rates enthalpy and entropy of the process streams are used to calculate the available work potential as well as the exergy destruction and efficiency for all the unit operations. A set of parallel reference material streams duplicating all the main streams in the process model at reference environment condition was developed. These streams are mirror imaged and updated for any change in the process parameters (e.g. mole fraction) in their corresponding main streams. This update is necessary to generate accurate exergy data under various process conditions and changes in process parameters as well as change in environment conditions. This feature is included, utilizing a tool available in the software package, to keep the reference stream updated and provide accurate reference exergy data during any change in process parameters. A detailed mathematical analysis is also provided. In addition, the process improvements, based on the exergy analysis results, are implemented integrating multiple unit operations in all four sections of the plant. Moreover, new approaches are proposed to utilize the waste heat and improve plant efficiency. This flexible process model also allows generating detailed process and exergy data automatically at various plant capacity ranges or at different cooling water temperature conditions as set by the user or for a specific design condition set for a particular plant. These qualifications give the integrated oxy-fuel process model a

distinct advantage over any other models that were recently published. The developed model presented in this thesis can be considered as a first attempt at developing a process model with rigorous mathematical exergy modelling of an integrated oxy-fuel power generation system. This effort ulilizes a novel CO_2 capture process, known as the $CanCO_2$, and a unique boiler and flue gas section model which are not available in the public domain.

1.5 Thesis outline

This thesis is organized in the following order:

Chapter 1 describes the introduction, objectives, scope of work and research contribution.

Chapter 2 provides the background of the technology with respect to electricity generation, fossil fuel use and relevance with CCS; and literature reviews on oxy-fuel technology and exergy analysis.

Chapter 3 provides the process simulation and model development details including process description and steady state model validation.

Chapter 4 presents the details of the exergy and its components, exergy analysis with exergy data testing and verification from published literature.

Chapter 5 presents the results obtained from exergy analysis and accordingly, waste heat utilization is implemented in the model; finally an improved oxy-fuel model is developed and the results presented. Process sensitivity analysis for few selective parameters is also presented in this chapter.

Chapter 6 provides the conclusions of this research work and recommendations for further studies.

Chapter 2

Background and Literature Review

This chapter provides the background of power generation and the resulting CO_2 emission with respect to the use of fossil fuels, specifically coal. This also shows the significance of coal as a prominent energy source in the global and Canadian energy mix and portrays the extent of CO_2 emission from coal combustion. A brief description of oxy-fuel combustion technology which is a recent technology development initiative in the power generation sector is also included in this chapter. Moreover, literature reviews on exergy analysis of individual plant sections as well as the overall integrated oxy-fuel plants are also provided.

2.1 Electricity generation from coal and CO_2 emission

Coal plays a significant role in the global energy mix which meets about 28 per cent of global primary energy demand. It is one of the cheapest primary energy sources due to its abundance and wide global distribution. Power generation accounts for two-thirds of coal consumption worldwide, and the rest is used mainly by the steel industries. According to the international energy agency (IEA), coal is the largest source of power generation worldwide, and currently accounting approximately 41% in total. This growth in electricity generation from coal will increase to 48% by the year 2035 as predicted by IEA (IEA, 2011b). So, coal will remain a major player in the overall growth of the world energy mix in the years to come. Canada is reach in fossil fuel resources. It has about 6.6 billion tonnes of proven recoverable coal reserves, which translates into 100 years of production at the current rate of production in the Canadian economy. In 2012, the total electricity generation capacity in Canada reached to 134 GW and the total power generation was 595 TWh (CEA, 2012; NEB, 2012b). Coal fired power plants were a significant part of this generation capacity. However, there is a growing trend to shift to the low carbon and renewable energy sources and reduce the dependence on coal for power generation in order to reduce the CO_2 emission from coal combustion and power generation. Figure 2-1 indicates the overall fuel mix in electricity generation sector for Canada in 2012.
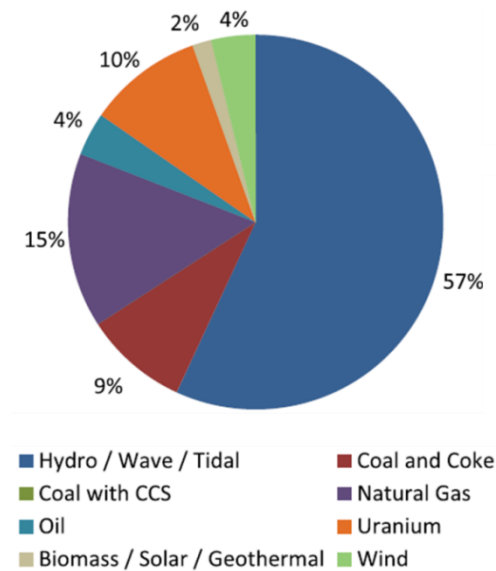
Figure 2-1 Fuel capacity mix by primary fuel for electricity generation in in Canada (NEB, 2012b)

The use of fossil fuels within the current energy infrastructure is considered to be the largest source of anthropogenic emissions of carbon dioxide. Figure 2-2 indicates the total greenhouse gas (GHG) emissions in Canada for the year 2010 which was 692 Megatonnes of CO_2 equivalent from all sectors, including power generation. The sectorial distribution of these emissions for the energy sector (603 megatonnes) is also presented in the same figure. It indicates that fossil fuel industries and electricity generation sector together contributes about 27.3 % of the total emission (CEA, 2012). There are numbers of ways to reduce the level of CO_2 emissions from fossil fuel usage such as, 1) increasing the "fuel to end-use" energy conversion efficiency; 2) replacing high-carbon fuels with lower-carbon fuels; and, 3) capturing, converting, reusing or storing CO_2 in suitable geological formations. While the first two are effective options, they alone cannot fully mitigate the global increase in CO_2 emissions. The storage option de-couples the use of fossil fuels from CO_2 emissions, thus allowing for the continued use of fossil fuel in a sustainable way. Hence, there are immense opportunities for a significant reduction in greenhouse gas (GHG) emissions from industrial processes and power plants through the aforementioned ways (Gale et al, 2000).
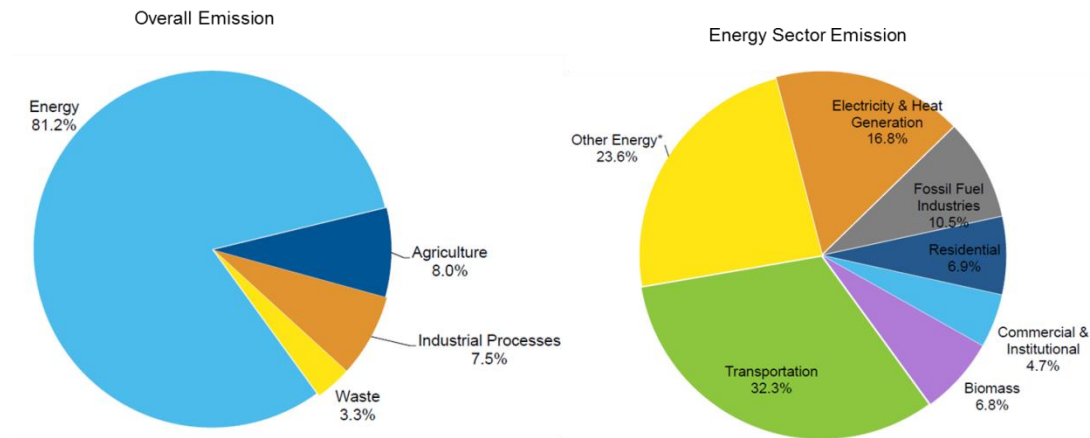
Figure 2-2 Greenhouse gas emission (GHG) by sector in Canada, 2010 (CEA, 2012)*[1]

Currently, there are three main approaches to capturing CO_2 from the fossil fuel energy conversion systems, namely, pre-combustion capture, post-combustion capture, and oxy-fuel combustion with CO_2 capture. Among these approaches, pre-combustion and oxy-fuel combustion take advantage of the fact that CO_2 capture is facilitated by increasing the concentration of CO_2 in the flue gas stream, or by increasing the flue gas pressure, or both. Pre-combustion processes through gasification remove pollutants and CO_2 from fossil fuels prior to their conversion into electric power, or hydrogen and chemicals (Kreutz et al, 2002). Oxy-fuel combustion, on the other hand, has a unique advantage over other approaches to CO_2 capture, in that it generates a flue gas stream that is mostly composed of CO_2 and H_2O. Hence, CO_2 capture from this flue gas stream is relatively straightforward, involving no solvents and requiring only compression and cooling. On the other hand post-combustion capture, applicable to existing conventional power plants, uses solvents to capture CO_2. However, solvent based processes have several issues related to fugitive emission, solvent degradation and safe disposal problems. The degradation products are typically separated in a reclaimer and disposed of as hazardous waste and subsequently incinerated at a permitted facility (DOE /NETL 2004).

---

[1] *includes all the other energy sector emission sources, such as mining, manufacturing, and construction, fugitive sources and agriculture/forestry/fisheries (CEA, 2012)

In all cases CO_2 capture is associated with energy penalty and efficiency loss. However, at the current state of development, the risks and costs of non-fossil energy alternatives, such as nuclear, biomass, solar, and wind energy, are so high that they cannot replace the entire share of fossil fuels in the near future timeframe. Additionally, any rapid change towards non-fossil energy sources, even if possible, would result in large disruptions to the existing energy supply infrastructure. As an alternative, the existing and new fossil fuel-based plants can be modified or designed to be either "capture" or "capture-ready" plants in order to reduce their emission intensity through the capture and conversion, reuse or storage of carbon dioxide. This would give the coal-fired power generation units the option to sustain their operations for longer time, while meeting increasingly stringent environmental regulations on air pollutants and carbon emissions in years to come.

2.2 Fossil fuel power generation systems:

Fossil fuel power plants are generally energy conversion systems where fossil fuels are converted into mechanical and electrical energy. The energy conversion system is usually integrated with a steam cycle based on a Rankine cycle or a Brayton cycle or the combination of the two (Steam, 2005; Smith et al, 1987). The Brayton cycle usually requires a cleaner fossil fuel (e.g. natural gas or oil) as the combustion flue gas directly passes through turbine blades. However, all types of fossil fuels can be used in a Rankine cycle, as only clean steam passes through the turbines. This research work focuses on identifying point sources for heat loss in a specific type of power plant, based on Rankine cycle, in order to improve its efficiency. Any improvement in the power plant efficiency by reducing waste heat generation or utilizing low grade heat will have significant impact on the overall efficiency of the power plants and will contribute to the sustainable use of fossil energy resources. The present study deals only with pulverized coal (PC) based power plants that would operate in oxy-fuel mode. However, this model is equally applicable for any other fossil fuel applications e.g. natural gas, bitumen, heavy oil etc. A brief description of conventional (air combustion) PC power plants is given below for reference.

2.2.1 Conventional fossil fuel power plants and CO_2 capture:

A conventional PC power plant generates heat through combustion of fossil fuel with air in the boiler. In these plants air is used as combustion medium where air bound nitrogen plays a vital role for flame temperature moderation inside the boiler. The heat is transferred to the steam cycle through the boiler water tubes which produces high pressure super-heated steam and subsequently converts the steam energy into electrical energy via a set of turbines and generators. The exhaust steam from the turbines is condensed and recycled back to the boiler as boiler feed water (BFW) to generate steam again and thus completing the cycle. The combustion flue gas contains different pollutants and impurities such as CO_2, SO_x, NO_x, Hg, trace metals and ash. High efficiency low NO_x burners are used to keep the NO_x formation minimum and within an acceptable limit. A couple of different flue gas treatment units are used at the downstream of the boiler to clean the flue gas to an acceptable limit before venting to the atmosphere. These units include electrostatic precipitator (ESP) and/or bag house for ash, selective catalytic reduction (SCR) unit for NO_x, and flue gas desulphurisation (FGD) unit for SO_X and mercury. Finally, the flue gas goes to the atmosphere through a stack at a temperature around 150 ^{o}C above the saturation temperature (Steam, 2005). A typical pulverized coal fired power plant is shown in Figure 2-3.
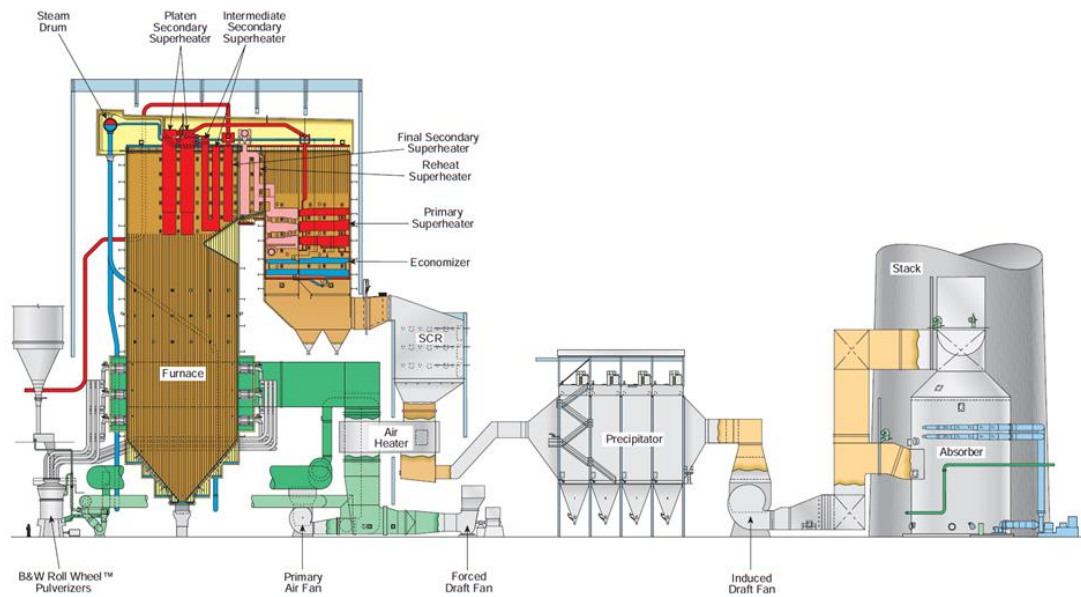
Figure 2-3 Modern coal fired utility boiler system with environmental control equipment (Steam, 2005)

The CO_2 concentration of the stack gas is usually between 5 and ~15% (mole), depending on natural gas or coal combustion, and the rest mainly N_2. A suitable CO_2 capture technology for these type of plants is a solvent based technology where CO_2 is absorbed by a suitable solvent (amines and its derivatives) in an absorber at low pressure and the captured CO_2 (> 99% mol purity) is released in a stripper, with application of heat, and at the same time the regenerated solvent is recycled back to the absorber for reuse. The energy penalty for the CO_2 capture is very high and reduces the overall plant efficiency by a few percentage points. All the plant efficiencies referred here are based on higher heating value (HHV) and the same convention will be used throughout the document. These plants have normally an efficiency range between 39 and 45% without CO_2 capture depending on the types of technology and fuel used. However, with CO_2 capture the efficiency drops down to a range of 29~33% based on the types of plant and technology used for CO_2 capture (BERR, 2007; DOE, 2008). As the CO_2 capture penalty is very high for post-combustion capture, there are alternative and promising technologies for power generation and CO_2 capture that are currently being investigated. For this reason, the concept of oxy-fuel power generation technology is gaining

13

momentum and several pilot and demonstration scale facilities are now in operation worldwide (Wall et al., 2009; Wall et al., 2011; CALLIDE, 2014; Levasseur et al., 2009; Strömberg et al., 2009). The facilities are being used to investigate the technology and further improve it to demonstrate the technology at a commercial scale.

2.2.2 Oxy-fuel combustion power plants:

The use of oxy-fuel combustion process in power generation systems is a relatively new concept that is actively being considered by utilities and industries. The technology is still in the development stage. Combustion in an oxy-fuel system takes place in pure oxygen environment, in absence of air. As a result, the flue gas from the oxy-fuel combustion process contains mainly CO_2 and water vapour along with some other impurities, such as nitrogen, argon, oxygen, nitrogen oxides, heavy metals and sulphur oxides. The presence of N_2 is mainly because of air leakage into the boiler and the percentage of the fuel bound N_2. O_2 (95% mol) stream also contains N_2 (2~3% mol) which contributes a small percentage to the overall N_2. The other impurity concentrations may vary based on the type of fuel, combustion conditions, plant configuration, and other process related parameters. In oxy-fuel combustion, nitrogen contained in air is first separated in an air separation unit (ASU) so that a stream of nearly pure oxygen (95% mol) is produced in the ASU. The O_2 is then used as a combustion medium, in place of air, and burned with coal or with other fossil fuels in the boiler. Combustion in pure O_2 environment creates very high temperature (~3000 ^{o}C) in the boiler and, as a result, part of the flue gas is recycled back to the boiler to moderate the flame temperature. The amount of recycle flue gas is controlled in such a way that it keeps the adiabatic flame temperature inside the boiler similar to that in a conventional air fired case (in order to use existing proven boiler technology) which is close to ~2000 ^{o}C (DOE, 2008). The resulting flue gas is then mostly composed of CO_2 and H_2O and ultimately forms the primary and secondary recycle after necessary processing through flue gas treatment systems. The portion of the flue gas which is not recycled is further processed in a CO_2 capture and compression unit where CO_2 is separated from the other pollutants. Finally, the relatively pure CO_2 (> 95% mol) is sent to pipeline at a pressure greater than 110 bar for transportation and reuse or storage. The CO_2 capture is relatively straight forward in oxy-fuel mode as

simple phase separation achieved by compression and expansion is sufficient to separate CO_2 from other impurities. In this particular study a proprietary (WIPO, 2014) CO_2 capture and compression unit (CanCO$_2$ in Figure 2-6) is used for CO_2 capture from the power plant. The working principle for the steam cycle, also known as balance of plant (BOP), in the oxy-fuel power plant is the same as in conventional power plants. The efficiency of an oxy-fuel power plant with CO_2 capture can be maximized if all the subsections (ASU, CO_2 capture Unit, BOP) are integrated and heat loss is minimized from the overall plant. A simplified process flow diagram of an integrated oxy-fuel combustion process with CO_2 capture is shown in Figure 2-4. In this plant configuration, ASU is connected to the boiler by the O_2 feed line. The BOP is connected by the main steam generation line from the boiler to the BOP. The CO_2 capture unit (CanCO$_2$) is connected by the flue gas line from the combustion loop to the CanCO$_2$. The BOP is similar irrespective of advanced oxy-fuel or conventional air combustion systems. Hence, no major change is anticipated in the steam cycle i.e., the BOP section.
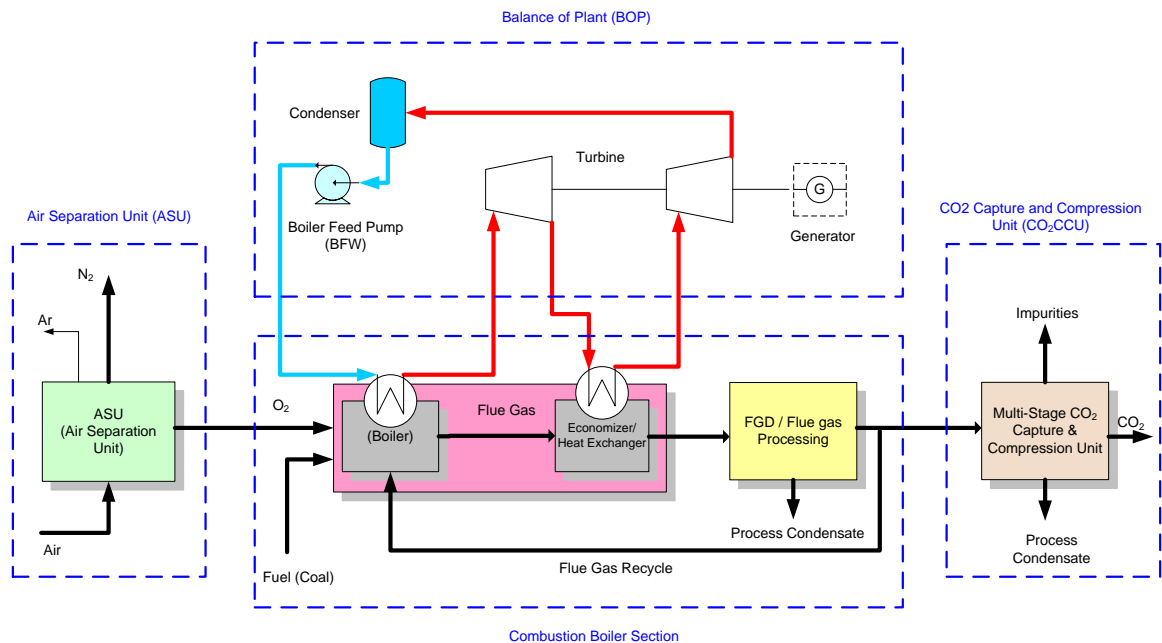
Figure 2-4 Integrated oxy-fuel combustion process: simplified diagram

Due to the elimination of N_2 from the combustion stream, the overall flue gas volume in oxy-fuel case is significantly lower, resulting in a size reduction of the plant components significantly and in some cases (flue gas cleaning equipments) almost to one fourth of a conventional combustion systems (IPCC, 2005). This size reduction ultimately translates into cost reduction as less material is needed to build the power plant. Also the parasitic power demand for the auxiliary equipments reduces significantly as the volume of flue gas reduces which translates into increased energy efficiency of the plant. The other advantage is a concentrated CO_2 stream in the combustion flue gas which requires less efforts and energy for CO_2 separation compared to a solvent based capture process used in the conventional post-combustion capture from PC plants (Gupta et al., 2007; Zanganeh et al., 2007a; 2007b; 2007c). Currently, there are no commercial oxy-fuel plants built. However, a chronology of event on oxy-fuel combustion R&D and pilot scale demonstration is well documented by IEA (Santos, 2013) and presented in Figure 2-5 with a minor modification.
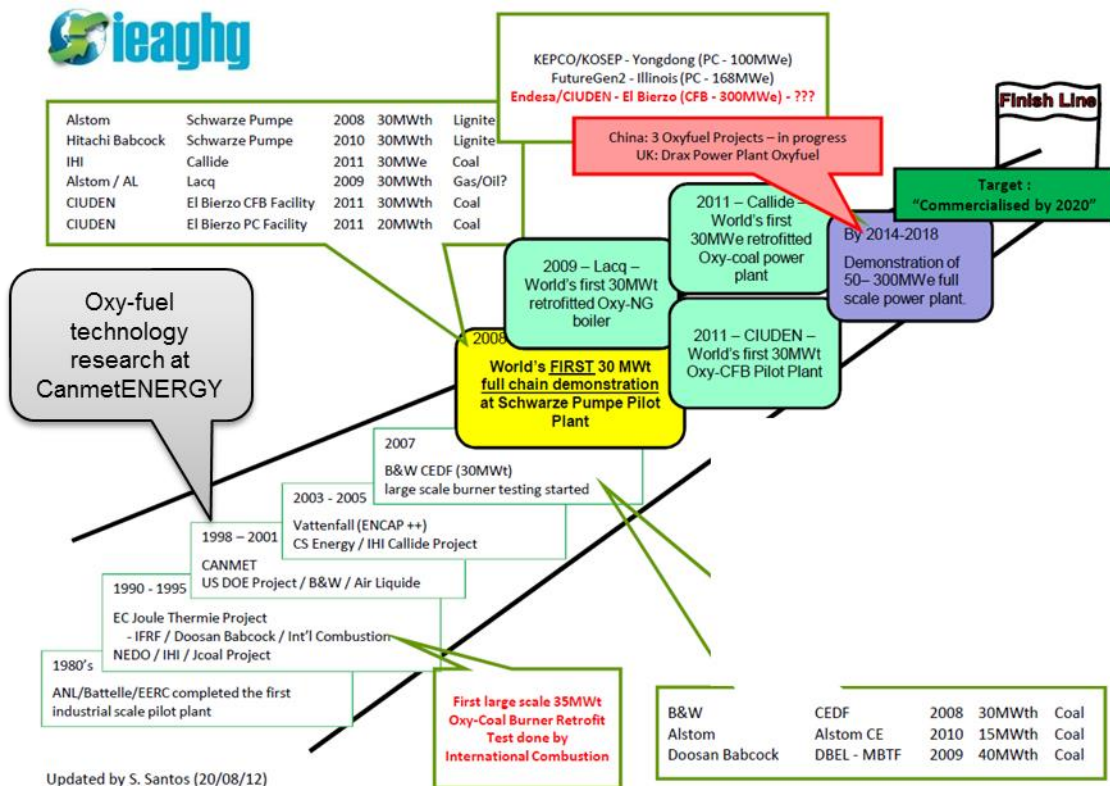
Figure 2-5 Chronology of oxy-fuel power generation research and development (modified after Santos S., 2013)

CanmetENERGY in Ottawa is one of the pioneers in oxy-fuel combustion research since early 1990. It established a $0.3MW_{thermal}$ oxy-fuel combustion pilot scale research facility. In 2008, a CO_2 capture and compression unit ($CanCO_2$) was added and integrated with the pilot facility. Together with the CO_2 capture unit it became the first of a kind pilot-scale research facility for oxy-fuel combustion integrated with CO_2 capture. Since then, experimental results from this pilot facility have been disseminated to the scientific community (Shafeen et al., 2010; Zanganeh et al., 2010, 2009a, 2009b; 2008a, 2008b, 2008c; 2007a; 2007b; 2007c; 2006; Gupta et al., 2007). However, the first oxy-fuel demonstration project was built in Germany (Schwarze Pumpe Pilot plant-Vattenfall) in 2008. The capacity of this plant was 30MWthermal and the experimental results are available in open literature which is very promising (Strömberg et al., 2009; Vattenfall, 2014). In addition, CIUDEN in Spain also commissioned a $30MW_{thermal}$ oxy-CFB (circulating fluidised bed) demonstration boiler in

17

December 2011. A few details of this plant are also available in open literature (Hack et al., 2011).

Several detailed studies were also performed to clearly understand the techno economic feasibility of the oxy-fuel power plants including CO_2 capture (IEA, 2005; IEA, 2006, BERR, 2007; DOE, 2008). All these studies describe the oxy-fuel combustion technology with minimum discussion about integration of all the individual sections of the power plant, which is actually necessary for the efficiency improvement of these plants. An integrated oxy-fuel plant will be more promising and sought after technology for its implementation at a commercial scale. Details of the current research and process description of an integrated oxy-fuel plant are included in Chapter 3.

2.2.3 Oxygen supply and air separation unit (ASU)

Unlike conventional power plants, the oxy-fuel combustion process uses nearly pure oxygen, instead of air, for the combustion in the boiler. Different technologies are available for oxygen production. These include cryogenic, ion transport membrane (ITM) and vacuum pressure swing adsorption (VPSA) technologies. Oxygen purities (% mol) from these technologies can reach up to 99.9%, 99+%, and 90~94% respectively. The current commercial applicability of ITM and VPSA technologies are limited in size (very small scale application) as the technology is still not matured and not yet developed for large scale application. However, cryogenic ASU is very common in industries and the technology is mature since many years. Details of these technologies are available in the public domain (PraxAir, 2014; Linde, 2014; Airproducts, 2014, Cornelissen et al., 1998). This study considers a cryogenic ASU technology, the detail of which is derived from an existing study (IEA, 2005). With the current available technology, a single train cryogenic ASU can be built up to 3000-4000 tonne per day of oxygen produced. However, these plants are energy intensive and reduce the overall integrated oxy-fuel power generation efficiency significantly, by almost 5-10% (DOE, 2008; IEA, 2005, BERR, 2007).

The preferred ASU cycle in the oxy-combustion is the one in which gaseous oxygen is produced by boiling liquid oxygen, as the delivery pressure required for oxy-combustion is

low. In addition, no pumping or compression of liquid or gaseous oxygen is required for the oxy-combustion process. A low purity (95% mol) oxygen cycle is also identified as the optimum cycle for oxy-combustion process as there will be always some air leakage into the combustion boiler. Moreover, the power consumption for producing nearly pure (99.5% mol) oxygen is calculated to be greater than the increase in CO_2 compression power (in the CO_2 capture unit) to remove the impurities introduced by the low purity oxygen (IEA, 2005; Fu, C., 2012).

There are limited opportunities to increase the efficiency of a cryogenic ASU; however an integrated approach in the context of an overall oxy-fuel power plant with CO_2 capture may present some opportunities to maximize the energy efficiency of these plants. On the other hand, a commercial scale oxy-fuel power plant would probably do the start up with air combustion and slowly transitions to pure oxygen combustion. Hence, efficiency improvement for the ASU might be a tricky issue with respect to its full load or part load operation during the transition period. Load following capability for ASU also will have immense impact on the operation of oxy-fuel power plants and specific strategy needs to be devised to minimize the overall efficiency penalty at that time (Goloubev, D., 2012). There are different approaches being considered by the industry to overcome these issues, however the current study does not focuses on those issues as it considers that the plant is running at full load and hence load variation does not apply here.

2.2.4 CO_2 separation capture and compression systems (CanCO$_2$)

As discussed earlier, the oxy-fuel combustion process generates a concentrated stream of CO_2 gas mixture in the flue gas. The concentration of CO_2 ranges from 70 to 90% (mol), depending on the purity of oxygen and air leakage into the combustion system. There are various technologies available for CO_2 capture and compression. However, the technology used here is based on a novel proprietary patented (WIPO, 2014) CO_2 capture and compression process co-developed by the author (Shafeen et al., 2010; Zanganeh et al., 2010, 2009a, 2009b; 2008a, 2008b, 2008c; 2006). This capture process removes multi-pollutants from the process stream and generate nearly pure CO_2 (> 95% mol) as a product stream. The

CO_2 recovery rate from this process is also very high (~85%). It is to be noted that the recovery rate always vary with the impurities present at the inlet process gas stream to the $CanCO_2$. A concentrated CO_2 stream usually provides higher recovery rate. However, more impurities require the system pressure to be raised for high recovery rate with more compression energy penalty. Capture of multi pollutants, especially SO_x, NO_x, and mercury, along with CO_2 can be efficiently done through $CanCO_2$. This can be achieved while the flue gas is pressurized and cooled down to liquefy and separate CO_2. The simultaneous removal of SO_x and NO_x in the presence of oxygen and water is achieved by taking advantage of a very old and well known process, known as "lead-chamber" process (Wilfrid Wyld, 1924). Nitrogen oxides mainly act as a catalyst for the overall SO_x transformation to produce sulfuric acid, while NO_x gets absorbed and regenerated during the process until all the SO_x is consumed. At this point NO_x is converted to nitric acid and any unconverted NO_x comes out mainly with the product CO_2 stream. If mercury is present in the flue gas, it reacts with nitric acid producing mercuric nitrate and further NO_x (Shafeen et al., 2010).

Several reaction mechanisms have been proposed involving the lead-chamber reactions. However, a more plausible reaction mechanism proposed to be occurring in high pressure and low temperature systems, typical of the underlying $CanCO_2$ low-temperature gas separation process, is (White et al., 2008):

Reaction # 1: $2NO + O_2 = 2NO_2$

Reaction #. 2: $2 NO_2 = N_2O_4$

Reaction #. 3: $NO_2 + SO_2 + H_2O = NO + H_2SO_4$

Reaction # 4: $2 NO_2 + H_2O = HNO_2 + HNO_3$

Reaction #. 5: $3HNO_2 = HNO_3 + 2NO + H_2O$
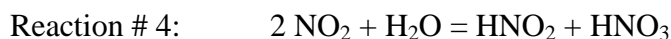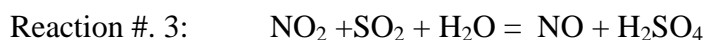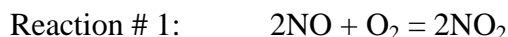
At low pressures, equation 1 is a slow reaction; however, at low temperatures and high pressures the rate of this reaction significantly increases, as it is known to have a third-order kinetics. The equilibrium of equation 2 is assumed to be always towards NO_2 formation as the system temperature always remains high after each stage of compression. The potential

energy difference between the NO_2 and N_2O_4 is very small and a slight heating up of the N_2O_4 should convert, at least theoretically, all the N_2O_4 generated during the compression process to NO_2. Nevertheless a very small quantity of N_2O_4 might always remain once the inter stage cooling is done.

Reaction # 3 is a fast reaction and is known as the lead-chamber process reaction for producing sulphuric acid. Reaction # 4 is a slow reaction and assumed to be occurring after all the SO_2 is consumed by reaction # 3. In order to have these reactions proceeding at a moderate rate to remove NO, NO_2 and SO_2 simultaneously, they require the presence of water vapor in the gas mixture; good vapour liquid interaction and adequate residence time within the $CanCO_2$ inter stage separator vessels.

On the other hand, if mercury is present in the flue gas, it will react with nitric acids in several ways, Two possible reaction mechanisms are:

Reaction # 6: $\quad\quad Hg + 4HNO_3 = 2NO_2 + 2H_2O + Hg(NO_3)_2$

Reaction # 7: $\quad\quad 6Hg + 8HNO_3 = 3Hg_2(NO_3)_2 + 2NO + 4H_2O$

Depending on the concentration of nitric acid in the condensate stream and residence time, in addition to mercuric nitrate or mercurous nitrate, also NO, or NO_2, or both can be formed. Mercuric nitrate, or mercury {II} nitrate [$Hg(NO_3)_2$], and mercurous nitrate, or mercury {1} nitrate [$Hg_2(NO_3)_2$], are both water soluble and are removed from the process with the condensate stream. The reactions in reactions 6 and 7 needs further investigation and are subject of ongoing research. Figure 2-6 shows a trailer mounted version of the $CanCO_2$ process which is currently in operation at CanmetENERGY since 2008. A detail process description of $CanCO_2$ is provided in Chapter 3.

Figure 2-6 Trailer mounted CanCO$_2$ unit at operation at CanmetENERGY, Ottawa

There are ample opportunities to increase the energy efficiency in an integrated oxy-fuel plant with CO$_2$ capture. This research work will focus on the ways and means to achieve that higher efficiency by improving the exergy efficiency of different unit operations and utilizing waste heat in the plant.

2.3 Irreversibility and exergy analysis

This section reviews the exergy (available useful energy) analysis of different unit operations in the overall plant. Exergy analysis identifies the exergy destruction points and the amount of exergy destruction rate due to irreversibilities in the process. This information is used to improve the efficiency of the overall plant, as it is well understood that the efficiency of the plant increases if the irreversilities are minimized. Exergy is also a measure of the departure of a system from the environment. Exergy can be defined as the maximum theoretical useful work potential of a system at a specified state. It does not represent an actual work delivered by a work producing device; rather it is a representation of the upper limit of the work that the device can deliver. So there will be always a difference between the exergy and the actual work delivered. This is because the final state of an exergy analysis is

22

always assumed to be the dead state which is never the case for an actual engineering system. Exergy is destroyed whenever an irreversible process occurs. It is important to recognise irreversibilities, evaluate their influence, and develop cost effective means for reducing them in an industrial system, which ultimately helps achieving profitable production rate, high heat transfer rates and high efficiency in all sections of the production unit. However irreversibilities are allowed to happen in some extent in all systems as it turns out to be very costly to minimize them. Hence, every system has some sorts of irreversibilities associated with them (Cengel et al., 2006; Bejan et al., 1988).

Exergy is also defined as a measure of departure of the state of the system from that of the environment. During an exergy analysis of a power plant, the thermodynamic imperfections can be quantified as exergy destruction. Based on the exergy destruction values, corrective measures could be suggested to improve the efficiency of the overall system. According to Dincer and Rosen (Dincer et al., 2007) some important characteristics of exergy are as follows, as quoted from the above reference:

• "A system in complete equilibrium with its environment does not have any exergy. No difference appears in temperature, pressure, concentration, etc. so there is no driving force for any process.

• The exergy of a system increases the more it deviates from the environment. For instance, a specified quantity of hot water has a higher exergy content during the winter than on a hot summer day. A block of ice carries little exergy in winter while it can have significant exergy in summer.

• When energy loses its quality, exergy is destroyed. Exergy is the part of energy which is useful and therefore has economic value and is worth managing carefully.

• Exergy by definition depends not just on the state of a system or flow, but also on the state of the environment.

• Exergy efficiencies are a measure of approach to ideality (or reversibility). This is not necessarily true for energy efficiencies, which are often misleading.

23

• Exergy can generally be considered a valuable resource. There are both energy or non-energy resources and exergy is observed to be a measure of value for both.

• Energy forms with high exergy contents are typically more valued and useful than energy forms with low exergy. Fossil fuels, for instance, have high energy and energy contents. Waste heat at near environmental condition, on the other hand, has little exergy, even though it may contain much energy, and thus is of limited value. Solar energy, which is thermal radiation at the temperature of the sun (approximately 5800 K), contains much energy and exergy.

• A concentrated mineral deposit 'contrasts' with the environment and thus has exergy. This contrast and exergy increase with the concentration of the mineral. When the mineral is mined the exergy content of the mineral is retained, and if it is enriched or purified the exergy content increases. A poor quality mineral deposit contains less exergy and can accordingly be utilized only through a larger input of external exergy. Today this substitution of exergy often comes from exergy forms such as coal and oil. When a concentrated mineral is dispersed the exergy content is decreased."

2.3.1 Exergy analysis for power plants

There are several papers available in open literature related to the exergy analysis of the different units of conventional power plants, but mainly concentrating the BOP section. However, only two exergy analysis, to the best of the author's knowledge, is published with respect to the integrated oxy-fuel power plant.

Fu and Gunderson (2013) evaluated an integrated oxy-coal plant configuration with exergy analysis. The exergy analysis was done for an oxy-combustion supercritical pulverized coal power plant with waste heat utilization. The overall integrated plant was modelled for a 792 MWgross fixed plant capacity. The thermal efficiency (on the basis of higher heating value) was calculated to be 39.8% (HHV) for an air fired power plant without CO_2 capture and 30.4% (HHV) for the oxy-combustion plant with CO_2 capture. The efficiency penalty was reported to be mainly caused by the ASU (cryogenic) and the CO_2 purification unit (CPU). The actual work for the ASU was reported as 0.230 kWh/kg O_2. The total efficiency penalty

was reported as 9.7% out of which ASU was 6.3% and the rest caused by the CPU. The actual work for CO_2 capture was reported as 0.114 kW/kg of CO_2 captured. The exergy destruction/loss reported for the combustion boiler including the BOP, ASU and CPU was 91.3%, 6.6% and 2.1% respectively. The exergy input by the coal was reported as 2211 MW. The largest exergy loss was reported in the boiler area which was 1158MW. The cooling water inlet/outlet temperature was used as 25/35°C and the sea water (used for cooling too) inlet/outlet temperature was used as 15/25°C. The waste heat integration was done by compression heat from the CPU with the steam cycle. The efficiency improvement of the overall plant by utilizing waste heat was reported as 0.72 percentage points.

Hagi et al. (2013) published an integrated oxy-pulverized coal plant configuration with exergy analysis. The integrated plant was modelled for a 1000 MWgross fixed plant capacity. The thermal efficiency (on the basis of lower heating value) was presented as 36.1% (LHV) for the improved plant where as the base plant's efficiency was 32.6%. The actual work for the ASU was reported as 0.220 kWh/kg O_2 and 0.201 kWh/kg O_2 for the base and improved models. The actual work for CO_2 capture was reported as 0.106 kW/kg of CO_2 0.0916 kW/kg of CO_2 for the base and improved model. ASU power consumption was 14.55% and CO2 processing unit power consumption was reported as 8.9% of the gross power for the improved model. The total energy efficiency penalty was reported as 11.4% and 7.9% for the base and improved model compared to a reference air fired plant with an efficiency of 44%. The steam cycle condition was 300 bar/600°C/620°C and the reheat steam pressure was 60 bars. The exergy input by the coal was reported as 2275 MW. The largest exergy loss was reported in the boiler area which was 1119MW. The cooling water inlet temperature was used as 18.2°C. This paper mainly suggested a few scattered improvements in the plant but no global plant wide integration potential and optimization approach was carried out which was specified in the paper. The scattered improvements proposed here were also based on heuristic rules. There was no detail exergy analysis provided in the paper.

The following publications deal with exergy analysis for individual sections of conventional power plants. A few publications are also available related to the exergy analysis of the ASU. However, the boiler and flue gas sections in these cases are for

conventional air fired boilers and not an oxy-fuel boiler. Most of these studies considered the boiler and flue gas section as a single control volume and detailed description and analysis for the steam cycle were provided.

Islam H. Aljundi (2009) studied an exergy analysis on the steam cycle of an existing 396 MW power plant. The boiler system was reported to have the maximum exergy destruction percentage which was 77%. The exergy destruction percentage for the turbine system was reported as 13%. The exergy efficiency of the power cycle was reported as 25%. A sensitivity analysis was presented with respect to the exergy analysis with the various reference environment temperatures. The increase in dead state temperature increases exergy destruction and hence reduces the efficiency.

Modesto et al. (2009) presented an exergy analysis of an actual power generation system using blast furnace and coke oven gas from an existing steel mill. The maximum exergy destruction was reported for the boiler which accounted for more than 75%. Plant improvement measures were incorporated based on exergy analysis resulting in a 3% increase in global efficiency.

Yilmazoglu et al. (2011) performed an exergy analysis of a 373MW combined cycle power plant and did a sensitivity analysis. The net exergy efficiency was reports as 50.11%. The maximum exergy destruction was calculated in the combustion chamber which was 77.39%. They also reported improvement of the exergy efficiency with the increase in ambient temperature up to the dead state temperature (25°C); however this relationship is inversed with further increase in temperature beyond the dead state. A detailed sensitivity analysis with respect to various process parameters and their effect on the exergy analysis was reported in this paper.

Sengupta et al. (2007) evaluated an exergy analysis of an existing 210 MW coal-based thermal power plant with design data and different operating conditions. The entire plant was divided in to three control volumes for the analysis. It was reported that the boiler causes the maximum exergy destruction amounting almost 60%. Different load variations such as 100%, 75%, 60% and 40% were considered. In all loads the boiler exergy destruction

26

remained constant at 60%. Effect of two different condenser pressures, i. e. 76 and 89 mmHg (abs), on steam cycle exergy efficiency was analysed. The lower pressure resulted in a higher exergy efficiency.

Ameri et al. (2008) presented an exergy analysis of a 420 MW combined cycle power plant. The analysis was done on the boiler and steam cycle. Most of the exergy destruction, approximately 83%, was reported for the boiler section including the combustion chamber, gas turbine, duct burner and the heat recovery steam generator. The exergy efficiency of the combined cycle power plant was reported as 44~47%.

Saidur et al. (2010) studied the exergy and economic analysis of industrial boilers. This is a theoretical study and no specific plant was considered. In this study the boiler was identified as the major source of exergy loss and the exergy efficiency for the boiler was reported as 24.89%. An energy analysis was also performed for the overall plant.

Ganapathy et al. (2009) performed an exergy analysis on an existing 50 MWe plant. The overall plant was divided into three control volumes for the analysis. This study indicated an exergy loss of 57% in the boiler section. Exergy efficiency of individual feed water heaters was also reported. The exergy loss was indicated due to the irreversibility inherent in the combustion process, heat loss, incomplete combustion, and exhaust losses. The exergy efficiency of the overall plant was reported as 27%.

In general there are different papers in the open literature that discusses exergy analysis of conventional steam cycles with the boiler/combustion chamber including in the overall analysis. Most of these analyses combined the turbine section in one control volume and the combustion chamber in a different control volume and performed the analysis. Moreover, all these analysis reported a wide range of exergy efficiency numbers and destruction rate for the control volumes under study. The reason for this variation is the different operating temperature and pressure conditions of the plants unique to each study. There are almost no literatures, to the best of the author's knowledge, available for the exergy analysis of the CO_2 capture and compression section. As CO_2 capture is considered to be a new concept with

respect to the current emission concern, hence exergy investigation for these process are scarce or not available at this time.

2.3.2 Exergy analysis for ASU

Fu and Gunderson (2012) performed an exergy analysis on a low pressure (1.20 bar) and low purity (95% mol) double column ASU which was part of an oxy-fuel combustion power generation system. The air compression section and the distillation system were considered to be the largest contributors to the exergy losses: 38.4% and 28.2% respectively. This study also indicated that the exergy losses in the air compression and the distillation section can be reduced by 17.2% and 14.7% respectively, if an intermediate reboiler is placed in the low pressure column.

Cornelissen and Hirs (1998) did a study on the exergy analysis of a high purity (99.6% mol) ASU having a low (3 bar) and a high pressure (6 bar) distillation column. Nitrogen was pressurised to 46 bar and liquid nitrogen purity was reported to be 99.99 mol%. The maximum exergy loss was reported for the compressor section (31%). Exergy loss in the distillation section was calculated to be only 9%. However, the high pressure liquefaction unit shared the maximum exergy loss of 55%. The main heat exchangers had very minimum exergy loss (3.8%).

Van der Ham, L. (2011) in his PhD dissertation investigated the efficiency improvement measures of an ASU for an integrated gasification combined cycle (IGCC) unit. This research was carried out at the Norwegian University of Science and Technology (NTNU-Trondheim) and the research title was "Improving the Second law efficiency of a cryogenic air separation unit". This study presented the exergy analysis results of a two and a three-column design of cryogenic ASU. Both designs used the same feed and the product specifications were also the same. The three-column design was identified to be better than the two-column design. Most of the exergy destruction was located in feed pre-processing including compression section and the inter-stage coolers. The exergy destruction percentage reported for the feed pre-processing section was 47.1% and 54.1% for the two column and three column designs respectively. The waste heat from the compressor inter-stage coolers

was proposed to be used elsewhere in the IGCC plant and improve the overall plant efficiency. The exergy destruction percentage for the distillation column sections for the two and three column designs were reported as 26.5% and 20.8% respectively.

There are several other papers available in the public domain related to the exergy analysis of the boiler and steam cycles. However, these are only a few that have been mentioned here. These papers were selected mainly because of their relevance with the power generation systems and their reporting of various exergy efficiency and exergy destruction numbers for conventional unit operations used in power plants. A summary of these papers is presented in Table 2-1.

Table 2-1 Summary performance data of exergy analysis of boiler, steam cycle and ASU

Source	Process Type	Exergy Destruction						
		Combustion and Steam Cycle		ASU		CO_2 Capture	Exergy Efficiency	Thermal Efficiency Improvement
Journal Paper		Boiler (%)	BOP (%)	Compressoion (%)	Distillation (%)	(%)	(%)	(%)
Fu and Gunderson (2013, 2012)	Oxy-combustion	85.4		6.3		2.1		0.72
Islam H. Aljundi (2009)	Air Combustion	77	13				25	
Modesto et al. (2009)	Air Combustion	75						3
Yilmazoglu et al. (2011)	Air Combustion	77.4					50.1	
Sengupta et al. (2007)	Air Combustion	60						
Ameri et al. (2008)	Air Combustion	83					44% - 47%	
Saidur et al. (2010)	Air Combustion						24.9	
Ganapathy et al. (2009)	Air Combustion	57	15.4				27	
Fu and Gunderson (2012)	ASU			38.4	28.2			
Cornelissen and Hirs (1998)	ASU			31	9			
Van der Ham, L. (2011)	ASU			47.1% - 54.1	20.8% - 26.5%			

Acir et al., (2012) in their study on the impact of various dead state temperatures on the energy and exergy efficiency of the thermal power plants presented a comprehensive

collection of exergy efficiency data reported by various authors. Table 2-2 shows the collection of these results.

Table 2-2 Exergy efficiency of different thermal power plants (Acir et al., 2012)

Power plants	Capacity/MW	Per cent exergy destruction		Exergy efficiency η_{II}/%		
		Boiler	Turbine	Boiler	Turbine	Overall
Çayırhan, Turkey (this study)	160	58·05	5·68	41·95	83·40	33·48
Neyveli, India[11]	50	57·35	…	41·72	81·2	26·95
Kostolac, Serbia[12]	348·5	88·2	9·5	46·4	86·8	35·80
Uniten, Malaysia[13]	120	71·45	14·14	55·43	85	…
NGS, Canada[21]	500	…	…	49·51	…	35·81
Chennai, India[22]	32	86·76	7·60	…	…	25·39
Zarqa, Jordan[24]	396	76·75	12·99	43·8	73·5	24·80
Hamedan, Iran[26]	250	…	…	53	92·25	36·80
Beijing, China[28]	300	91·98	2·09	48·55	92·71	44·07
Xiaolongtan, China[29]	300	67·78	18·54	…	…	51·88

Chapter 3

Process Simulation and Model Development

This chapter deals with the process simulation and model development for the base process of an oxy-fuel power plant that includes four separate section models (Boiler, BOP, ASU and CO_2CCU) integrated in a single process flow sheet. An improved version of the same model is presented in chapter 5 after implementing all the necessary process improvement measures as identified by the exergy analysis in chapter 4. The model was developed in detail in a state-of-the-art process simulation software package named Aspen HYSYS. Peng-Robinson (PR) equation of state and ASME steam property packages were used to develop the model. A systematic approach was undertaken to develop the base and improved integrated process models which is presented here. Process descriptions and model details including process model automation features are also included in this chapter.

3.1 Model development approach

The process simulation and model development were carried out in a systematic approach following five major stages as shown in Figure 3-1. These include: model formulation, problem definition, problem evaluation, decision making and sensitivity analysis. These steps were followed in sequence to complete the overall task.
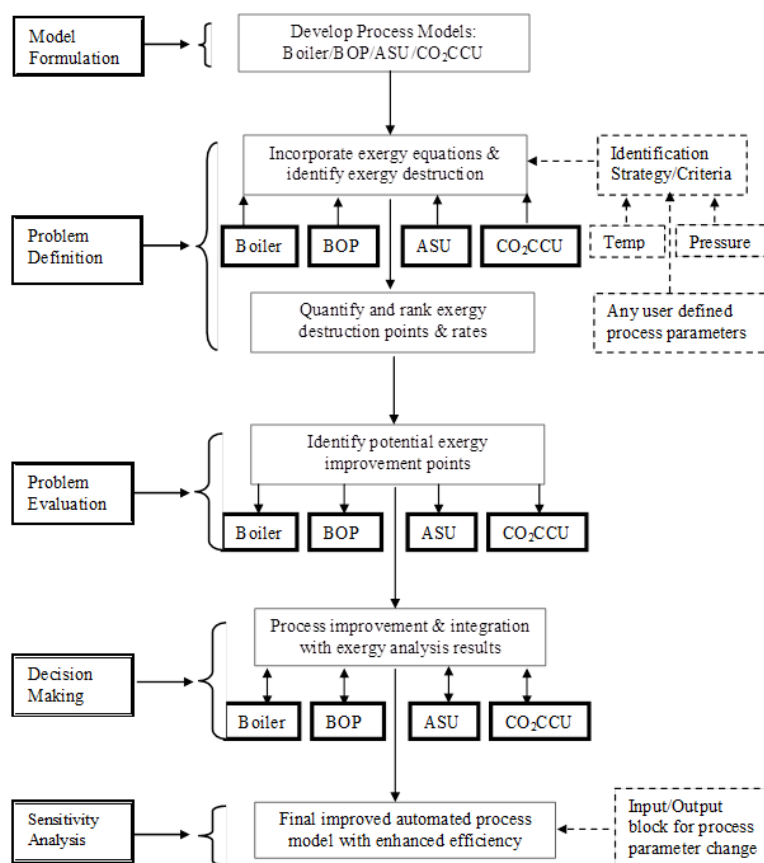
Figure 3-1 Process simulation and model development approach

3.1.1 Model formulation

The major activities in this step included the development of separate process models for the four major sections in Aspen HYSYS and combine the models to develop the base model for the integrated oxy-fuel power generation system with CO_2 capture. The models of these four sections are independent and developed separately in separate process flow sheets (so-called sub flow sheets, a terminology used in HYSYS) and then combined into a single integrated flow sheet. The HYSYS process flow diagrams are presented in Figures 3-7 to 3-10. In this step the process models were also verified for their accuracy compared to the published data in available literature. The model verification was done for the BOP and ASU as these two models were incorporated from published reports (IEA, 2005; DOE, 2008).

The system was modelled in a unique way such that it can accept changes in the major process parameters within a wide range without having any model convergence issues. An input/output block, which is a spreadsheet calculation block, was created where all the user input parameters can be set and subsequently updated results are generated automatically. As an example, a single change in exergy reference temperature in the input/output block will generate a new set of exergy analysis data for the overall plant. Similarly several other parameters can be changed in this block. Details of the process automation measures are discussed later.

3.1.2 Problem definition

The problem definition step included the incorporation of exergy analysis equations in the model and perform the exergy analysis. In most of the cases all the major unit operations were selected as individual control volumes for exergy calculation. However in few instances a combination of multiple unit operations were considered as a single control volume. An example of this is the compressors in ASU and CO_2CCU section where interstage separators are included in a single control volume with the respective compressors. This was necessary as the interstage separators are considered as an integral part of a compressor section.The exergy analysis was carried out for the major components in each section of the integrated plant. This was done to determine the exergy destruction rate and accordingly process improvement measures were incorporated. At this stage all the major exergy destruction point sources within the integrated plant were identified and ranked based on the exergy efficiency. A few process parameters (pressure, temperature, enthalpy, entropy and flow rates) were used to perform the exergy calculation for the different unit operations and control volumes.

3.1.3 Problem evaluation

This step dealt with the evaluation of a few potential exergy destruction point sources for their efficiency improvement opportunities. The potential exergy destruction point sources were selected based on their ranking in previous step and appropriate improvement measures were investigated and proposed. These improvement measures were based on sound

33

engineering judgement and process improvement approaches generally practiced in industries. The focus of the improvement method was to utilize the waste heat through cooling water loop and reduce the temperature difference (in/out) in the targeted exchangers or the control volumes.

3.1.4 Decision making

In this step the potential exergy destruction point sources which were already evaluated for their efficiency improvement were further integrated in the overall oxy-fuel model by design changes in the process flow sheet. The design changes were made according to the process requirement and finally an improved oxy-fuel power generation system model was developed and presented in Chapter 5. The HYSYS process flow diagrams for the improved process are also included in Chapter 5.

Finally, a sensitivity analysis with respect to a few parameter changes was done. The sensitivity analysis was made easy in this process model as a single change in the parameter values generates an updated set of data in the model. A few examples of these process parameters include: fuel composition, O_2 purity (ASU), CO_2 capture efficiency, flue gas exhaust (boiler)/inlet to CO_2CCU temperature, change in environmental reference state etc. The model was built so that additional user defined process parameters could be included in the input/output block for more sensitivity analysis. After completing all these steps, an improved and efficient oxy-fuel model was developed.

3.2 Process description

A brief process description of the oxy-fuel power plant is given in the following section. The overall plant was classified into four separate areas based on the four sections (BOP, Boiler, ASU and CO_2CCU). This is done in order to group together the process streams of each section and have distinct stream numbers. The areas are as follows:

- Area 000: BOP section
- Area 100: CO_2CCU section
- Area 200: Boiler and flue gas section

- Area 300: ASU Section

3.2.1 Oxy-fuel boiler and flue gas section

The model of the oxy-fuel boiler and flue gas section was developed for a capacity of 786 MWgross. This plant capacity was chosen as it resembles a standard single unit utility boiler and also sufficient data are available in the open literature for a representative similar size of existing conventional air fired power plant (DOE, 2008). The process model for the boiler and flue gas section was developed based on the author's experience from an existing pilot scale oxy-fuel combustion boiler (0.3 MWt) at CanmetENERGY in Ottawa and based on available literature in the public domain, as there is currently no commercial unit available. The combustion boiler and flue gas section was modelled based on the required heat input to the BOP to generate 786 MWgross electricity. A simplified process flow diagram is presented in Figure 3-2 for the boiler and flue gas section. In this process description the nomenclature of the fans and preheaters are kept as conventional names (e.g. Air fans or Air preheaters), though recycle flue gas, instead of Air, is being used in the process as primary and secondary "air". This is done to avoid introducing new nomenclature for the already existing conventional equipment names in industrial practice. In the combustion boiler pulverized coal is carried by the recycle flue gas (238), and in presence of nearly pure oxygen (204) combustion takes place. Nearly pure oxygen from ASU is fed to the boiler by premixing with the primary and secondary recycle flue gas. The ratio of oxygen premix with the primary and secondary depends on the actual burner design, O_2 concentration in the primary and secondary line, and the overall amount of oxygen needed into the system. However in this particular simulation all the required O_2 is directly mixed with the primary and secondary line (235, 238) which made the O_2 concentration in these lines about 31% (mole). The maximum O_2 concentration, with respect to fire, safety and material compatibility, should not exceed 40% to avoid the need to specify pure oxygen construction materials standards for ducting (IEA, 2005; NFPA, 2014, ASTM 2014a; ASTM 2014b). A 30% (mole) or lower is more desirable to avoid drastic change in existing boiler design (IEA, 2005). In order to maintain optimum O_2 concentration in the lines, alternate arrangement of

O_2 feed will be made in an actual plant design. The excess O_2 in the boiler exit flue gas (213) was maintained at around 3% (mole) in wet basis.
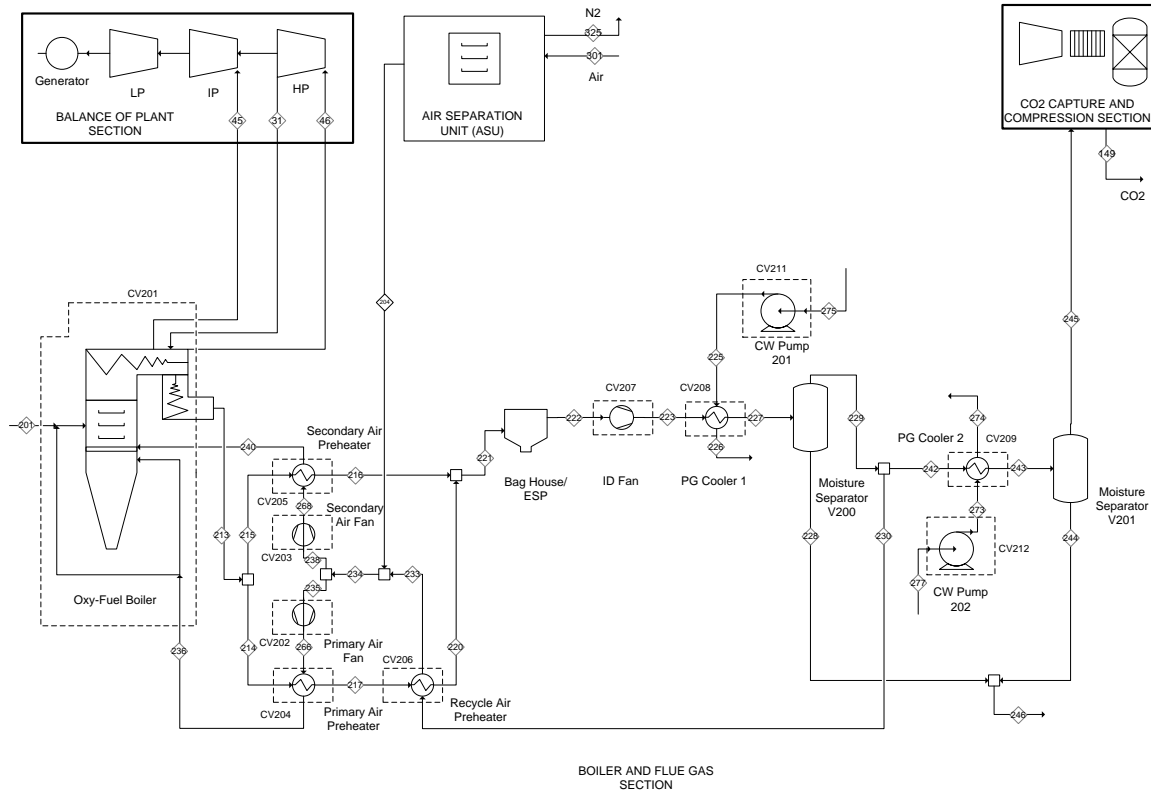
Figure 3-2 Process flow diagram for Boiler and Flue Gas Section

In this plant configuration, the exit gas from the boiler (213) splits into two streams (214, 215) and pass through primary and secondary air pre-heaters after giving up heat, to the incoming recycle flue gas, and cooled down to 210°C and 169°C respectively (217 and 216). Stream 217 is further cooled down to 187°C via recycle air preheater where it pre heats the recycle flue gas (230) to 78°C (233) and thus bring its temperature above saturation point. This is necessary to avoid saturation point inside the fan blades of the primary and secondary air fans. Finally the split gases (216, 220) combines together (221) and goes to the bag house at 178°C. Subsequently the flue gas passes through the ID fan, a process gas cooler (PG Cooler 1) and a moisture separator. A part of the relatively dry process gas from the moisture

separator is recycled back to the combustor as stream 230 at 57°C. The recycle stream (230) first passes through recycle air preheater and split into two streams as primary (235) and secondary stream (238). The primary and secondary streams pass through primary and secondary fans and air preheaters before entering the combustor. The temperatures at the outlet (236, 240) of these two heaters are maintained at 355°C. The temperature limit for primary recycle is determined by the coal feed mill temperature limitations as the primary recycle is used as the coal carrier to the boiler. The overall recycle ratio (ratio of 230/229) is maintained around 0.65 to moderate the boiler temperature to maintain the adiabatic flame temperature inside the boiler around 1750 °C. The recycle ratio could be varied as needed to moderate the flame temperature for complete combustion and maintain enough primary and secondary recycle flow for the process. The part of the flue gas which is not recycled (242) passes through a second process gas cooler (PG Cooler 2) to cool down to 50°C, then enters a moisture separator and finally goes (245) to the CO_2 capture and compression unit (CO_2CCU) for further processing.

The leak air into the boiler and the flue gas section is maintained at 0.0175 kg air/ kg of the flue gas which is well within the acceptable range (0.01~0.02 kg air/kg flue gas) for the combustion boilers (IEA, 2005). This process design does not include a flue gas desulfurization (FGD) unit as the fuel coal used in the model contains less than < 1% of sulfur. A higher percentage of sulfur content (>1%) in coal will require a FGD unit included in the system (DOE, 2008). In general SO_x removal is necessary to avoid corrosion in the downstream piping structure, in the CO_2 capture unit and building up of sulfur content in the recycle loop. As no FGD is used, the combination of PG cooler 1 and the moisture separator removes SOx from the flue gas in these systems. Figure 3-2 also shows the integration of all the subsections of the oxy-fuel power generation system.

For exergy analysis the flue gas section is divided into eleven control volumes and those are represented as dotted line in Figure 3-2. The control volumes for the boiler and the BOP are listed in Table 3-1. The exergy analysis is described in details in chapter-4.

Table 3-1 List of control volumes in Boiler and BOP section used in exergy analysis

Boiler Section		BOP Section	
Control Volume (CV) Name	CV Number	Control Volume (CV) Name	CV Number
Boiler	CV201	Turbine Section	CV01
Primary Air Fan (PAF)	CV202	Feed Water Heater 1	FWH1
Secondary Air Fan (SAF)	CV203	Feed Water Heater 2	FWH2
Primary Air Preheater (PAPH)	CV204	Feed Water Heater 3	FWH3
Secondary Air Preheater (SAPH)	CV205	Feed Water Heater 4	FWH4
Recycle Air Preheater (RAPH)	CV206	Deaerator	Deaerator
ID Fan	CV207	Feed Water Heater 6	FWH6
PG Cooler 1	CV208	Feed Water Heater 7	FWH7
PG Cooler 2	CV209	Feed Water Heater 8	FWH8
CW Pump 201	CV211	BFW Pump	P001
CW Pump 202	CV212	CW Pump	P002
		Condensate Pump	P003
		Condenser	Condenser

3.2.2 Balance of Plant (BOP) section:

The BOP model was developed based on the process parameters and model layout published by DOE for a 786 MWgross oxy-fuel power plant (DOE, 2008). The single reheat BOP steam cycle condition is 242 bar/593°C/622°CRankine cycle. The main steam temperature is 593°Cand the reheat steam temperature here is 622°C. This layout design consists of seven feed water heaters (FWH), a deaerator, steam condenser, pumps and turbine section. Details of the BOP plant layout are presented in Figure 3-3. In this plant configuration boiler feed water (1) from condensate pump (P003) discharge at 39°Cand 17.5 bar initially passes through four feed water heaters (FWH 1-4) before entering the deaerator. The boiler feed water from the deaerator is further pressurized to 289.6 bar by the BFW pump (P001) and passed through three additional heaters (FWH 6-8) before entering the boiler at 292°Cand 289 bar (HTS12). The boiler feed water is pre-heated in the FWHs by the extraction steam taken from different stages of the turbine. The extraction steam streams used for the preheating are 21, 22, 23, 25, 26, 27, 28, 29, 30, and 34, as shown in Figure 3-3. The main steam (46) generated from the boiler enters the high pressure turbine (HP) turbine at 593°C

and 242 bar at supercritical state. The cold reheat steam (31), which is the exhaust from HP turbine section, goes back to the boiler/economizer and gets reheated. The hot reheat steam (45) then enters the intermediate pressure turbine (IP) at 622°Cand 45 bar. The exhaust from the IP turbine enters the low pressure turbine (LP) at 386°Cand 9.5 bar. A portion of the IP exhaust steam is used to drive the boiler feed pump (BFW) turbine drive. Finally the exhaust from the LP (36), BFW pump turbine drive (37), make up (38) and all the seal and gland steam condensate (35) enters the condenser and recycled back again as boiler feed water (1) to the condensate pump (P003) suction in the closed loop system shown in Figure 3-3.
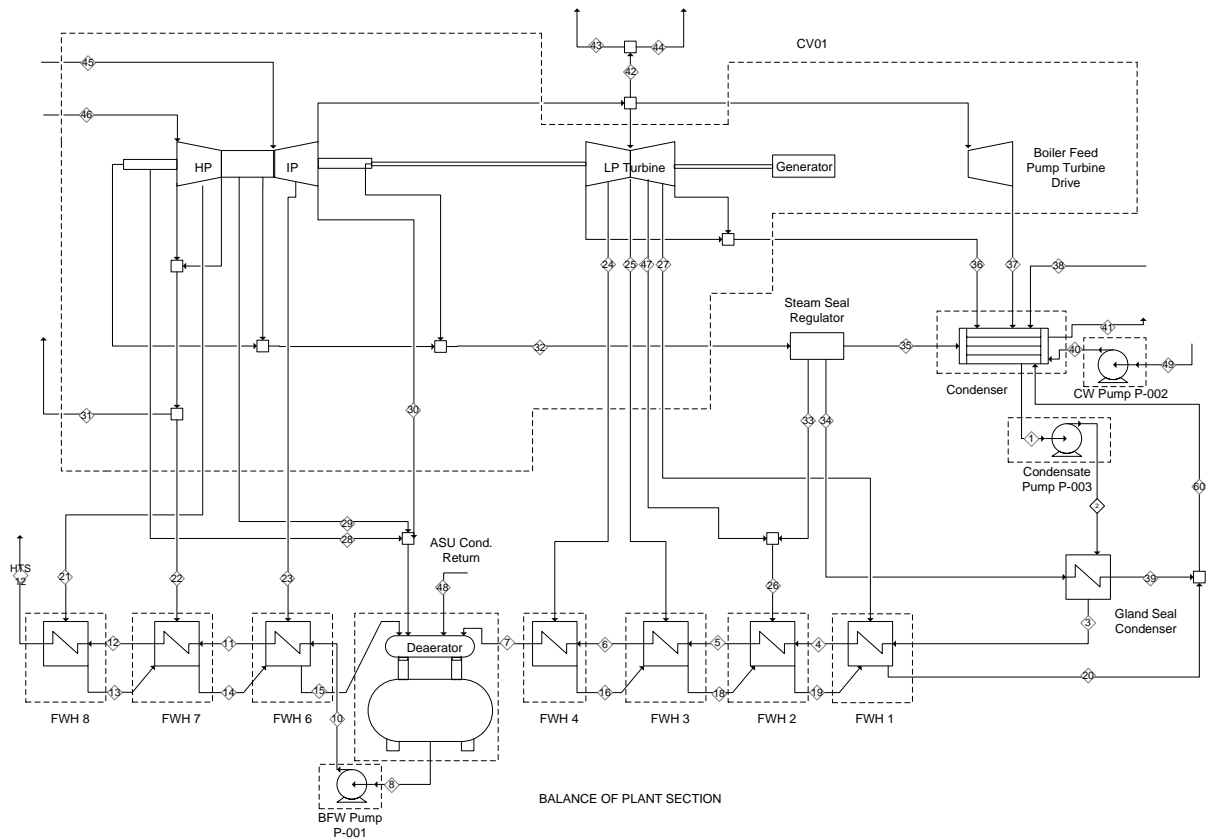
Figure 3-3 Process flow diagram for the Balance of Plant Section (BOP)

The dotted line in the figure represents control volumes used for the exergy calculation. There are, in total thirteen control volumes in the BOP section. The turbine section was kept as a single control volume (CV01). The other unit operations were considered as individual

control volumes. All these control volumes are listed in Table 3-1. In most cases the nomenclature for the control volumes and the unit operations were kept the same in the BOP section except the turbine.

3.2.3 Air Separation Unit (ASU) section:

The ASU model was developed based on the process parameters and model layout published by the International Energy Agency (IEA, 2005). Figure 3-4 shows a representative model of the ASU as proposed in IEA report.
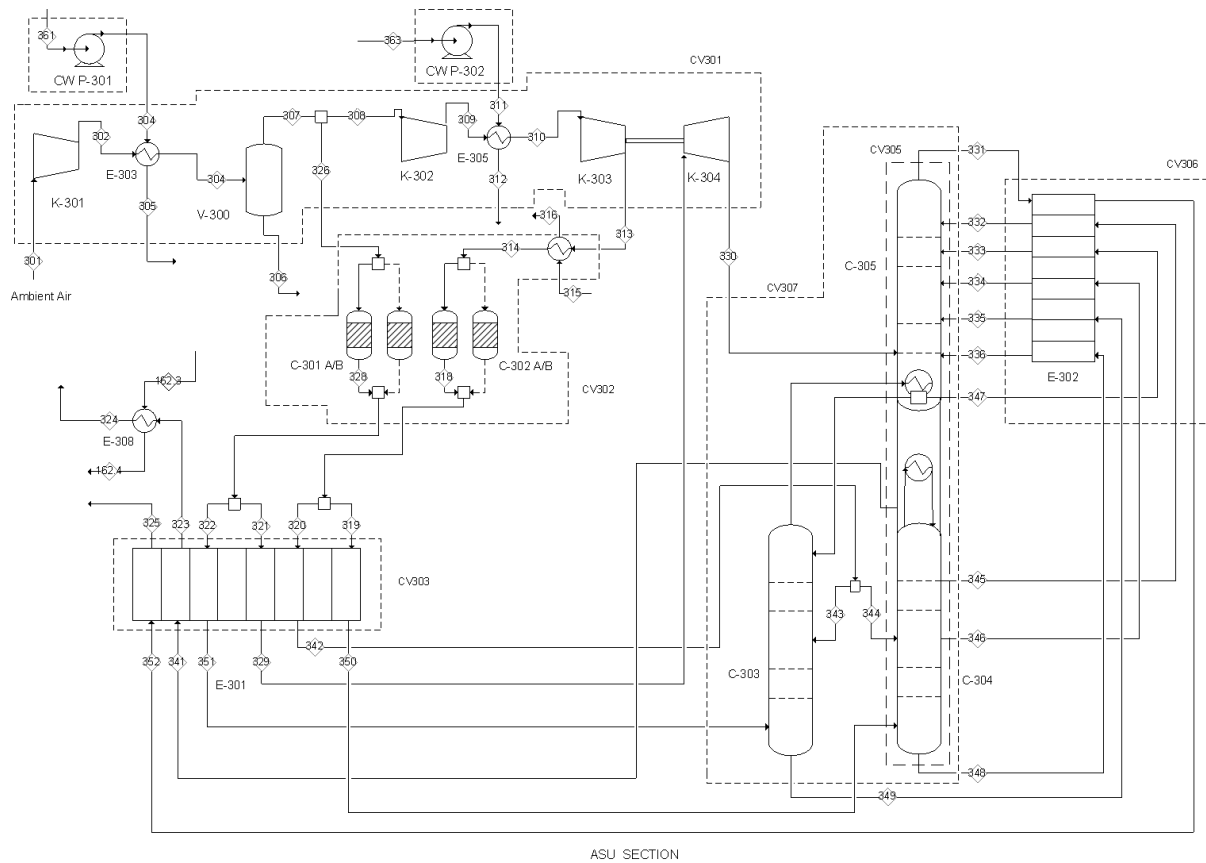
Figure 3-4 Process flow diagram for the Air Separation Unit (ASU)

In the ASU process configuration a standard double column (C304 & C305) along with an additional third column (C303) was modelled. A combination of high (5 bar), low (1.4 bar) and intermediate pressure (3 bar) was maintained in C304, C305, and C303 distillation

columns respectively. As stated in the IEA document this specific design, consisting of three columns, minimizes the air compression and reduces the power demand for the ASU. In this plant configuration the major components include a compression module (K301, K302 and K303), an adsorption front end air purification system (dryers C301A/B and 302A/B), and cold box containing the columns and heat exchanger equipment (C303, C304, C305, E301 and E302).

Ambient air (301) is initially compressed to 3 bar and passed through a moisture separator (V300). Part of the exhaust stream (326) from the moisture separator goes to the dryer (301A/B) and exchanger E301 and finally enters the intermediate pressure column (C303) and expander (K304) as stream 351 and 329 respectively. The rest of the exhaust stream (308) from V300 is compressed further to 5 bar and passed through dryer (302A/B) and exchanger E301 and finally enters the intermediate and high pressure columns (C303 and C 304) as process streams 343, 344 and 350. All these process streams are integrated in a complex flow path as shown in the Figure 3-4. Finally a nearly pure (~95% mol) oxygen stream (324) is produced and fed to the boiler. A highly pure (~98% mol) N_2 stream (325) is also generated as a by-product and released to atmosphere. This N_2 stream can be used for different purpose e.g. coal drying, plant utilities or could be sold separately as a by-product.

Table 3-2 List of control volumes in ASU and CO₂CCU section used in exergy analysis

ASU Section		CO₂CCU Section	
Control Volume (CV) Name	CV Number	Control Volume (CV) Name	CV Number
Compressor Section	CV301	MP Compressor	CV101
Dryer Section (C301A/B, 302A/B)	CV302	HP Compressor	CV102
LNG Exchanger (E301)	CV303	MP Expander	CV103
Columns (C304 &305)	CV305	Pump P101	CV104
LNG Exchanger (E302)	CV306	Expander K106	CV105
Columns (C303, C304 & 305)	CV307	LNG Exchanger 101	CV106
Cooling Water Pump (CWP301)	CWP301	LNG Exchanger 102	CV107
Cooling Water Pump (CWP302)	CWP302		

The dotted line in Figure 3-4 represents the control volumes used for exergy calculation. There are in total eight control volumes in the ASU section. All the control volumes for the ASU and CO_2CCU section are listed in Table 3-2.

3.2.4 CO_2 Capture and Compression Unit (CO_2CCU) section

The novel CO_2 capture and compression unit model is successfully being demonstrated at a pilot-scale level as a standalone trailer mounted CO_2 capture unit located at CanmetENERGY in Ottawa. It is currently being extensively used to generate valuable data for CO_2 capture from oxy-fuel combustion systems. Details of this unit can be found in different publications (Shafeen et al., 2010; Zanganeh et al., 2010, 2009a, 2009b; 2008a, 2008b, 2008c; 2006). A simplified diagram is show here in Figure 3-5. The boiler exit flue gas stream (101) enters at 1bar and 50°Cinto the multi stage compression, intercooling and separation section where it is finally compressed and cooled (112) to approximately 30 bar and 35°C. The pressurized stream 112 then passes through a dryer (C101) and heat exchanger E111 before entering the flash separator (V104) as stream 117. The dryer brings down the dew point temperature of the process gas to approximately -70°C. The gaseous stream (119) from V104 is split into two streams (121, 132). One of the split streams (121) is expanded (15 bar) and flashed through expander (K106) and flash separator V106. The separated gas (123) from V106 is recycled back to an intermediate stage of the compressor. This expansion of the process gas supplies the cooling effect to the exchanger E111. The other split gas stream (132) passes through exchanger E112 and enters the flash separator V105. The gaseous stream (134) from V105, mainly impurities, passes through exchangers E112 and E111 and comes out at 29 bar and 7°C as stream 137. Stream 137 is preheated to 300°Cthrough heaters E106 and E107 and finally released to the atmosphere at 1 bar and 21°C (140) after an expansion through the expander K107. The liquid streams (120 & 125) from V104 and V106 are combined together and throttled (127) to 19 bar to supply cooling effect to E111 before entering K105 as gaseous CO_2 product stream (128) for compression. The liquid stream (135) from V105 is also throttled (142) to 10 bar to supply cooling effect to E112 and E111 respectively and then enters K104 as gaseous CO_2 product stream (144)

for compression to a pressure of 19 bar (145). The CO_2 product streams 128 and 145 then combined together and compressed to a higher pressure (110 bar, 43°C) for pipeline transportation (149).
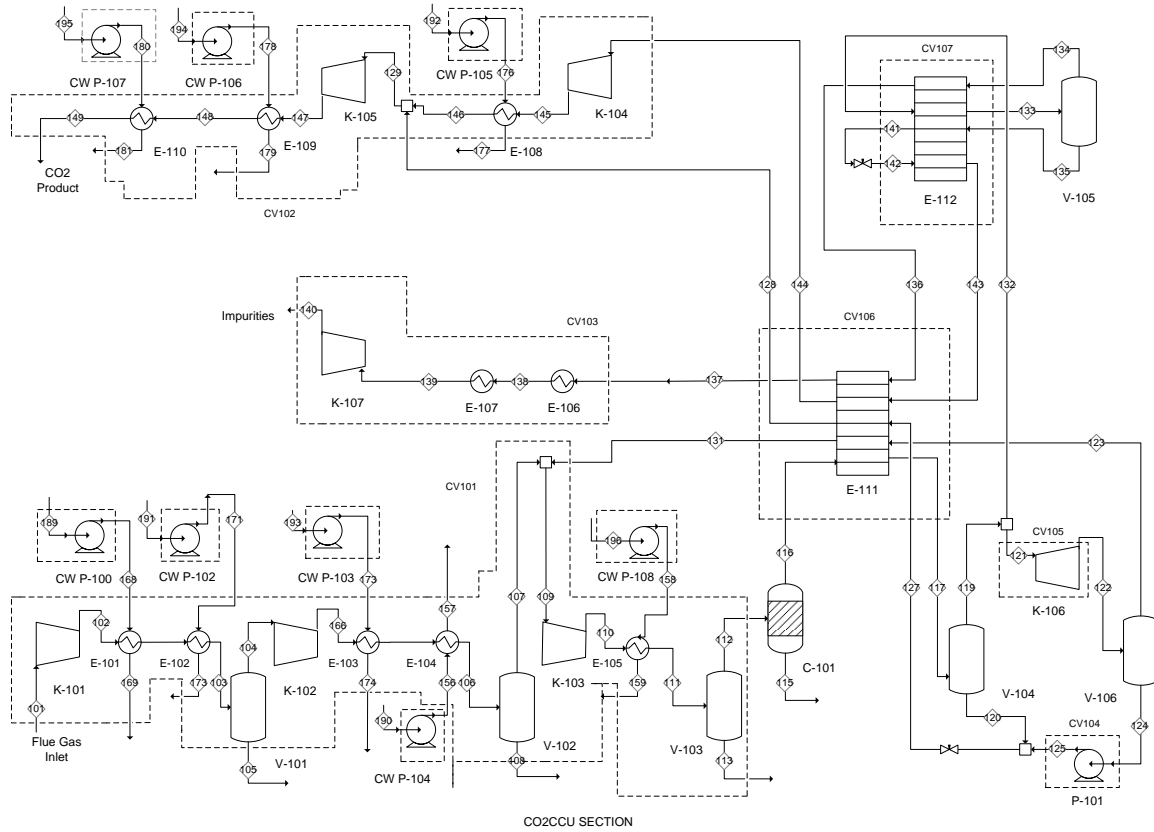
Figure 3-5 Process flow diagram for CO_2 Capture and Compression Unit (CO_2CCU)

In between all the compression stages throughout the process there are intercoolers and flash separators to keep the temperature and moisture content of the process gas to an acceptable range as a design requirement.

The dotted lines in Figure 3-5 represent the control volume identified for the exergy calculation. There are in total fifteen control volumes in the CO_2CCU section and eight of them are for cooling water pumps. The exergy variations for the eight cooling water pumps (CW P-100, 102, 103, 104, 105, 106, 107, 108) were insignificant as the adiabatic efficiency (default value at 75% in HYSYS) and the inlet/outlet cooling water temperatures were kept

constant for the pumps. The remaining seven control volumes that are used for exergy calculation in the CO_2CCU section are presented in Table 3-2.

3.3 Steady State Process Model Development

The overall model was developed in the AspenHYSYS process simulation software package. It is an integrated model consisting of four major sections as stated earlier, i.e. the boiler and flue gas section, BOP, ASU and CO_2CCU. These four sections are independent models developed separately in separate process flow sheets (so-called sub flow sheets) and then combined into a single integrated flow sheet. A snapshot of the integrated base process model is presented in Figure 3-6. In this figure each individual sub flow sheets (ASU, Boiler, CO_2CCU and BOP) contains a detailed process diagram of the respective sections which are graphically presented in Figures 3-2, 3-3, 3-4 and 3-5. An improved version of the base model, after incorporating all the exergy analysis results, is presented in chapter 5. The actual HYSYS process flow diagrams are presented in Figures 3-7, 3-8, 3-9 and 3-10. Figure 3-6 also points out the input/output block and the fuel chemical exergy calculation block.
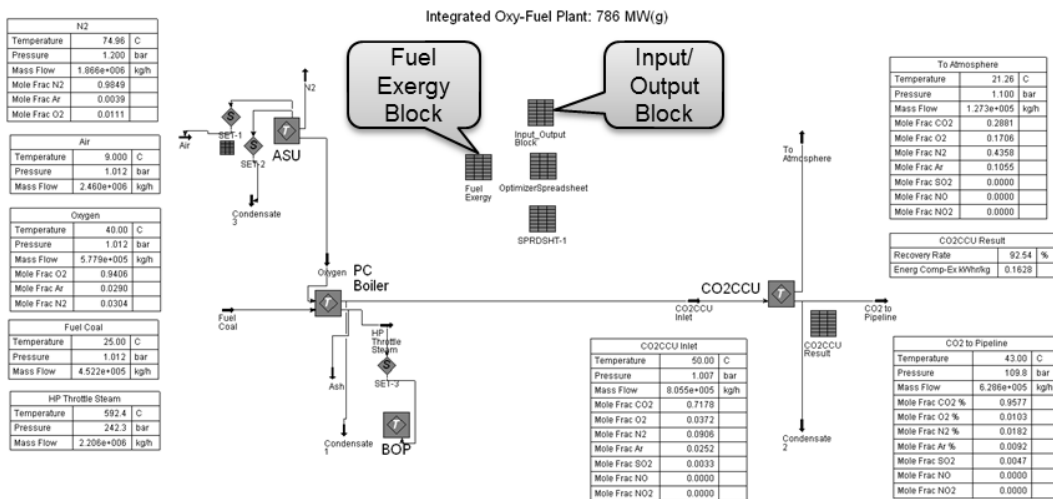

Figure 3-6 Snapshot of integrated oxy-fuel combustion power plant in HYSYS

It can be noted in Figure 3-6 that the ASU is connected to the PC boiler by the O_2 feed line. The BOP is connected by the main steam generation line from the boiler to the BOP. The

CO_2 capture unit (CO_2CCU) is connected by the flue gas line from the combustion boiler to the CO_2CCU. All these interconnections make this process model an integrated oxy-fuel power generation system model.

3.3.1 Model development methodology

Three major steps have been followed while developing the integrated process model. The first step was the development of four individual process models which were later combined to form the integrated base model (Figure 3-6). The second step was to develop the exergy analysis tool which was incorporated directly into the flow sheet model. The exergy analysis tool was developed as an automated tool. It is automated in the context that a single change in exergy reference temperature will recalculate the exergy in the overall process and generate a new set of data. The third step was to incorporate the improvement measures into the base model and develop the improved model as presented in Chapter 5. Figure 3-1 displayed a graphical representation of this approach.

3.3.2 Input parameters and model assumptions

There are several input parameters for the process model. As noted earlier the input/output block is the only place where all the user input process parameters can be changed. One of the main input parameters to the model is coal composition. Numerous types of coal can be used in this model, and accordingly chemical exergy of the fuel is calculated automatically. The coal type used in this particular study is a lignite coal which has high moisture content. A typical coal analysis data used for this study is presented in Table 3-3. A different type of coal or any other fuel can easily be incorporated in the model as it requires only the fuel composition input to the model. The other input parameters and various process modelling assumptions that were used for developing the integrated model are presented in Table 3-4. Only the major parameters are listed in this table.

Table 3-3 Lignite coal analysis data used for the process model

Proximate Analysis		Ultimate Analysis	
Component	Weight %	Component	weight %
Moisture	33.54	Moisture	33.54
Volatile Matter	24.39	Carbon	39.58
Fixed Carbon	28.61	Hydrogen	2.57
Ash	13.46	Sulfur*	0.49
Total	100.0	Nitrogen	0.67
		Oxygen	9.7
Heating Value		Ash	13.46
BTU/lb (HHV)	6,433	Total	100.0
kJ/kg (HHV)	14,963		
Element	**ppm dry basis**	***Sulfur Forms**	**wt %**
Arsenic	5	Sulfur (Pyritic)	0.14
Cadmium	0.107	Sulfur (Organic)	0.35
Chlorine	<80		
Mercury	0.12		
Selenium	0.87		

Table 3-4 Process modelling input parameters and assumptions

Parameters	Values
Coal HHV (lignite coal), kJ/kg	14,963
Boiler adiabatic flame temperature, °C	1750
Main steam pressure, kPa	24,200
Main steam temperature, °C	593
Reheat steam temperature, °C	622
Condenser pressure, kPa	6.9
Cooling water supply temperature, °C	30
Cooling water in to condenser, °C	30
Cooling water out from condenser, °C	38
Cooling water supply pressure, kpa	400
Turbine adiabatic efficiencies, %	79~99
ASU Oxygen purity, %	94.25
Compressor adiabatic efficiencies, %	75~87
Flue gas processing for CO_2 capture, %	100
CO_2 product condition, kPa/°C	11,000/44
Exergy reference condition, kPa/°C	101.3/25

A nearly pure oxygen stream was used in the overall oxy-fuel system model. The oxygen and nitrogen purity from the ASU is reported in Table 3-5 below.

Table 3-5 ASU process parameters for O$_2$ and N$_2$ Stream

ASU Parameters	Unit	O$_2$ Stream	N$_2$ Stream
Pressure	bar a	1.012	1.2
Temperature	$^\circ$C	40.09	75
Flow rate	tonne/hr	577.9	1866
Composition	mol%		
O$_2$	%	94.02	1.11
N$_2$	%	3.08	98.49
Ar	%	2.9	0.39

3.3.3 Cooling water supply and return

In this plant configuration the cooling water return temperatures from different unit operations were maintained at three different temperature levels, i.e. 38/60/85°C in order to keep the CW return temperature as high as possible for maximum utilization of waste heat. A few units generated low grade waste heat and hence the cooling water return temperature from those units was low. In this model it was maintained at 38°C for these low temperature CW return streams by manipulating the CW flow rate. A few units generated moderate amount of waste heat and hence the cooling water return temperature from those units was also moderately high. In this model it was maintained at 60°C for those streams by manipulating the CW flow rate. Similarly a few units generated high grade of waste heat and hence the cooling water return temperature from those units was also kept high for best utilization of the waste heat. In this model it was maintained at 85°C for those streams by manipulating the CW flow rate. By adopting this approach it was possible to utilize the waste heat rejected from the high temperature unit operations of the integrated plant and use it in appropriate locations effectively as identified by the exergy analysis. More details about the CW temperatures are available in section 5.4.1. The cooling water supply and return temperatures were modelled as user input variable and can be altered at any reasonable value

depending on the plant location and source of cooling water supply (e.g. underground or sea water). In this base model the cooling water supply temperature was set at 30°C. As mentioned earlier the cooling water return temperatures at different unit operations were maintained at 38/60/85°Cfor this particular oxy-fuel process model.

3.3.4 Equation of State (EOS)

Peng-Robinson (PR) equation of state was used to relate the pressure, temperature, and specific volume of a substance in the overall oxy-fuel plant except the BOP section. The ASME steam property package was used for the BOP section. ASME Steam accesses the ASME 1967 steam tables. The limitations of this steam package are the same as those of the original ASME steam tables, i.e., pressures less than 1020 bar (15,000 psia) and temperatures greater than 0°C (32°F) and less than 815.5°C (1,500°F). However, the BOP model was well within of these constraints. The Van Der Waals equation of state (1873) was the first equation to predict vapour-liquid coexistence. A modification was later done by Redlich and Kwong in 1949 with the proposal of Redlich-Kwong equation of state that improved the accuracy of the Van Der Waals equation. Soave in 1972 and later Peng and Robinson (1976) proposed additional modifications to the Redlich-Kwong equation and more accurately predicted the vapour pressure, liquid density, and equilibrium ratios. The Peng-Robinson equation of state is generally the recommended property package for oil, gas, and petrochemical applications. It rigorously solves most single-phase, two-phase, and three-phase systems with a high degree of efficiency and reliability. Peng-Robinson EOS is used to determine the relationship between pressure (P), temperature (T) and molar volume (V_m) of substances in the oxy-fuel process as expressed in equation (3.1) (HYSYS, 2014; Peng et al. 1970; Stryjek et al., 1986).

$$P = \frac{RT}{(V_m - b)} - \frac{a}{V_m(V_m + b) + b(V_m - b)} \qquad (3.1)$$

where

$$a_i = \alpha_i \; 0.045724 \frac{R^2 T_{ci}^{\;2}}{P_{ci}} \tag{3.2}$$

$$b_i = 0.07780 \frac{R T_{ci}}{P_{ci}} \tag{3.3}$$

$$\alpha_i = \left[1 + m_i \left(1 - T_{ri}^{\frac{1}{2}}\right)\right]^2 \tag{3.4}$$

$$m_i = 0.37464 + 1.54226\omega_i - 0.26992\omega_i^2 \tag{3.5}$$

The symble, ω_i represents the acentric factor which is used for characterizing how non-spherical a molecule is, thereby assigning it to EOS. The abbreviations, T_{ci} and P_{ci}, represent the critical temperature and pressure while T_{ri} is the reduced temperature of each substance. The Peng-Robinson EOS can also be written in another form in terms of compressibility factor, Z, as follows:

$$Z^3 - (1-B)Z^2 + (A - 3B^2 - 2B)Z - (AB - B^2 - B^3) = 0 \tag{3.6}$$

where
$$A = \frac{aP}{R^2 T^2} \tag{3.7}$$

$$B = \frac{bP}{RT} \tag{3.8}$$

$$Z = \frac{P V_m}{RT} \tag{3.9}$$

For a mixture, the mixing rule is applied to calculate the parameters "a" and "b" as shown in the following equations.

$$a = \sum_{i=1}^{n} \sum_{j=1}^{n} x_i \, x_j \sqrt{a_i a_i} \left(1 - k_{ij}\right) \quad and \quad b = \sum_{i=1}^{n} x_i b_i \tag{3.10}$$

In equation (3.10), k_{ij} is a binary parameter to determine the binary interaction between component i and component j. This parameter can be obtained from the regression of phase equilibrium data, but in this case it is retrieved from ASPEN Plus databank since the experimental data are not available.

3.3.5 Fuel chemical exergy calculation block

A user input spreadsheet block for fuel composition is incorporated into the process model for exergy analysis. This is done to calculate the fuel chemical exergy automatically as soon as any change is made in the fuel composition. With this calculation block the model became fuel agnostic with respect to exergy analysis and all the subsequent changes takes place automatically with respective changes in fuel composition. Details of the fuel exergy calculation block are shown in Table 3-6.

Table 3-6 Fuel chemical exergy calculation spread sheet in HYSYS.

Coal Analysis					Chemical Exergy Calculation		
Coal Sample	Mass Comp	Properties			Absolute Entropy DAF	HHV of DAF	Chemical Exergy of Fuel
H2O	0.335	HHV		6433 Btu/lb	s^{DAF} (kJ/kmol*K)	(MJ/kg)	e^{CHDAF}(kJ/kg)
Ash	0.135	HHV	14962.1142	kJ/kg	1.326	29.259	29870.029
Carbon	0.396	T_o	298.15	K			
Hydrogen (H)	0.026	P_o	101.325	kPa			
Oxygen (O)	0.097						
Nitrogen (N)	0.007				**Input**: Fuel Composition		
Sulfer S	0.005					**Output**: Fuel Chemical Exergy	
Total	1.000						
Total Dry Ash Free	0.530						
Standard Input Data for Fuels							
Coal Sample	Dry Ash Free Coal-DAF			Conversion		Standard Molar Chemical Exergy	Absolute Entropy
Symbol	Mass Comp	MW	kmol/kg	Product	Stoichiometric (kmol/kg) DAF	e^{CHi} (kJ/kmol)	s^i (kJ/kmol*K)
Carbon C	0.746	12.0107	0.062	CO2	0.062	14176	213.794
Hydrogen (H)	0.048	2.01588	0.048	H2O	0.024	45	69.948
Oxygen (O)	0.183	31.9988	0.011	O2	0.069	3951	205.146
Nitrogen (N)	0.013	28.0134	0.001	N2	0.000	639	191.61
Sulfer S	0.009	32.065	0.000	SO2	0.000	301939	284.094
Total DAF	1.000						

The calculation details are included in section 4.2.6. The only input parameters to this calculation block is the fuel mass fraction as shown in the table filled with reference coal composition of Table 3-3. HYSYS fuel chemical exergy data was validated with published data (Bejan et al. 1996) and no discrepancy was observed.

3.3.6 Process automation

The overall plant model, including the base and improved model, is a fully automated model. However, the word 'automation' does not refer here to an automated process control. It only reflects the steady state model's characteristics with respect to the interconnected material and energy streams. The connections are done in such a way that no manual changes in process streams are necessary to investigate the perturbations and generate updated results. All changes in the integrated process happen with a single parameter change in the input/output block. The input/output block in the main flow sheet as displayed in Figure 3-6 is actually a spread sheet tool that provides a central location where all the major process parameters can be manipulated and subsequently the update takes place in the whole flow sheet and generates a new set of results. The manipulated variables include, but are not limited to:

- total power output
- cooling water inlet/supply temperature
- cooling water outlet/return temperature
- cooling water pressure
- oxygen preheating temperature
- exergy reference temperature
- CO_2 capture efficiency etc.

Additional manipulated variables or automation parameters could be included in the input-output block according to the end user requirements. The input-output block is thus the main user interface where the changes in basic plant parameters are only allowed. This also eliminates any possibility of errors and securing the process model from being corrupted. A

change in any parameter in this block such as plant capacity or exergy reference temperature will translate into a new simulation with updated data. This automation also allows to carryout plant sensitivity analysis with enhanced flexibility while selecting various process variables. As the model is created in an integrated fashion so that a small change in major independent variables will cause the overall model to adjust and update accordingly.

Moreover, the model was developed with a minimum number of fixed parameters and included ratio based calculations as much as possible to define various streams. The inclusion of the ratio based calculations allows the model to be more flexible for a wide range of applications. Ratio based calculations are implemented by adopting control logic calculation box that accepts different numerical values, set by an individual/user, to define a particular stream parameter with respect to a base parameter. Most of the flow rates of various process streams in the BOP section are defined as a specific ratio to the main steam (46) flow rate entering the HP turbine section. As an example the extraction steam (21) for heating up of the FWH8 has a ratio of 0.07763 with respect to the main steam (46) flow. These ratios can also be changed, if necessary, for a particular stream if a new turbine design is introduced. These ratios allow the BOP model to float around any capacity range when a user input capacity is changed (e.g. >0 MW…1000 MW or more) in the main input/output block for various plant capacity ranges. Similarly for the ASU section a few flow rates were set as a ratio of the main air flow input (301) to the ASU. As an example, the exit gas streams (345 and 346) from the distillation column C304 to C305 have a ratio of 0.1246 and 0.1736 to that of the air inlet flow (301). A few other ratios were also set for the internal streams within the columns C 303 and C304 which made these three columns flexible and allowed them to float around at various plant capacity ranges as dictated by the overall oxy-fuel plant model. It is often difficult to converge rigorous distillation column models for different process parameters. However, the use of ratio-based calculator blocks aided column convergence for various process parameters. No convergence difficulties were observed with respect to the ASU and three interconnected distillation columns in this model.

In the overall oxy-fuel model, a change in the capacity range (at input/output block) instantaneously generates an updated set of process and exergy analysis data for the oxy-fuel

52

plant. As an example, if the desired power generation capacity in the input-output block is changed from base 786 MW gross to 700 MW gross or any other number, then the ASU, Boiler and CO_2CCU process parameters will be adjusted accordingly by the model. There is no limitation for size reduction or size increment for this integrated model. Each of the increment and reduction happens in each block according to the process demand. In the current study, however, the model results are presented for the base 786 MW_{gross} power plant.

This process model is a fuel agnostic model and it requires no adjustments for the model convergence. In case of a new user it requires only to provide an input (e.g. desired plant capacity) number into the input/output block and the simulation results are generated automatically for the overall process. However, an advanced user might change process parameters and customize the plant design. Novel modelling features, e.g. ratio based calculations, into the ASU, BOP CO_2CCU and FG boiler section, make them ideal for any scale up or scale down case study and the plant calculations are done automatically. A typical simulation run steps in this automated flow sheet takes place in the following manner.

A change in plant capacity number (MW_{gross} electricity) at the input-output block communicates this information to the boiler which adjusts the fuel input to the boiler automatically and sets a new value for fuel flow rate. At the same time the steam generation is adjusted in the boiler for the BOP section and an updated O_2 flow requirement determines the ASU size and capacity. The ASU size is also dependent on the air infiltration to the boiler and excess O_2 composition in the exit flue gas from the boiler. Finally, the flow rate of the boiler exit flue gas determines the capacity of the CO_2CCU and its size is adjusted accordingly. The size of the CO_2CCU also depends on the CO_2 capture efficiency set by the user. All these actions take place simultaneously by a single change in input to the plant capacity number in the input-output block.

3.4 Process models developed in HYSYS

Following are the snapshots of the four process flow diagrams developed in HYSYS for the individual sections of the oxy-fuel power generation system. The boiler, BOP, ASU and CO_2CCU process flow diagrams are presented in Figures 3-7, 3-8, 3-9 and 3-10.
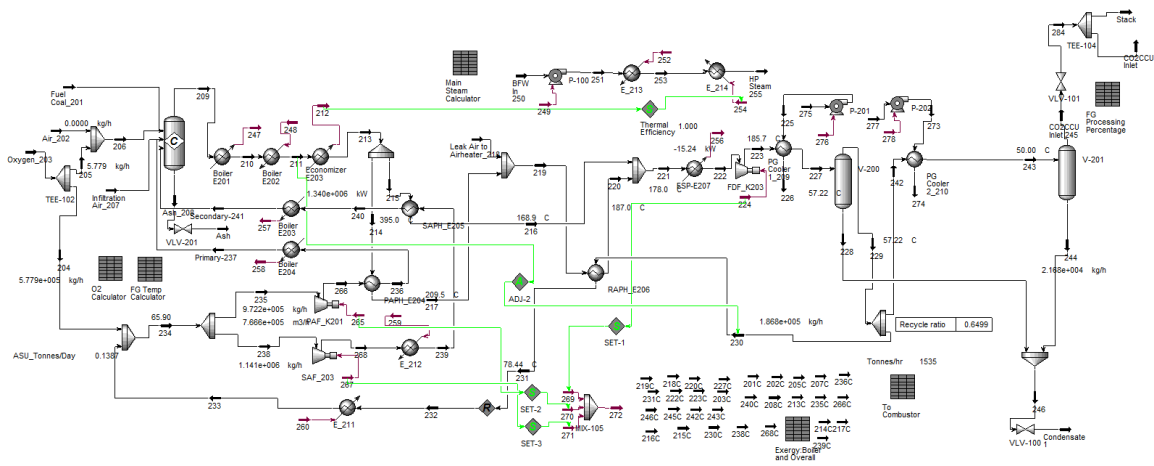
Figure 3-7 Boiler section process flow diagram developed in HYSYS
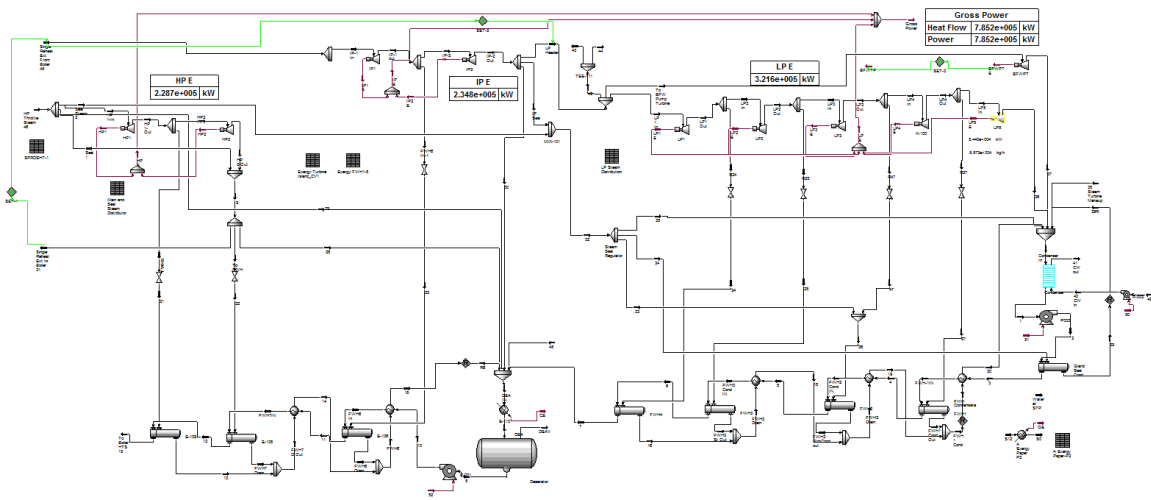
Figure 3-8 BOP process flow diagram developed in HYSYS

54
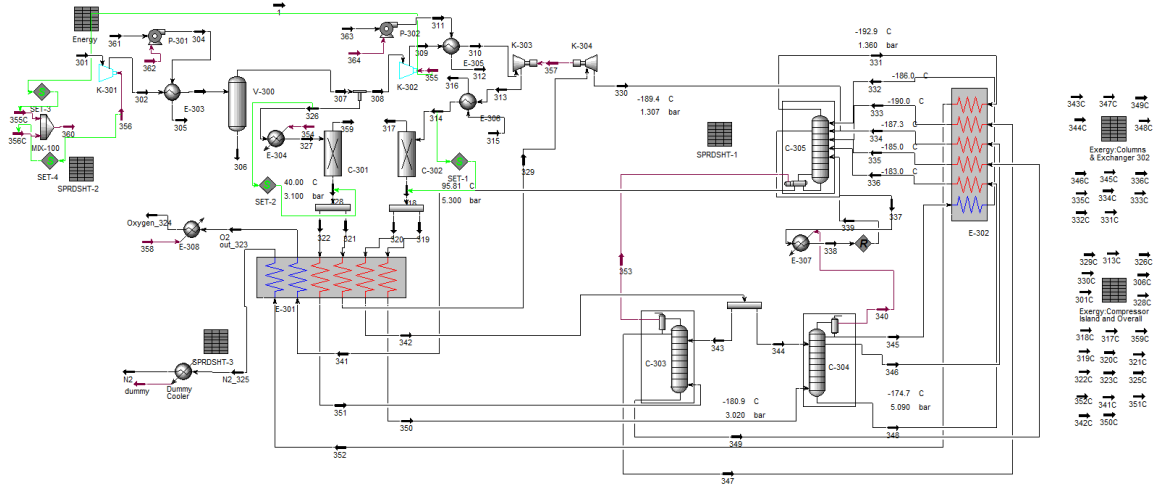
Figure 3-9 ASU process flow diagram developed in HYSYS
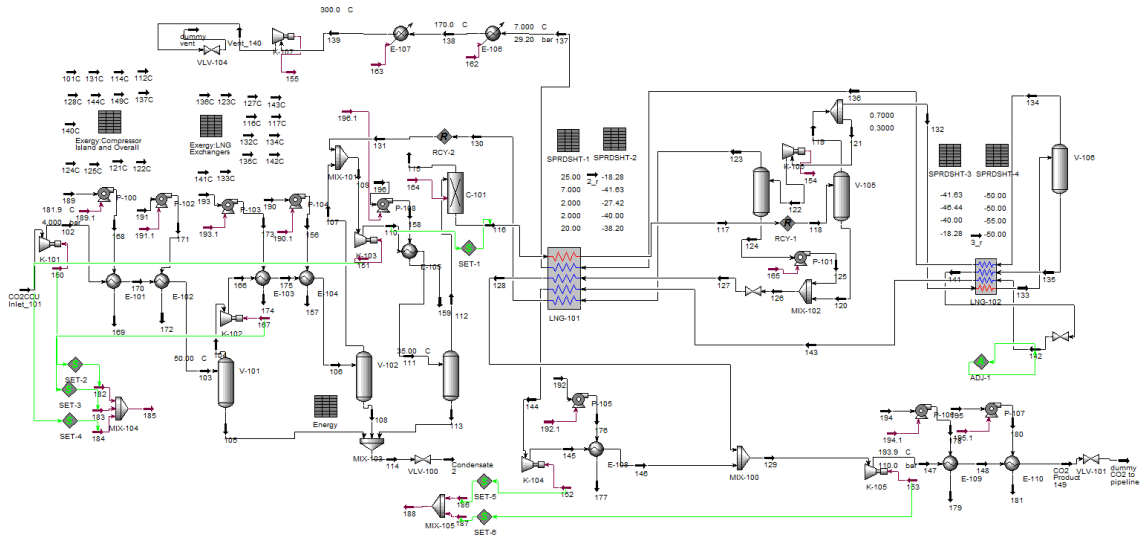
Figure 3-10 CO₂CCU process flow diagram developed in HYSYS

3.5 Process model validation

3.5.1 Model validation for ASU

The process model validation is only performed for the BOP and ASU sections as these two models were developed and simulated from existing publications (DOE, 2008; IEA, 2005) and for which the model data are available in the open literature. Table 3-7 compares a few selected main process stream data for the ASU model developed in this research work and the published model. Minor deviations can be observed between the two models in the table. The difference calculations were performed on the flow rates and the maximum difference was observed to be 1.74% for the oxygen stream, stream 34. The process flow diagram with stream numbers for the ASU in the IEA report is presented in Figure 3-11. The same process model was developed in HYSYS and presented in Figure 3-4 and 3-9. In case of the BOP the comparison, data are also similar between the DOE model and the current thesis and the discrepancies are minor and negligible. The comparison data for BOP are attached as Appendix A and presented in Table A-1

Figure 3-11 IEA report: ASU process flow diagram

56

Table 3-7 Model validation for ASU: IEA report (figure 3-11) and current thesis (figure 3-4)

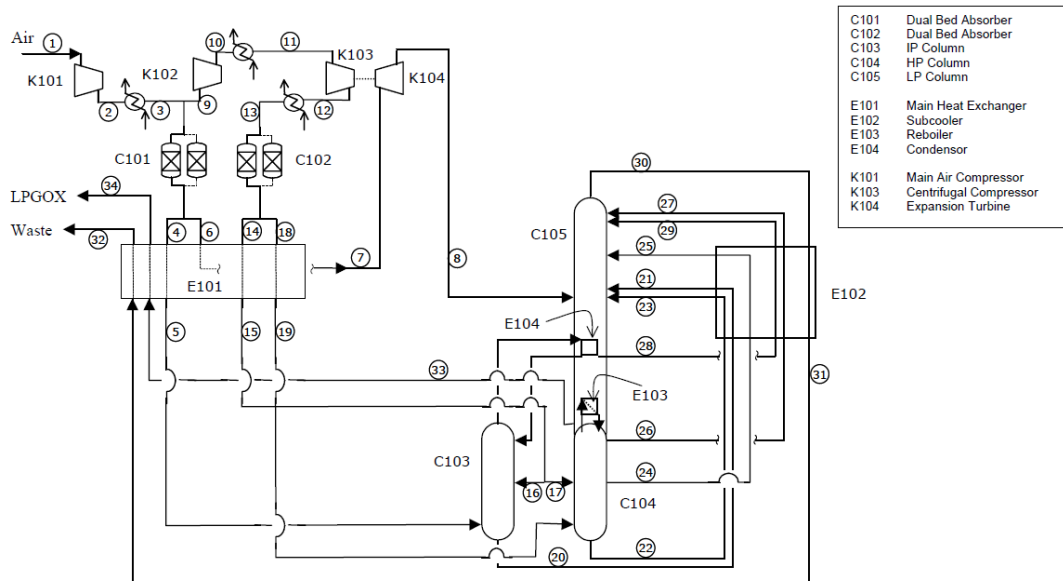| IEA Report: Selected Process Parameters for ASU								
Stream No#	1	5	8	20	22	30	32	34
Composition (mol%)								
N2	77.3	78.1	78.12	54.41	58.89	99.04	99.04	1.98
Ar	0.92	0.93	0.93	1.55	1.53	0.35	0.35	3.03
O2	20.73	20.95	20.95	44.04	39.58	0.608	0.608	94.98
Water	1	0	0	0	0	0	0	0
CO2	0.04	0	0	0	0	0	0	0
Flow (kg/hr)	962,422	188,577	290,223	110,843	152,635	727,040	727,040	228,788
Pressure bar (a)	1.01	3.02	1.46	3.02	5.09	1.36	1.2	1.6
Temperature ^{o}C	9	-178.54	-188.16	-180.78	-174.64	-193	15.5	15.5
Current Thesis Model Validation: Selected Process Parameters for ASU								
Stream No#	301	351	330	349	348	331	325	324
Composition (mol%)								
N2	77.3	78.12	78.12	54.42	59.12	98.55	98.55	2.23
Ar	0.92	0.93	0.93	1.48	1.45	0.42	0.42	2.83
O2	20.73	20.94	20.95	44.1	39.43	1.03	1.03	94.94
Water	1	0	0	0	0	0	0	0
CO2	0.04	0	0	0	0	0	0	0
Flow (kg/hr)	962,422	188,600	290,200	110,800	152,600	731,100	731,100	224,800
Pressure bar (a)	1.01	3.02	1.47	3.02	5.09	1.36	1.2	1.6
Temperature ^{o}C	9	-178.5	-188.3	-180.8	-174.7	-192.9	14.36	15.54
Relative error for flow (%)	0.000	-0.012	0.008	0.039	0.023	-0.558	-0.558	1.743

3.5.2 Model consistency and testing for exergy calculation tool

In order to test the accuracy of the exergy model and the exergy data generated by HYSYS, a combustion process with available exergy analysis data was modelled in HYSYS. This is an air combustion case study with exergy analysis presented by Bejan et al (1996). As the exergy test data does not depend on air or oxy-combustion process, hence this published data was selected for the exergy model accuracy test for HYSYS. The objective was to check if the HYSYS model can generate the same data as in the published literature (Bejan et al., 1996). First the published process was modelled and simulated in HYSYS and presented in Figure 3-12.
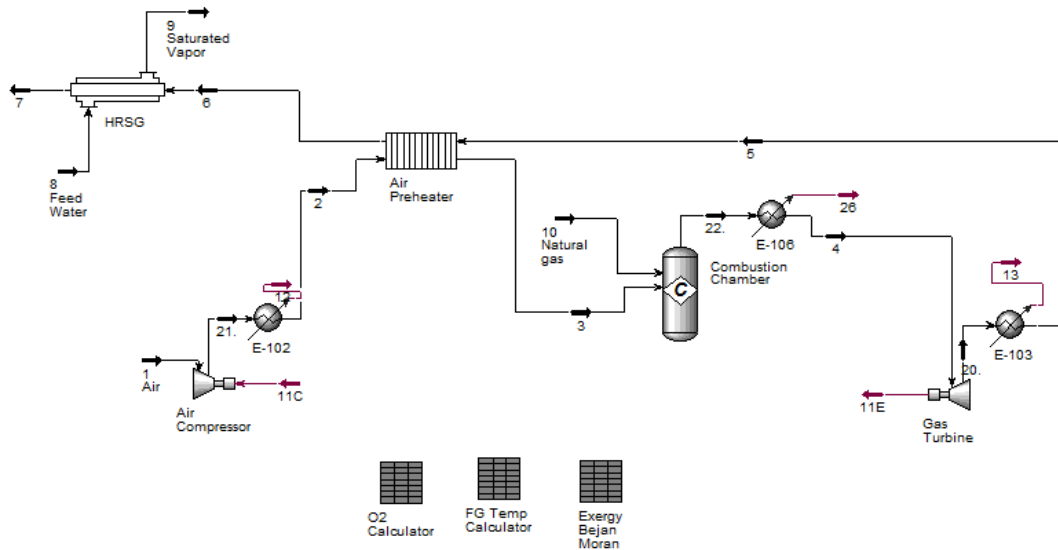
Figure 3-12 Exergy model developed for model data validation (after Bejan et al., 1996)

The combustor was modelled for a 85MW plant capacity, as specified in the publication. The components included in the process model were air compressor, combustion chamber, gas turbine, air preheater and the heat recovery steam generator. After completing the model development, all the exergy analysis equations were included in the HYSYS process model. The comparison results between the HYSYS model and the source data (Bejan et al., 1996) are presented in Table 3-8. No significant discrepancy was observed in the physical $(\dot{E}^{PH})$ as well as total exergy $(\dot{E})$ rate data generated by the HYSYS model and the source data. The contribution of chemical exergy $(\dot{E}^{CH})$ was found to be very insignificant for all the process streams. For most of the streams the amount of chemical exergy with respect to the physical exergy $(\dot{E}^{CH}*100/\dot{E}^{PH})$ was less than 2%. For the two low temperature streams (streams 7 and 8 in Table 3-8) the share of chemical exergy is significant compared to that of the physical exergy which are 15.23% and 131.6% respectively. However the low temperature streams have much less total exergy (2.77 MW and 0.06 MW respectively) compared to that of the overall exergy input to the system and which are less than 0.5% as shown in the impact

58

column in Table 3.8. The chemical exergy is associated with change in chemical composition of the substances (Sato N., 2004). In an oxy-fuel combustion system the chemical change of the flue gas or other streams are very negligible within the process streams. Also as seen in the Table 3-8 the chemical exergy contribution of the individual process streams are insignificant and hence not included in this exergy analysis.

Table 3-8 Exergy analysis comparison data for model validation (after Bejan et al., 1996)

State	Substance	Mass Flow rate	Temperature	Pressure	Exergy Rates (MW)			Share of E^{CH} (%)	Impact of E^{CH} (%)	Error
					$\dot{E}^{PH}$ +	$\dot{E}^{CH}$	= (Total) $\dot{E}$	$\dot{E}^{CH}*100/\dot{E}^{PH}$	$(\dot{E}i*100)/(\dot{E}_{10}+\dot{E}_{8})$	
		kg/s	K	bars						%
full	Bejan et al., 1996 (pg 139): Sample combustuion system exergy data									
1	Air	91.28	298.15	1.013	0	0	0			
2	Air	91.28	603.74	10.13	27.54	0	27.538	0.00	0.00	
3	Air	91.28	850	9.623	41.94	0	41.938	0.00	0.00	
4	Combustion products	92.92	1520	9.142	101.08	0.3665	101.454	0.36	0.43	
5	Combustion products	92.92	1006.2	1.099	38.42	0.3665	38.782	0.95	0.43	
6	Combustion products	92.92	779.8	1.066	21.39	0.3665	21.752	1.71	0.43	
7	Combustion products	92.92	426.9	1.013	2.406	0.3665	2.773	15.23	0.43	
8	Water	14	298.15	20	0.0266	0.035	0.0616	131.58	0.04	
9	Water	14	485.6	20	12.775	0.035	12.81	0.27	0.04	
10	Methane	1.642	298.15	12	0.627	84.3668	84.994		99.19	
full	Current Thesis: Sample combustuion system exergy data									
1	Air	91.28	298.15	1.013	0	0	0			
2	Air	91.28	603.75	10.13	27.43	0	27.43			0.39
3	Air	91.28	850	9.623	41.8	0	41.8			0.33
4	Combustion products	92.92	1520	9.623	101.4	-	101.4			0.05
5	Combustion products	92.92	1006.2	1.099	37.95	-	37.95			2.15
6	Combustion products	92.92	780.15	1.066	21.06	-	21.06			3.18
7	Combustion products	92.92	420.45	1.066	2.611	-	2.611			5.84
8	Water	14	298.15	20	0.0266	0.035	0.0616			0.00
9	Water	14	485.55	20	12.78	0.035	12.815			-0.04
10	Methane	1.642	298.15	12		85.05	85.05			-0.07

Only the fuel chemical exergy was considered as it has the most exergy amount in the overall process. This assumption is also justified by the insignificant exergy variation observed in the data presented in Table 3-8. These results indicate that the exergy data generated by HYSYS is well within the acceptable range for any analysis. Similarly exergy calculations were also tested after the data presented by Dincer et al. for an air/water heat pump system as shown in Figure 3-13 (Dincer et al., 2007).
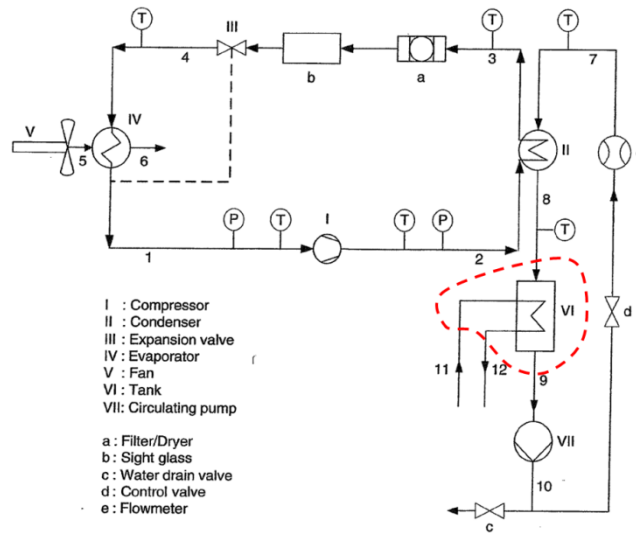
Figure 3-13 Exergy model developed for model data validation (after Dincer et al., 2007)

The data accuracy test was done partially for the tank (unit#VI in Figure 3-13) only, which relates to the streams 8, 9, 11 and 12 and presented in Table 3-9.

Table 3-9 Exergy analysis comparison data for model validation (after Dincer et al., 2007)

				Specific enthalpy	Specific entropy	Specific exergy	Exergy rate	Error
	Mass Flow	Temperature	Pressure					
Stream No	m (kg/hr)	°C	kPa	h (kJ/kg)	s (kJ/kg-K)	e (kJ/kg)	$\dot{E}$ (kW)	%
Dincer et al. 2007 (pg 100): Unit VI Tank exergy data								
8	39.6	24.6	220	103.3	0.361	3.96	0.044	
9	39.6	16	200	67.3	0.239	1.55	0.017	
11	86.4	9.1	500	38.7	0.0138	0.76	0.018	
12	86.4	13.1	500	54.9	0.196	1	0.024	
Current Thesis : Unit VI Tank exergy data in HYSYS								
8	39.6	24.6	220	102.957	0.361	3.730	0.041	6.73
9	39.6	16	200	66.387	0.237	1.490	0.016	3.61
11	86.4	9.1	500	38.353	0.138	0.755	0.018	-0.69
12	86.4	13.1	500	55.114	0.197	1.278	0.031	-27.80

The data for 8, 9 and 11 were a very close match; however a slight variation in enthalpy data for stream 12 made a significant impact on the exergy value of stream 12. In general, the discrepancies noted here in the table are only because of the slight variation in enthalpy and the entropy values generated by HYSYS and the software package (Engineering Equation Solver-EES) used by Dincer et al.

60

Chapter 4
Exergy Analysis

4.1 Exergy

4.1.1 Definition

A system delivers the maximum work if it undergoes a reversible process from a specified initial state to the state of its environment, also known as dead state. This represents the maximum work potential of the system at the specified state and is defined as exergy. The reference environment must be specified prior to any exergy analysis. The exergy of the system or flow depends on the state of both the system or flow and the reference environment. According to first law energy cannot be destroyed, however, it is important to know when something can be destroyed (a second law concept) or the cause of irreversibilities and which can be quantified by an exergy (availability) analysis (also a second law concept). This is very useful in designing and analyzing thermal systems (Cengal et al., 2006; Bejan et al., 1996).

4.1.2 Cause of irreversibilities

A process is said to be irreversible if there is no way to undo it or if both the system and the surroundings could not be exactly restored to their respective initial state. There are many effects that cause the process to be irreversible. Some of these include but are not limited to heat transfer, compression, expansion, chemical reaction, mixing of matter having different compositions or states, friction, electric current flow, magnetization, inelastic deformation etc. Improved thermodynamic performance can reduce these irreversilbilities. However, the steps needed to address the issues are always constrained by the economic factors. As an example for a heat exchanger to reach ideality, it requires infinite residence time or surface area. Similarly a distillation column needs an infinite number of stages. These designs are not feasible from process and economic perspectives. In this isolated approach, the efficiency of an individual unit operation can be improved with size (e.g. area or trays), however the overall process will be inefficient in terms of the cost. Hence, reducing the irreversibilities by

better process design, integration and waste heat utilization in a thermal system is the most favoured approach to mitigate some of these issues.

4.1.3 Environment or the reference/dead state

The reference environment or the dead state is usually considered to be the actual environment in which the overall system exists. In this particular research work the environmental or reference state is considered to be 1 atm (p_o) and 25°C (T_o). However for real world applications the temperature and pressure may be specified differently. For example, p_o and T_o may be taken as the average ambient temperature and the pressure for the location where the system operates (Bejan et al., 1996).

4.2 Exergy components

4.2.1 Types of exergy

The exergy of a system or a stream of substance can be divided into four components such as physical exergy E^{PH}, kinetic exergy E^{KN}, potential exergy E^{PT}, and chemical exergy E^{CH}. The sum of the kinetic, potential and physical exergies is also in some literature referred to as thermo-mechanical exergy. For the current study physical or thermo-mechanical exergies were considered for all the streams of the integrated oxy-fuel power plant and chemical exergy was considered for the fuel stream only. The total exergy of a system is then expressed as

$$E = E^{PH} + E^{KN} + E^{PT} + E^{CH} \qquad\qquad 4.1$$

It is convenient to work with total exergy on a unit mass or molar basis. In that case the total specific exergy on a mass basis is given by e where e is represented as

$$e = e^{PH} + e^{KN} + e^{PT} + e^{CH} \qquad\qquad 4.2$$

If the system is considered at rest (dead state) with respect to the environment, then the kinetic and potential exergy terms becomes zero ($e^{KN} = e^{PT} = 0$). At this state it has zero velocity and zero elevation above the reference level with respect to the environment. In this context the thermo-mechanical exergy, which essentially becomes physical exergy, is the maximum

theoretical useful work that can be obtained as the system passes from an initial state (T, p) to a dead state or to the environment condition (T_0, p_0). Physical exergy is also in literature classified (Sato N., 2004) into thermal exergy (due to change in temperature), pressure exergy (due to change in pressure) and exergy of mixing (due to change in concentration).

4.2.2 Thermal exergy

Thermal energy cannot be completely converted into work; rather only part of it is converted to work. An ideal reversible heat engine can convert thermal energy into work as given below (Sato N., 2004).

$$W_{rev} = Q - Q_o = Q[1 - Q_o/Q] \qquad\qquad 4.3$$

where, Q is the thermal energy received by a working fluid (e.g. an ideal gas) in the engine from an outside heat source at temperature T and releasing an amount of thermal energy Q_o into an outside heat reservoir at a lower temperature T_o in the absolute temperature scale similar to what is shown in Figure 4-1 (Smith et al., 1987).
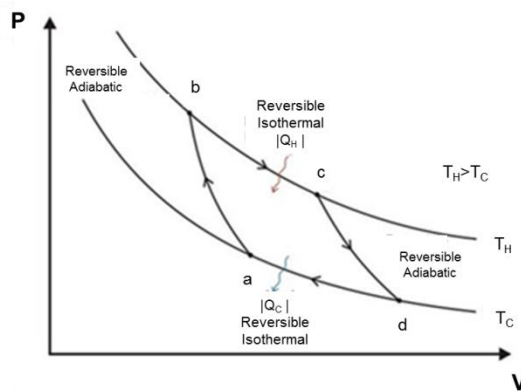
Figure 4-1 PV diagram for an ideal gas (Carnot Cycle)

Details of this analysis are given in Appendix B. In Figure 4-1, Q is referred as Q_H, Q_o as Q_C, T as T_H, and T_o as T_C. If T_C is set at the environment temperature (same as T_o) to which exergy is referred, W_{rev} will become the exergy of the thermal energy at temperature T. So the exergy, E,

of an amount of heat Q at a temperature T can be written as according to equation B 1.10 in Appendix B (Smith et al., 1987).

$$E = W_{rev} = Q[1 - T_o/T]$$ 4.4

This is the maximum work that can be reversibly gained from an amount of thermal energy Q at a temperature T. Again the thermal energy that is released from the engine as Q_C (or Q_0) can be written as

$$Q_o = Q - E$$ 4.5

After substitution of equation 4.4 we get

$$Q_o = Q - Q[1 - T_o/T] = Q[T_o/T]$$ 4.6

Equation 4.6 represents the amount of energy that cannot be used. Hence the efficiency of the reversible heat engine can be written as

$$\lambda = \frac{W_{rev}}{Q} = \frac{E}{Q} = \frac{Q[1 - T_o/T]}{Q} = 1 - T_o/T$$ 4.7

If the heat engine operates in an irreversible way, then the efficiency λ drops as the amount of work W_{irr} is less than W_{rev} and hence less than exergy, E, of heat energy Q at temperature T as some of the exergy is lost due to the irreversibility in the energy transformation.

4.2.3 Pressure exergy

If we consider a gas phase of volume V and pressure p that expands reversibly at constant temperature T_0 toward a volume V_0 and at pressure p_0 (equilibrium with atmosphere), the reversible work done will be (Sato N., 2004; Smith et al., 1987)

$$W_{rev} = \int_{p}^{p0} pdV$$ 4.8

The work done here is against the atmospheric pressure of the outside environment where work done is for removing a volume of atmospheric gas. This work cannot be utilized. So the available work or exergy will be less than W_{rev}. However if p is much greater than p_0 we may assume W_{rev} to be approximately equal to E. From the equation of state of an ideal gas we know $pV = nRT_o$. By differentiating we get

$$pdV + Vdp = 0, \text{ and } dV = -\left(\frac{V}{p}\right)dp = -\left(\frac{nRT_0}{p^2}\right)dp \qquad 4.9$$

Substituting these in equation 4.8 we get exergy of an ideal gas expressed as a function of pressure.

$$E = W_{rev} = -nRT_0\int_p^{p_0}\frac{dp}{p} = nRT_0 \ln \frac{p}{p_0} \qquad 4.10$$

4.2.4 Exergy of mixing

The exergy of mixing of a substance for one mole of the mixture is given by the free enthalpy for the mixing of substances i.e

$$\varepsilon^M = h^M - T_0 S^M \qquad 4.11$$

Where h^M and S^M are the enthalpy and entropy for the mixing of substances for one mole of mixture. For a perfect mixture (e.g. ideal gas mixture) or solution h^M is zero. For a perfect mixture consisting of mole fraction x_i of each of the substance present, the entropy of mixing is

$$S^M = -\sum x_i(s_i^{mixture} - s_i^{pure}) = -\sum_i - x_i ds_i = -\sum - x_i(C_p\frac{dT}{T} - \frac{R}{P}dP) \qquad 4.12$$

where $S_i^{mixture}$ and S_i^{pure} are the partial molar entropy of each of the substances "i" in the pure state and in mixture. At constant temperature the entropy of mixing becomes:

$$S^M = -\sum_i - x_i ds_i = -\sum - x_i (Rd \ln P) \quad at \quad constant \quad T \tag{4.13}$$

Integrating from partial to the total pressure of the mixture

$$S^M = -\int_{p_i}^{P} \sum_i - x_i ds_i = -\sum - x_i (R \ln \frac{P}{p_i}) = -\sum - x_i R \ln \frac{P}{x_i P} = -\sum x_i R \ln x_i$$

$$\tag{4.14}$$

The molar exergy for the mixing of substances in an ideal mixture ($h^M = 0$) can be written after equation 4.11 and 4.14.

$$\varepsilon^M = h^M - T_0 S^M = h^M + \sum x_i T_o R \ln x_i = \sum x_i T_o R \ln x_i \tag{4.15}$$

The molar exergy (exergy of mixing) for an ideal gas mixture ($h^M = 0$) at the environment condition (T_o and p_o) therefore can be written as (Norio Sato, 2004; Smith et al., 1987)

$$\varepsilon = \sum_i x_i \varepsilon_i^{pure} + \varepsilon^M = \sum_i x_i \varepsilon_i^{pure} + h^M - T_0 S^M \tag{4.16}$$

$$= \sum_i x_i \varepsilon_i^{pure} + \sum_i RT_o x_i \ln x_i \tag{4.17}$$

Considering the environment conditions of temperature T_o and pressure p_o the mole fraction of i_{th} gas x_i is different from the value of x_i^e where subscript ^{e} denotes the stable environment condition of atmospheric air. In this stable condition the partial molar exergy value is zero.

The exergy of the i_{th} gas component with respect to the atmospheric air can be written as (after equation 4.17)

$$\varepsilon_i = RT_o \ln x_i - RT_o \ln x_i^e = RT_o \ln \frac{x_i}{x_i^e} \qquad 4.18$$

This equation can be extended to the gas mixture whose compositional values x_i are different from those of x_i^e. So the exergy equation for the gas mixture relative to the atmospheric air will be

$$\varepsilon = \sum_i RT_o \, x_i \ln \frac{x_i}{x_i^e} \qquad 4.19$$

4.2.5 Thermal exergy of high temperature substances

Assume that a substance at high temperature (and at constant pressure) supplies an amount of heat $dQ(= dH)$ to a reversible heat engine. In this case the reversible work done by the engine dW_{rev} will be achieved by releasing an amount of heat $dQ_o(= dH_o)$ to the environment at temperature T_0 and the heat supply by the substance will continue until its temperature reaches the environment temperature. The temperature drop of the substance due to the heat supply dQ will be dT where,

$$dQ = dH = C_p dT \qquad 4.20$$

and the exergy drop dE will be equal to dW_{rev} work done by the engine where (after equation 4.4)

$$dE = dW_{rev} = \frac{T - T_o}{T} dQ > 0 \qquad 4.21$$

So the thermal exergy (at constant pressure) for the high temperature substance (which is supplying heat to the heat engine), when the temperature decreases from T to T_o will be (Sato N., 2004)

$$E = -W_{rev} = \int_{T_0}^{T} \frac{T - T_0}{T} dQ = \int_{T_0}^{T} \frac{T - T_0}{T} dH = \int_{T_0}^{T} C_p \left(\frac{T - T_0}{T} \right) dT = \int_{T_0}^{T} C_p dT - T_0 \int_{T_0}^{T} \left(\frac{C_p}{T} \right) dT$$

$$= \int_{T_0}^{T} C_p dT - T_0 \int_{T_0}^{T} \frac{dQ}{T}$$

$$= \int_{T_0}^{T} C_p dT - T_0 \int_{S_0}^{S} dS \quad \text{(at constant pressure } dH = C_p dT)$$

$$= (H - H_0) - T_0 (S - S_0) \qquad\qquad\qquad 4.22$$

Where H and H_0 are the enthalpy of the substance and S and S_0 are the entropy of the substance at temperature T and T_0 respectively. In terms of molar quantities, where molar enthalpy is h and molar entropy is s, equation 4.22 can be written for the specific exergy in the following form (Smith et al., 1987).

$$e = (h - h_0) - T_0 (s - s_0) \qquad or\ in\ general,\ \ e_j = (h_j - h_0) - T_0 (s_j - s_0) \qquad 4.23$$

The exergy equation can be expressed in various forms that may be more appropriate for a particular application. The specific exergy of a fluid stream in equation 4.23, with negligible kinetic and potential exergies, can be used to express the rate of exergy flow associated with a mass flow rate of $\dot{m}$ as follows:

$$\dot{E}_j = \dot{m}_j e_j = \dot{m}_j \left[(h_j - h_0) - T_0 (s_j - s_0) \right] \qquad\qquad 4.24$$

Equation 4.24 is identified as the physical component (physical exergy) of the exergy transfer associated with temperature and pressure. The enthalpy and entropy values of the process streams cover not only the physical components but also the chemical contributions of the process streams (Norio Sato, 2004; Szargut et, al., 1988). As a result, the exergy values calculated by equations 4.22 or 4.24 will give the value of total exergy of a process stream. In

68

this context this study did not consider to calculate the exergy components separately and rather used equation 4.24 as the main deciding equation for all exergy calculations for the process streams. However, for the case of solid fuel the chemical exergy of the fuel was calculated and used in the total exergy calculation.

4.2.6 Chemical exergy

Chemical exergy is the work that can be obtained by taking a substance having the parameters T_o and p_o to the state of thermodynamic equilibrium with the datum level components of the environment. The datum level components consists of a set of reference substances with standard concentrations reflecting closely the chemical makeup of the natural environment. The reference substances are generally divided into three groups: a) gaseous components of the atmosphere, b) solid substances from the lithosphere, and c) ionic and non-ionic substances from the oceans. Two alternative exergy reference environments named as model-I and model-II are normally used for engineering calculations where all the standard chemical exergies for various components are listed. Details of these models can be found in Bejan et, al. (1996).

Considering a control volume where a gas i enters at temperature T_o and pressure p_o and expands isothermally with heat transfer with the environment only and exits to the environment at temperature T_o and partial pressure $x_i^e p_o$. The maximum theoretical work per mole of gas i is reached when expansion occurs without irreversibilities. Accordingly, the chemical exergy for the i_{th} gas arising from its mixing exergy (after eq.4.15) can be written as

$$e_i^{CH} = RT_o \ln p_o - RT_o \ln x_i^e p_o \qquad 4.25$$

$$e_i^{CH} = RT_o \ln \frac{p_o}{x_i^e p_o} \qquad 4.26$$

$$e_i^{CH} = -RT_o \ln x_i^e \qquad 4.27$$

where subscript ^{e} denotes the environment. Now instead of i_{th} gas, we consider a gas mixture where gas i is present whose mole fraction in the gas mixture is x_i at T_o and p_o. It enters the same control volume at T_o and the partial pressure $x_i\, p_o$ and exits at T_o and partial pressure $x_i^e\, p_o$. Similar to the previous derivation we can write the exergy per mole as follows:

$$e_i^{CH} = RT_o\, \ln x_i p_o - RT_o\, \ln x_i^e p_o \qquad\qquad 4.28$$

$$e_i^{CH} = RT_o\, \ln \frac{x_i p_o}{x_i^e p_o} \qquad\qquad 4.29$$

$$e_i^{CH} = -RT_o\, \ln \frac{x_i^e}{x_i} \qquad\qquad 4.30$$

Extending this equation over a number of components per mole of gas mixture we can write the chemical exergy per mole of gas mixture as

$$e^{CH} = -RT_o\, \sum x_i \ln \frac{x_i^e}{x_i} \qquad\qquad 4.31$$

Expanding the logarithmic term and replacing with Eq 4.27 we can re write the chemical exergy equation as follows (Bejan et al., 1996: Norio Sato, 2004; Smith et al., 1987).

$$e^{CH} = \sum x_i e_i^{CH} + RT_o\, \sum x_i \ln x_i \qquad\qquad 4.32$$

4.2.7 Chemical exergy of fuel

The chemical exergy of the fuel is the most important chemical exergy as it participates in the combustion reactions and assumes chemical changes. Consider an idealized device for evaluating maximum work as shown in Figure 4-2. The fuel used here for combustion is a generic hydrocarbon fuel C_aH_b which is being combusted with oxygen (O_2).

70
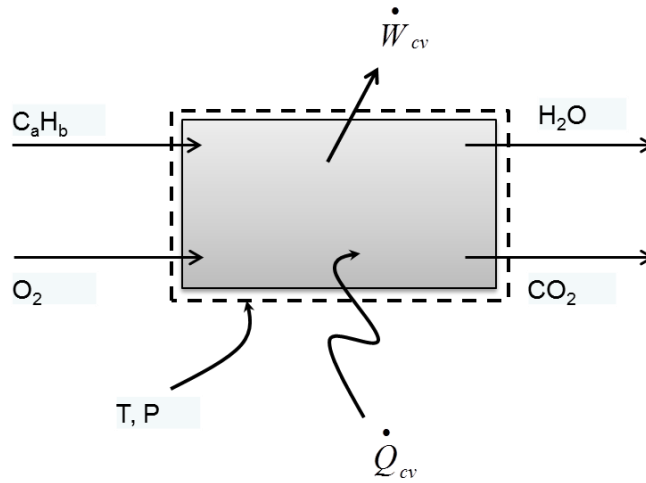
Figure 4-2 Control volume representing a device for evaluating maximum work

Let's assume the reaction to be complete, with entering and exiting streams leaving a combustion device (control volume) at same temperature T and pressure p (Bejan et al., 1996). Following is the complete reaction for this fuel combustion

$$C_aH_b + \left(a + \frac{1}{4}b\right)O_2 \rightarrow aCO_2 + \frac{1}{2}bH_2O \qquad 4.33$$

For steady state operation, at per mole of fuel, the energy rate balance for the system is as follows

$$a\overline{h_{co2}} + \frac{1}{2}b\overline{h_{H2O}} - \overline{h_F} - \left(a + \frac{1}{4}b\right)\overline{h_{o2}} = \frac{\dot{Q}_{cv}}{\dot{n}_F} - \frac{\dot{W}_{cv}}{\dot{n}_F} \qquad 4.34$$

or

$$\frac{\dot{W}_{cv}}{\dot{n}_F} = \frac{\dot{Q}_{cv}}{\dot{n}_F} + \overline{h_F} + \left(a + \frac{1}{4}b\right)\overline{h_{o2}} - a\overline{h_{co2}} - \frac{1}{2}b\overline{h_{H2O}} \qquad 4.35$$

where, subscript F denotes fuel, $\overline{h}$ is the molar enthalpy, $\dot{Q}\ and\ \dot{W}$ are the rate of heat input to the device and work done by the device respectively. Here the potential and kinetic energy

71

effect are considered negligible. Similarly, considering heat transfer occurs only at temperature T, then the entropy balance for the control volume, per mole basis, will be as follows

$$a\overline{s_{co2}} + \frac{1}{2}b\overline{s_{H2O}} - \overline{s_F} - \left(a + \frac{1}{4}b\right)\overline{s_{o2}} - \frac{\dot{Q}_{cv}/\dot{n}_F}{T} = \frac{\dot{S}_{gen}}{\dot{n}_F}$$

4.36

or

$$\frac{\dot{Q}_{cv}}{\dot{n}_F} = T\left[a\overline{s_{co2}} + \frac{1}{2}b\overline{s_{H2O}} - \overline{s_F} - \left(a + \frac{1}{4}b\right)\overline{s_{o2}}\right] - T\frac{\dot{S}_{gen}}{\dot{n}_F}$$

4.37

From equation 4.35 and 4.37

$$\frac{\dot{W}_{cv}}{\dot{n}_F} = \left[\overline{h_F} + \left(a + \frac{1}{4}b\right)\overline{h_{o2}} - a\overline{h_{co2}} - \frac{1}{2}b\overline{h_{H2O}}\right] - T\left[\overline{s_F} + \left(a + \frac{1}{4}b\right)\overline{s_{o2}} - a\overline{s_{co2}} - \frac{1}{2}b\overline{s_{H2O}}\right] - T\frac{\dot{S}_{gen}}{\dot{n}_F}$$

4.38

The maximum value of work is obtained when the entropy generation term is set to zero in equation 4.38.

$$\left(\frac{\dot{W}_{cv}}{\dot{n}_F}\right)_{rev} = \left\{\left[\overline{h_F} + \left(a + \frac{1}{4}b\right)\overline{h_{O_2}} - a\overline{h_{CO_2}} - \frac{1}{2}b\overline{h_{H_2O}}\right](T,p)\right\} - T\left[\overline{s_F} + \left(a + \frac{1}{4}b\right)\overline{s_{O_2}} - a\overline{s_{CO_2}} - \frac{1}{2}b\overline{s_{H_2O}}\right](T,p)$$

4.39

When the temperature and pressure in equation 4.39 correspond to 25ºC ($T_0 = 298.15K$) and 1 bar (or $p_0 = 1\,atm$), respectively the enthalpy term corresponds to standard heating values. It will be $\overline{HHV}$ when water exits from the system as liquid in Figure 4-2 and $\overline{LHV}$ when water exits as vapour (Bejan et al., 1996). Assuming the particular case where water comes out as liquid,

$$\left(\frac{\dot{W}_{cv}}{\dot{n}_F}\right)_{rev} = \overline{HHV}(T_0, p_0) - T_0\left[\overline{s_F} + \left(a + \frac{1}{4}b\right)\overline{s_{O2}} - a\overline{s_{CO2}} - \frac{1}{2}b\overline{s_{H2O}}\right](T_0, p_0) \qquad 4.40$$

In order to calculate the chemical exergy of the fuel we take a special case of the steady syate system referred in Figure 4-2 where the system boundary temperature is T_0 (298.15K) at which heat transfer occurs. The flowrate in the control volume is assumed to be a stoichiometric flowrate on mole basis per unit time at steady state condition. All substances enter and exit the control volume at temperature T_0 and pressure p_0 (1bar). Assuming no irreversibilities ($\dot{S}_{gen} = 0$), the steady-state exergy rate balance equation per mole of fuel will be as follows (Bejan et al., 1996):

Exergy input – Exergy output – Exergy consumption / destruction = Exergy accumulation

$$\overline{e_F}^{CH} + \left(a + \frac{1}{4}b\right)\overline{e_{O2}}^{CH} - a\overline{e_{CO2}}^{CH} - \frac{1}{2}b\overline{e_{H2O(l)}}^{CH} + \sum_j \frac{\dot{E}_{Q,j}}{\dot{n}_F} - \left(\frac{\dot{W}_{cv}}{\dot{n}_F}\right)_{rev} - \dot{E}_D = 0 \qquad 4.41$$

where $\overline{e}^{CH}$ refers to chemical exergy per mole, $\dot{E}_{Q,j}$ refers to net input of exergy rate associated with heat at location "j" where temperature is T_j , $\dot{E}_D (= T_0 \dot{S}_{gen})$ refers to exergy rate of destruction or consumption ($= 0$ here as no irreversibilities are assumed), and at steady state condition the accumulation term becomes zero (Dincer et al., 2007; Bejan et al., 1996). With these assumptions and substituting equation 4.4 in equation 4.41 we get

$$0 = \overline{e_F}^{CH} + \left(a + \frac{1}{4}b\right)\overline{e_{O2}}^{CH} - a\overline{e_{CO2}}^{CH} - \frac{1}{2}b\overline{e_{H2O(l)}}^{CH} + \sum_j \left(1 - \frac{T_0}{T_j}\right)\frac{\dot{Q}_j}{\dot{n}_F} - \left(\frac{\dot{W}_{cv}}{\dot{n}_F}\right)_{rev} \qquad 4.42$$

Where $(1-\dfrac{T_0}{T_j})\dot{Q}_j$ represents the time rate of exergy transfer associated with heat transfer at the

rate $\dot{Q}_j$ occurring in the boundary at location "j" where the instantaneous temperature is T_j. In this particular case $T_j = T_0$ and as a result

$$\overline{e}_F^{\,CH} = \left(\frac{\dot{W}_{cv}}{\dot{n}_F}\right)_{rev} + a\overline{e}_{CO2}^{\,CH} + \frac{1}{2}b\overline{e}_{H2O(l)}^{\,CH} - \left(a+\frac{1}{4}b\right)\overline{e}_{O_2}^{\,CH} \qquad \text{4.43}$$

Substituting equation 4.40 in equation 4.43 we get the chemical exergy of a hydrocarbon fuel as stated below.

$$\begin{aligned}
\overline{e}_F^{\,CH} = \;& \overline{HHV}(T_0, p_0) - T_0\left[\overline{s}_F + \left(a+\frac{1}{4}b\right)\overline{s}_{o_2} - a\overline{s}_{co_2} - \frac{1}{2}b\overline{s}_{H_2O}\right](T_0, p_0) \\
& + \left\{a\overline{e}_{CO2}^{\,CH} + \frac{1}{2}b\overline{e}_{H2O(l)}^{\,CH} - \left(a+\frac{1}{4}b\right)\overline{e}_{O_2}^{\,CH}\right\}
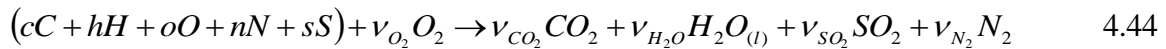\end{aligned} \qquad \text{4.43}$$

4.2.8 Chemical exergy of coal

Equation 4.43 is a generalized equation applicable to any fuel for exergy calculation. It is applied to calculate the exergy of coal used in the current study. In case of coal the assumptions made here are: coal and oxygen entering at (T_0, p_0), complete combustion taking place inside the control volume as shown in Figure 4-3, combustion products (CO_2, SO_2 and $H_2O_{(l)}$) exiting separately at (T_0, p_0), N_2 in the coal exiting separately at (T_0, p_0), and all heat transfers occur at (T_0) (Bejan et al., 1996).
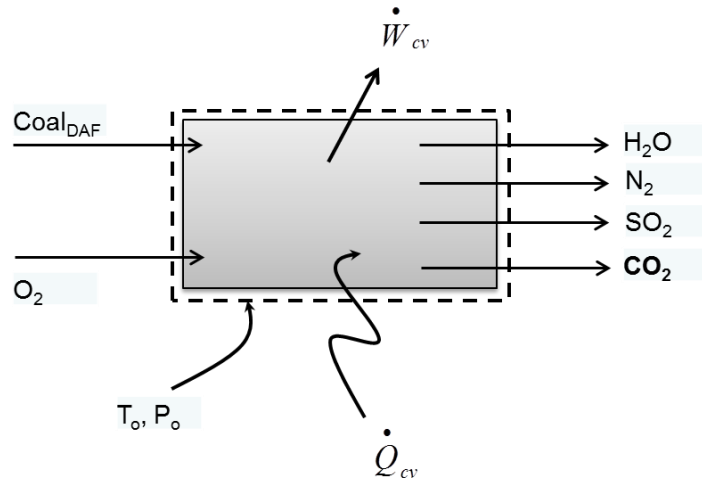
Figure 4-3 Control volume for dry and ash free coal combustion

The generalized combustion reaction is given below

$$\left(cC + hH + oO + nN + sS\right) + v_{O_2}O_2 \rightarrow v_{CO_2}CO_2 + v_{H_2O}H_2O_{(l)} + v_{SO_2}SO_2 + v_{N_2}N_2 \qquad 4.44$$

Where c, h, o, n and s each in kmol/kg$_{DAF}$ as mentioned in Table 3-6 and for balancing the reaction we get

$$v_{CO_2} = c, \qquad v_{H_2O} = \frac{1}{2}h, \qquad v_{SO_2} = s, \qquad v_{N_2} = \frac{1}{2}n, \qquad v_{O_2} = c + \frac{1}{4}h + s - \frac{1}{2}o \qquad 4.45$$

For this particular case with coal, equation 4.43 takes the form as follows

$$\overline{e_{DAF}}^{CH} = \overline{HHV_{DAF}} - T_0\left[\overline{s_{DAF}} + v_{O_2}\overline{s_{O_2}} - v_{CO_2}\overline{s_{CO_2}} - v_{H_2O}\overline{s_{H_2O}} - v_{SO_2}\overline{s_{SO2}} - v_{N_2}\overline{s_{N_2}}\right]$$

$$4.46$$

$$+ \left\{ v_{CO_2}\overline{e_{CO_2}}^{CH} + v_{H_2O}\overline{e_{H_2O(l)}}^{CH} + v_{SO_2}\overline{e_{SO2}}^{CH} + v_{N_2}\overline{e_{N_2}}^{CH} - v_{O_2}\overline{e_{O_2}}^{CH} \right\}$$

Values of entropy $\overline{s}\left(= absolute\ entropy\ values\ \overline{s}_0\ kJ/kmol.K\right)$ and standard molar chemical exergy $\overline{e}^{CH}\left(kJ/kmol\right)$ at *298.15 K* and p_0 can be inserted from available data in the literature.

These values are (Bejan et al., 1996):

$\overline{s}_{O_2} = 205.15 \ kJ/kmol.K, \qquad \overline{s}_{CO_2} = 213.79 \ kJ/kmol.K, \qquad \overline{s}_{H_2O(l)} = 69.95 \ kJ/kmol.K,$

$\overline{s}_{SO_2} = 248.09 \ kJ/kmol.K, \qquad \overline{s}_{N_2} = 191.61 \ kJ/kmol.K,$

$\overline{e}_{O_2}^{CH} = 3.951 \ MJ/kmol, \qquad \overline{e}_{CO_2}^{CH} = 14.176 \ MJ/kmol, \quad \overline{e}_{H_2O(l)}^{CH} = 0.045 \ MJ/kmol,$

$\overline{e}_{SO_2}^{CH} = 301.939 \ MJ/kmol, \ \overline{e}_{N_2}^{CH} = 0.639 \ MJ/kmol,$ \hfill 4.47

In the absence of measured values, HHV_{DAF} and absolute entropies $\overline{s}_{DAF}$ can be estimated by the following (Eiserman et al., 1980).

For HHV_{DAF} :

$$HHV_{DAF} = [152.19H + 98.767][(C/3) + H - (O - S)/8] \qquad 4.48$$

Where $H, C, O \ and \ S$ are the mass fractions of coal (DAF). In this study, the values are given in Table 3.6. Replacing the values we get from equation 4.48

$$HHV_{DAF} = [152.19(0.048) + 98.767][((0.746)/3) + (0.048) - (0.183 - 0.009)/8]$$
$$= 29.26 \ MJ/kg \ (DAF)$$

For $\overline{s}_{DAF}$:

$$s_{DAF} = c\left[37.1653 - 31.4767 \exp\left(-0.564682\frac{h}{c+n}\right) + 20.1145\frac{o}{c+n} + 54.3111\frac{n}{c+n} + 44.6712\frac{s}{c+n}\right]$$

\hfill 4.49

Where $h, c, o, n \ and \ s$ are the kmol/kg (of DAF), which are as given in Table 3.6 for the coal used in this study. Replacing the values we get from equation 4.49

$$s_{DAF} = 0.06217 \begin{bmatrix} 37.1653 - 31.4767 \exp\left(-0.564682\dfrac{0.0481}{0.063072}\right) + 20.1145\dfrac{0.01144}{0.063072} + \\ 54.3111\dfrac{0.0009}{0.063072} + 44.6712\dfrac{0.000288}{0.063072} \end{bmatrix}$$

$$= 1.326 \, kJ/kg_{(DAF)}.K$$

Substituting the values of equations 4.45, 4.47, 4.48 and 4.49 in equation 4.46 we get the specific chemical exergy of the dry and ash free coal as follows:

$$\overline{e_{DAF}}^{CH} = 29.26 \, MJ/kg_{(DAF)} - 298.15 \, K \begin{bmatrix} 1.326 + 0.06876 \times 205.146 \, kJ/kg \\ -0.06217 \times 213.794 - 0.02405 \times 69.948 \\ -0.000288 \times 284.094 - 0.000451 \times 191.61 \end{bmatrix} kJ/kg_{(DAF)}.K$$

$$+ \begin{Bmatrix} 0.06217 \times 14176 + 0.02405 \times 45 + 0.000288 \times 301939 + \\ +0.000451 \times 639 - 0.06876 \times 3951 \end{Bmatrix} kJ/kg_{(DAF)}.K$$

$$= 29.26 \, MJ/kg_{(DAF)} - 298.15 \, K[1.326 - 1.036] kJ/kg_{(DAF)}.K + 697.8 \, kJ/kg_{(DAF)}.K$$

$$= 29.87 \, MJ/kg_{(DAF)} \tag{4.50}$$

The specific chemical exergy of coal (as received), with reference to Table 3.6, can be calculated as follows. The chemical exergy of ash has been ignored in this calculation.

$$\overline{e}^{CH} = 0.7918 \, \overline{e_{(DAF)}}^{CH} + \frac{0.1112}{18.015} \overline{e_{H_2O(l)}}^{CH}$$

$$= 0.7918 \frac{kg_{(DAF)}}{kg} \times 29.87 \frac{MJ}{kg_{(DAF)}} + \frac{0.1112}{18.015} \frac{kmol}{kg} \times 0.045 \frac{MJ}{kmol}$$

$$= 23.65 \frac{MJ}{kg} \tag{4.51}$$

77

4.3 Exergy analysis

Exergy balance and analysis were performed on the components of the integrated model to identify the location and quantity of the exergy destruction rate for the components. This allows for implementation of corrective measures or incorporating better plant integration to minimize the losses. The exergy balance equation for a flow system can be obtained by combining the conservation law of energy and non-conservation law for entropy. Mass, energy and exergy balance for any control volume, with negligible potential and kinetic energy changes, at steady state can be expressed as follows (Dincer et al., 2007; Sato N., 2004; Bejan et al., 1996).

Mass balance: $\qquad \sum_{j=1}^{n} \dot{m}_i = \sum_{j=1}^{n} \dot{m}_e$ $\qquad\qquad\qquad\qquad$ 4.52

Energy balance: $\quad \sum_{j=1}^{n} \dot{Q} - \dot{W} = \sum_{j=1}^{n} \dot{m}_e h_e - \sum_{j=1}^{n} \dot{m}_i h_i$ $\qquad\qquad$ 4.53

Exergy balance:

Exergy input − Exergy output − Exergy consumption / destruction = Exergy accumulation

$$\sum_{j=1}^{n} \dot{m}_i e_i - \sum_{j=1}^{n} \dot{m}_e e_e + \sum_{j}\left(1-\frac{T_0}{T_j}\right)\dot{Q}_j - \dot{W} = \dot{I} \qquad\qquad 4.54$$

Where $\dot{I}$ is the irreversibility rate or the rate of exergy destruction from the control volume and the specific exergy e is represented by equation 4.23. Exergy transfer associated with heat transfer (at the rate $\dot{Q}_j$) occurs in the boundary at location j. The instantaneous temperature at location j is T_j, which is equal to the ambient condition i.e. 298.15K (Cengel et al., 2006; Ameri et al., 2008). Also for all components except the turbines, fans compressors, and pumps $\dot{W} = 0$. In this research work, the exergy destruction rate $(\dot{I})$ for each component and subsystem of the oxy-fuel plant was calculated. Finally, the overall exergy efficiencies (ψ) for

the individual components and the overall plant was calculated and ranked. Based on the exergy efficiencies, appropriate plant improvement measures were recommended and necessary plant design changes were implemented to improve the base integrated oxy-fuel process model. The general definition for the exergy (ψ) and energy efficiency (η) are given below in equations 4.55 and 4.56 (Dincer et al., 2007). However, for specific cases the exergy efficiencies were calculated by the equations presented in a generalised form in Table 4-1 (Bejan et al., 1996; Aljundi I.H., 2009)

Table 4-1 Typical exergy equations used for integrated oxy-fuel plant model

	Exergy destruction Rate	Exergy efficiency
Boiler	$\dot{I}_{Boiler} = \dot{E}_{Fuel} + \dot{E}_{in} - \dot{E}_{out}$	$\psi_{boiler} = \dfrac{(\dot{E}_{out} - \dot{E}_{in})_{Steam}}{\dot{E}_{fuel}}$
Pumps	$\dot{I}_{pump} = \dot{E}_{in} + \dot{W}_{pump} - \dot{E}_{out}$	$\psi_{pump} = \dfrac{\dot{E}_{out} - \dot{E}_{in}}{\dot{W}_{pump}}$
Feed Water Heaters	$\dot{I}_{FWH} = \dot{E}_{in} - \dot{E}_{out}$	$\psi_{FWH} = \dfrac{\dot{E}_{in} - \dot{I}_{FWH}}{\dot{E}_{in}}$
Turbine	$\dot{I}_{turbine} = \dot{E}_{in} - \dot{E}_{out} - \dot{W}_{el}$	$\psi_{turbine} = \dfrac{\dot{W}_{el}}{\dot{E}_{in} - \dot{E}_{out}}$
Compressor	$\dot{I}_{condenser} = \dot{E}_{in} + \dot{W}_{pump} - \dot{E}_{out}$	$\psi_{compressor} = \dfrac{\dot{E}_{out} - \dot{E}_{in}}{\dot{W}_{compressor}}$
Cycle	$\dot{I}_{cycle} = \sum \dot{I}_{cycle\ allcomponents}$	$\psi_{cycle} = \dfrac{\dot{W}_{el\ out}}{\dot{E}_{fuel}}$

$$\eta = \frac{Energy\ output}{Total\ energy\ input} \qquad 4.55$$

$$\psi = \frac{Exergy\ output}{Total\ exergy\ input}$$

4.56

The equations for the exergy analysis and subsequent process stream data for the base oxy-fuel model are described in this section. The results and the detailed comparison data for the base and the improved model are discussed in chapter 5 for further analysis and process improvement applications.

The overall cycle exergy efficiency can be expressed either with respect to the gross electrical output, as shown in Table 4.1, or with respect to the total exergy destruction mentioned below:

$$\psi_{cycle} = \frac{\dot{E}_{fuel} - \sum \dot{I}_{cycle\ allcomponents}}{\dot{E}_{fuel}}$$

4.57

In this study the cycle exergy efficiency is calculated by equation 4.57. The cycle exergy efficiency calculated by equation 4.57 gives a clear understanding about the exergy performance of the integrated power plant. However, the other method does not show directly the actual exergy performance of the plant. The cycle exergy efficiency expressed in Equation 4.57 will always be higher compared to the cycle efficiency calculated by the method shown in Table 4-1. This is because the electrical output is always much lower than the exergy utilization number $(\dot{E}_{fuel} - \sum \dot{I}_{cycle\ allcomponents})$ in an energy conversion system.

In general the equations mentioned in Table 4-1 are utilized for the exergy calculation for different unit operations in this study. Different process streams used for the exergy analysis are indicated in the respective HYSYS process flow diagrams attached in Appendix C.

4.3.1 Exergy reference environment streams

Reference streams are created in the process flow diagrams for each main stream that are involved in exergy calculation. Essentially all the process streams mentioned in Tables 4.2, 4.4 4.7 and 4.8 and few other relevant process streams have parallel reference streams that generates exergy data automatically at reference environment condition if there is any change in the process stream parameters, compositions or change in reference condition. The

reference data are necessary for all the exergy calculation. These reference streams are also connected with the input output block through temperature input parameter. If the reference temperature is desired to change for the overall flow sheet it can be done by a single change at the input/output block.
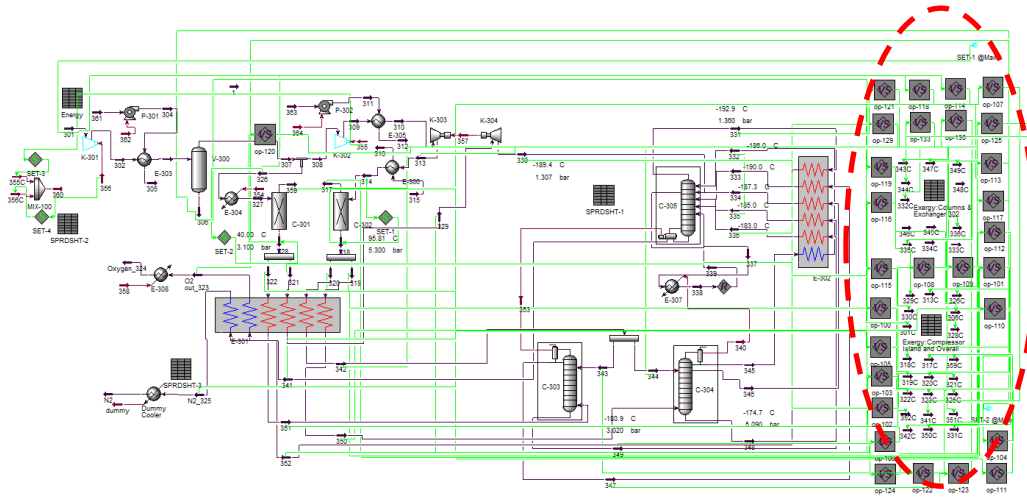
Figure 4-4 Exergy reference environment streams in HYSYS

The reference streams and the associated calculation box are shown in Figure 4-4 in the dotted area for the ASU process model. If any parameter change happens in the main process streams it mirror images the stream compositions and parameters in the reference streams. So the exergy data for the reference condition is always updated. As an example, if a new coal is used instead of the coal in this current study, it will change the process parameters and composition in the boiler and flue gas section as well as ASU, BOP and CO_2CCU for all the process streams. However, as the parallel reference streams are created with instantenious update facility, it will automatically update all the reference streams accordingly and generate new and accurate exergy data.

4.3.2 Exergy analysis for BOP

The BOP section is divided into 13 (thirteen) control volumes. However, detailed exergy equations are only provided here for FWH1 and the CV1 (Figures 3-3 and 3-8). The equations

81

for the other feed water heaters are similar but with different stream numbers. Equations for all the individual heaters, pumps and deaerator and condenser are implemented in HYSYS process model and the exergy results of those are presented in chapter 5. The generalised form of the equations for these equipment are given in Table 4-1. Details of the equations for these equipment are included in Table 4-3. Typical energy balance equations for FWH1 are given below in equations 4.58, 4.59 and 4.60. However, no results are presented here for the energy analysis for any equipment in the BOP or any other section as the energy data was already in use for the exergy calculation.

$$\sum_{j=1}^{n} \dot{Q} - \dot{W} = \sum_{j=1}^{n} \dot{m}_e h_e - \sum_{j=1}^{n} \dot{m}_i h_i \qquad 4.58$$

$$\dot{Q} = \dot{m}_4 h_4 + \dot{m}_{20} h_{20} - \dot{m}_{27} h_{27} - \dot{m}_3 h_3 - \dot{m}_{19} h_{19} \qquad 4.59$$

$$\eta_{FWH1} = \frac{\dot{m}_4 h_4 + \dot{m}_{20} h_{20}}{\dot{m}_{27} h_{27} + \dot{m}_3 h_3 + \dot{m}_{19} h_{19}} \qquad 4.60$$

The exergy analysis equations for FWH1 is presented below

$$\sum_{j=1}^{n} \dot{m}_i e_i - \sum_{j=1}^{n} \dot{m}_e e_e + \sum_j \left(1 - \frac{T_0}{T_j}\right) \dot{Q}_j - \dot{W} = \dot{I} \qquad 4.61$$

Assuming the heat exchangers are adiabatic or the temperature of the boundary (the outer surface of the heat exchanger) T_j is equal to T_0, the generalized equation 4.54 and the efficiency equation in Table 4-1 for the FWH1 takes the following form.

$$\dot{I}_{FWH1} = \dot{E}_{27} + \dot{E}_3 + \dot{E}_{19} - \dot{E}_{20} - \dot{E}_4 \qquad 4.62$$

$$\psi_{FWH1} = \frac{\dot{E}_4 + \dot{E}_{20}}{\dot{E}_{27} + \dot{E}_{19} + \dot{E}_3} \qquad 4.63$$

Exergy analysis data for all the process streams in the BOP section is presented in Table 4-2. Plugging in data from Table 4-2 into equation 4.62 and 4.63, we get the exergy destruction amount and exergy efficiency for FWH1 as $1454\ kW\ and\ 76.89\%$ respectively. The turbine island in the BOP section is considered to be one single control volume and it is shown in the BOP process diagram as CV1 (Figure 3-3). The exergy balance and efficiency equations for CV1 can be similarly written with reference to equation 4.54 and Table 4-1 as follows:

$$
\begin{aligned}
\dot{I}_{CV1} = &\ \dot{E}_{46} + \dot{E}_{45} - \dot{E}_{31} - \dot{E}_{21} - \dot{E}_{23} - \dot{E}_{28} - \dot{E}_{29} - \dot{E}_{30} - \dot{E}_{32} - \dot{E}_{24} - \dot{E}_{25} - \dot{E}_{22} - \\
&\ \dot{E}_{47} - \dot{E}_{27} - \dot{E}_{36} - \dot{E}_{37} - \dot{E}_{42}
\end{aligned}
\qquad 4.64
$$

$$
\psi_{CV1} = \frac{\dot{E}_{31} + \dot{E}_{21} + \dot{E}_{23} + \dot{E}_{28} + \dot{E}_{29} + \dot{E}_{30} + \dot{E}_{32} + \dot{E}_{24} + \dot{E}_{25} + \dot{E}_{22} + \dot{E}_{47} + \dot{E}_{27} + \dot{E}_{36} + \dot{E}_{37} + \dot{E}_{42}}{\dot{E}_{45} + \dot{E}_{46}}
\qquad 4.65
$$

Plugging in data from Table 4-2 into equation 4.64 and 4.65 we get the exergy destruction amount and exergy efficiency of CV1 as $96.88\ MW\ and\ 89.03\ \%$ respectively. Considering the efficiency numbers for FWH1 and CV01, it is clear that FWH1 could be a good candidate for implementing exergy efficiency improvement measures.

Table 4-2 Stream parameters for exergy analysis for the overall BOP section

Stream No.	Temperature	Pressure	Flow rate	specific enthalpy	specific entropy	Specific exergy	Exergy	Exergy
	°C	bar a	m (kg/hr)	h (kJ/kg)	s (kJ/kg-K)	e (kJ/kg)	$\dot{E}$ (kJ/hr)	$\dot{E}$ (kW)
1	38.39	0.069	1684554.65	160.40	0.55	1.12	1888775.35	524.70
2	38.56	17.24	1684554.65	162.64	0.55	2.87	4838974.51	1344.27
3	39.09	16.89	1684554.65	164.83	0.56	2.94	4946075.31	1374.02
4	60.86	16.55	1684554.65	255.76	0.84	9.89	16664524.24	4629.40
5	83.78	15.86	1684554.65	351.74	1.12	22.94	38646890.48	10736.11
6	105.7	15.51	1684554.65	443.98	1.37	40.37	68011230.20	18893.52
7	149.5	15.17	1684554.65	630.29	1.84	87.91	148095157.75	41140.83
8	176.2	9.17	2205131.45	745.99	2.10	124.01	273453659.70	75965.43
10	182.3	289.6	2205131.45	787.96	2.13	158.94	350473287.67	97361.48
11	215.8	289.2	2205131.45	933.78	2.44	212.62	468853120.35	130247.40
12	261.6	288.9	2205131.45	1141.84	2.84	299.41	660244180.87	183415.83
HTS12	292.2	288.5	2205131.45	1289.59	3.11	367.04	809367572.11	224842.31
13	290.3	74.81	171252.06	1291.49	3.16	352.83	60423548.97	16785.66
14	260.7	47.54	390988.19	1138.48	2.89	281.01	109872238.40	30522.51
15	214	20.67	482841.12	915.92	2.46	186.53	90066459.96	25020.46
16	108.9	1.382	119809.54	456.37	1.41	41.89	5018803.45	1394.22
18	86.89	0.624	179117.11	363.59	1.16	23.63	4231934.78	1175.63
19	66.33	0.269	238868.77	277.32	0.91	10.89	2601967.99	722.83
20	44.83	0.096	294599.28	187.34	0.64	2.54	748949.26	208.06
21	415.5	74.8	171252.06	3194.00	6.48	1268.20	217181558.26	60333.04
22	361.4	47.5	219736.13	3107.16	6.53	1163.82	255732361.91	71042.45
23	501	20.74	91852.94	3469.15	7.42	1261.75	115895838.41	32195.86
24	305	4.75	119809.54	3075.90	7.50	843.10	101011707.38	28061.05
25	160.7	1.25	59307.57	2796.25	7.56	547.68	32481559.10	9023.38
26	121.7	0.56	59751.66	2724.73	7.76	417.11	24923122.74	6923.64
27	63.56	0.24	55730.51	2550.04	7.66	270.89	15097093.03	4193.97
28	362.6	49	202.12	3107.16	6.52	1167.64	236005.76	65.56
29	598.9	242.3	11383.13	3494.15	6.38	1596.97	18178531.38	5050.00
30	386.2	9.5	41140.30	3236.60	7.45	1020.19	41970760.28	11659.48
31	362.6	49	1801274.60	3107.16	6.52	1167.64	2103247951.54	584282.28
32	429.2	9.5	6180.19	3327.62	7.58	1071.33	6621019.48	1839.32
35	429.2	9.5	1586.09	3327.62	7.58	1071.33	1699224.70	472.04
36	38.75	0.07	1234128.36	2391.36	7.70	99.21	122436407.45	34012.83
37	52.26	0.14	130692.98	2572.30	7.97	201.80	26373520.68	7326.56
38	15	1.014	22280.92	62.69	0.22	0.72	16119.14	4.48
39	100	1.014	1267.01	418.81	1.31	33.96	43029.07	11.95
40	21.11	4.826	60000000.00	88.62	0.31	0.49	29544127.80	8207.36
41	33.4	4.482	60000000.00	139.94	0.48	0.83	49866506.36	13852.92
42	386.2	9.5	8176.09	3236.60	7.45	1020.19	8341129.98	2317.17
45	621.1	45.22	1801274.60	3717.83	7.36	1526.73	2750057814.38	763966.06
46	598.9	242.3	2206032.00	3494.15	6.38	1596.97	3522971198.56	978681.40
47	103.6	0.56	56424.57	2689.18	7.66	409.04	23080157.32	6411.67
48	65.56	9.17	7284.19	274.80	0.90	11.39	82946.87	23.04

Table 4-3 Exergy balance equations for BOP section (Fig B-3)

Unit Operation	Exergy In $\dot{E}$	Exergy Out $\dot{E}$	Exergy Destruction $\dot{I}$	Exergy Efficiency ψ
FWH2	E18+E26+E4	E5+E19	E18+E26+E4-(E5+E19)	(E5+E19)*100/E18+E26+E4
FWH3	E5+E16+E25	E6+E18	E5+E16+E25-(E6+E18)	(E6+E18)*100/E5+E16+E25
FWH4	E24+E6	E16+E7	E24+E6-(E16+E7)	(E16+E7)*100/E24+E6
FWH6	E23+E10+E14	E11+E15	E23+E10+E14-(E11+E15)	(E11+E15)*100/E23+E10+E14
FWH7	E22+E11+E13	E12+E14	E22+E11+E13- (E12+E14)	(E12+E14)*100/E22+E11+E13
FWH8	E21+E12	E13+EHTS12	E21+E12-(E13+EHTS12)	(E13+EHTS12)*100/E21+E12
Deaerator	E28+E29+E30+E15+E7+E48	E8	E28+E29+E30+E15+E7+E48-E8	E8*100/E28+E29+E30+E15+E7+E48
Condenser	E36+E37+E38+E39+E40+E20+E35	E41+E1	E36+E37+E38+E39+E40+E20+E35-(E41+E1)	(E41+E1)*100/E36+E37+E38+E39+E40+E20+E35
Cond Pump P003	E1+W51	E2	E1+W51-E2	(E2-E1)*100/W51
BFW Pump P001	E8+W52	E10	E8+W52-E10	(E10-E8)*100/W52
CW Pump P002	E49+W50	E40	E49+W50-E40	(E40-E49)*100/W50

4.3.3 Exergy analysis for boiler and flue gas section

The boiler and flue gas section is divided into eleven (11) control volumes. The exergy data summarized for the boiler and flue gas section indicates that most of the exergy destruction in this section takes place in the combustion chamber as it is a major location for thermodynamic inefficiencies. The irreversibilities are associated with chemical reaction, heat transfer and friction where combustion reactions are the significant source of the exergy destruction. The exergy analysis equations for the control volume CV201 (in Figure 3-2) representing the main combustor is given below. The equations for the rest of the control volumes are included in Table 4-5. Following are the exergy analysis equations for the control volume CV201 derived from the generic equation of the boiler in Table 4-1. The generalized balance equation (4.54) takes the following form for the control volume CV201 for exergy destruction. The exergy analysis data for all the process streams of the boiler and flue gas section is presented in Table 4-4.

$$\dot{I}_{CV201} = \dot{E}_{201} + \dot{E}_{202} + \dot{E}_{205} + \dot{E}_{207} + \dot{E}_{236} + \dot{E}_{240} - \dot{E}_{212} - \dot{E}_{208} - \dot{E}_{46} + \dot{E}_{HTS12} - \dot{E}_{31} + \dot{E}_{45}$$

$$4.66$$

Plugging in data from Table 4-4 into equation 4.66 we get the exergy destruction amount of CV201 as $2259.3MW$ $(4629.3 - 2370)$. The exergy efficiency of CV201 is calculated using equation 4.67 where the total exergy input by the fuel is $\dot{E}_{201} = 3753MW$.

Table 4-4 Stream parameters for exergy analysis for the boiler and flue gas section

Stream No.	Temperature	Pressure	Flow rate	specific enthalpy	specific entropy	Specific exergy	Exergy	Exergy
	°C	bar a	m (kg/hr)	h (kJ/kg)	s (kJ/kg-K)	e (kJ/kg)	$\dot{E}$ (kJ/hr)	$\dot{E}$ (kW)
201	25.00	1.01	452240.39	10601.80	7.25	29870.03	13508433814.04	3752642.91
202	25.00	1.01	0.00	15924.99	5.38	0.00	0.00	0.00
203	40.00	1.01	577929.81	15938.59	5.17	0.33	190818.39	53.01
205	40.00	1.01	5.78	15938.59	5.17	0.33	1.91	0.00
207	25.00	1.01	44727.64	15924.99	5.40	0.13	5801.66	1.61
208	-	-	60865.47	28103.69	39.78	8219.33	500273544.27	138975.99
213	395.00	1.01	2549535.17	7734.38	6.02	178.89	456077697.39	126698.38
214	395.00	1.01	1274767.58	7734.38	6.02	178.89	228038848.69	63349.19
215	395.00	1.01	1274767.58	7734.38	6.02	178.89	228038848.69	63349.19
216	168.90		1274767.58	7470.53	5.54	58.28	74287912.45	20637.18
217	209.50	1.01	1274767.58	7515.85	5.64	74.35	94782454.50	26330.57
218	25.00	1.01	0.00	15924.99	5.38	0.00	0.00	0.00
219	209.50	1.01	1274767.58	7515.85	5.64	74.30	94713543.14	26311.42
220	187.00	0.97	1274767.58	7490.64	5.59	62.18	79261194.92	22018.76
222	178.00	0.97	2549535.17	7480.60	5.57	58.71	149682473.57	41581.79
223	185.00	1.03	2549535.17	7489.16	5.57	65.88	167950997.50	46656.79
225	30.00	4.00	6339907.50	125.82	0.44	0.47	3006491.30	835.20
226	60.00	4.00	6339907.50	251.11	0.83	8.26	52360124.01	14545.64
227	57.20	1.03	2549535.17	7177.60	4.71	12.90	32900051.07	9139.63
230	57.20	1.03	1535502.79	7725.40	4.80	13.41	20585223.28	5718.58
231	78.40	0.99	1535502.79	7746.32	4.87	13.44	20629936.16	5731.00
235	65.90	0.99	972176.34	9984.14	5.06	6.16	5990465.08	1664.15
236	355.00	1.11	972176.34	10282.77	5.67	124.01	120557877.58	33490.98
238	65.90	0.99	1141250.48	9984.14	5.06	6.16	7032285.09	1953.57
239	70.00	1.05	1141250.48	9988.06	5.06	10.69	12205199.90	3390.60
240	355.00	1.05	1141250.48	10282.78	5.68	120.19	137166680.20	38104.90
242	57.20	1.03	827208.47	7725.40	4.80	13.41	11089703.77	3080.72
243	50.00	1.01	827208.47	7656.21	4.60	5.76	4762958.30	1323.15
245	50.00	1.01	805525.24	7856.35	4.63	5.81	4676173.75	1299.04
246	56.47	1.01	208507.14	246.81	3.48	6.26	1305159.44	362.57
266	78.46	1.11	972176.34	9996.22	5.07	15.66	15228953.42	4230.60
268	72.33	1.05	1141250.48	9990.31	5.07	11.00	12549166.21	3486.16
273	30.00	3.80	1718348.43	125.79	0.44	0.45	780161.24	216.73
274	38.00	3.78	1718348.43	159.10	0.55	1.42	2446895.65	679.75
275	30.00	1.00	6339907.50	125.42	0.44	0.17	1085523.92	301.56
277	30.00	1.00	1718348.43	125.42	0.44	0.17	294216.96	81.73
212								1339912.56
265				Energy Streams				3260.61
267								1955.36
224								6060.55

86

$$\psi_{CV201} = \frac{(\dot{E}_{46} - \dot{E}_{HTS12}) + (\dot{E}_{31} - \dot{E}_{45})}{\dot{E}_{201} + \dot{E}_{202} + \dot{E}_{205} + \dot{E}_{207} + \dot{E}_{236} + \dot{E}_{240} - \dot{E}_{212} - \dot{E}_{208}} * 100$$

<div align="right">4.67</div>

Using the data from Table 4-4 in equation 4.67 we get the exergy efficiency of the combustion chamber as 39.67% . The total exergy destruction percentage in the combustion boiler with respect to the fuel exergy input is found to be 60.2 % (2259.3*100/3753). The details of the exergy analysis results for the boiler and flue gas section are analyzed in chapter 5.

Table 4-5 Exergy balance equations for boiler and flue gas section (Fig B-2)

Unit Operation	Exergy In $\dot{E}$	Exergy Out $\dot{E}$	Exergy Destruction i	Exergy Efficiency ψ
PAF CV202	E235+W265	E266	E235+W265-E266	(E266-E235)*100/W265
SAF CV 203	E238+W267	E268	E238+W267-E268	(E268-E238)*100/W267
PAPH CV 204	E214+E266	E217+E236	E214+E266-(E217+E236)	(E217+E236)*100/(E214+E266)
SAPH CV 205	E215+E239	E240+E216	E215+E239-(E240+E216)	(E240+E216)*100/(E215+E239)
RAPH CV 206	E219+E230	E220+E231	E219+E230-(E220+E231)	(E220+E231)*100/(E219+E230)
FDF CV 207	E222+W224	E223	E222+W224-E223	(E223-E222)*100/W224
PGCooler1_CV208	E223+E225	E226+E227	E223+E225-(E226+E227)	(E226+E227)*100/(E223+E225)
PGCooler2_CV209	E242+E273	E243+E274	E242+E273-(E243+E274)	(E243+E274)*100/(E243+E274)
CW P201	E275+W276	E225	E275+W276-E225	(E225-E275)*100/W276
CW P202	E277+W278	E273	E277+W278-E273	(E273-E277)*100/W278

4.3.4 Exergy analysis for ASU

The ASU section is divided into eight (8) control volumes (Figures 3-4 and 3-9). The compressor (CV 301) and the distillation section (CV307) have the highest exergy destruction. Detailed exergy equations for these two sections are given below. The results for all the control volumes, e .g. the individual heat exchangers, dryer section and pumps, including CV301, and CV307 are analyzed in chapter 5. The generalised form of the equations for these control volumes are given in Table 4-1. Details of the equations for the other control volumes are included in Table 4-6. Following are the exergy analysis equations for the control volumes CV301 and CV307 derived from the generic equations in Table 4-1. The generalized balance equation 4.54 and exergy efficiency equation in Table 4-1 take the following form for the

control volumes for exergy destruction and exergy efficiency calculation. The exergy analysis data for all the process streams of the ASU is presented in Table 4-7.

$$\dot{I}_{CV301} = \dot{W}_{compressor(360)} + \dot{E}_{301} + \dot{E}_{304} + \dot{E}_{311} + \dot{E}_{329} - \dot{E}_{330} - \dot{E}_{313} - \dot{E}_{312} - \dot{E}_{326} - \dot{E}_{306} - \dot{E}_{305}$$

4.68

$$\psi_{CV301} = \frac{\dot{E}_{330} + \dot{E}_{313} + \dot{E}_{312} + \dot{E}_{326} + \dot{E}_{306} + \dot{E}_{305} - \dot{E}_{301} - \dot{E}_{304} - \dot{E}_{311} - \dot{E}_{329}}{\dot{W}_{compressor(360)}} * 100 \qquad 4.69$$

Plugging in data from Table 4-7 into equation 4.68 and 4.69, we get the exergy destruction amount and exergy efficiency for the compressor section as 29.78 *MW and* 73.48% respectively. Similarly for control volume CV307 (distillation section) the equations are

$$\dot{I}_{CV307} = \dot{E}_{330} + \dot{E}_{342} + \dot{E}_{351} + \dot{E}_{350} + \dot{E}_{236} + \dot{E}_{335} + \dot{E}_{334} + \dot{E}_{233} + \dot{E}_{332} -$$
$$- \dot{E}_{341} - \dot{E}_{347} - \dot{E}_{349} - \dot{E}_{348} - \dot{E}_{346} - \dot{E}_{345} - \dot{E}_{331} \qquad 4.70$$

$$\psi_{CV307} = \frac{\dot{E}_{341} + \dot{E}_{347} + \dot{E}_{349} + \dot{E}_{348} + \dot{E}_{346} + \dot{E}_{345} + \dot{E}_{331}}{\dot{E}_{330} + \dot{E}_{342} + \dot{E}_{351} + \dot{E}_{350} + \dot{E}_{236} + \dot{E}_{335} + \dot{E}_{334} + \dot{E}_{233} + \dot{E}_{332}} * 100 \qquad 4.71$$

Table 4-6 Exergy balance equations for ASU (Fig B-4)

Unit Operation	Exergy In $\dot{E}$	Exergy Out $\dot{E}$	Exergy Destruction $\dot{I}$	Exergy Efficiency ψ
Dryer CV 302	E313+E315+E326	E316+E317+E359+ E328+E318	E313+E315+E326- (E316+E317+E359+E328+E318)	(E316+E317+E359+E328+E318)*100/ (E313+E315+E326)
LNG CV 303	E319+E320+E321+ E322+E352+E341	E329+E323+E325+ E351+E342+E350	E319+E320+E321+E322+E352+E341- (E329+E323+E325+E351+E342+E350)	(E329+E323+E325+E351+E342+E350) *100/ (E319+E320+E321+E322+E352+E341)
Column CV 305	E330+E353+E344+ E350+E336+E335+ E334+E333+E332	E341+E348+E346+ E345+E331	(E330+E353+E344+E350+E336+E335+ E334+E333+E332)- (E341+E348+E346+E345+E331)	(E341+E348+E346+E345+E331)*100/ (E330+E353+E344+E350+E336+E335+ E334+E333+E332)
LNG CV 306	E349+E348+E346+ E347+E331+E345	E336+E335+E334+ E333+E332+E352	E349+E348+E346+E347+E331+E345- (E336+E335+E334+E333+E332+E352)	(E336+E335+E334+E333+E332+E352) *100/(E349+E348+E346+E347+E331+ E345)
CW Pump P301	E361+W362	E304	E361+W362-E304	(E304-E361)*100/W362
CW Pump P302	E363+W264	E311	E363+W264-E311	(E311-E363)*100/W264

Table 4-7 Stream parapeters for exergy analysis for ASU

Stream No.	Temperature	Pressure	Flow rate	Specific enthalpyh	Specific entropy	Specific exergy	Exergy	Exergy
	°C	bar a	m (kg/hr)	h (kJ/kg)	s (kJ/kg-K)	e (kJ/kg)	$\dot{E}$ (kJ/hr)	$\dot{E}$ (kW)
301	9.00	1.01	2460379.30	15819.82	5.37	0.35	859569.15	238.79
304	30.00	3.80	7928976.96	125.79	0.44	0.45	3599898.80	1000.05
305	38.00	3.60	7928976.96	159.09	0.55	1.41	11151639.69	3097.93
306	40.00	3.30	0.00	149.28	3.19	2.18	0.00	0.00
311	30.00	4.00	21156.02	125.82	0.44	0.47	10032.54	2.79
312	85.00	3.80	21156.02	355.90	1.13	22.59	478017.17	132.79
313	97.80	5.41	1227943.32	15909.33	5.16	151.54	186080691.65	51693.22
315	30.00	2.00	9534.85	125.51	0.44	0.27	2588.90	0.72
316	92.80	1.80	9534.85	388.58	1.23	28.19	268790.91	74.67
317	152.00	5.30	8415.35	3054.45	8.86	630.69	5307472.82	1474.42
318	95.81	5.30	1219527.97	15995.98	5.12	148.86	181545012.07	50433.20
319	95.81	5.30	604999.29	15995.98	5.12	148.86	90063209.67	25019.56
320	95.81	5.30	614528.68	15995.98	5.12	148.86	91481802.40	25413.64
321	40.00	3.10	741921.44	15939.59	5.11	96.00	71225366.52	19786.41
322	40.00	3.10	482068.40	15939.59	5.11	96.00	46279156.32	12856.35
323	15.54	1.60	577851.33	15916.23	4.98	35.37	20440558.80	5678.39
325	74.99	1.20	1865666.29	15977.06	5.41	18.85	35166555.84	9769.27
326	40.00	3.30	1232435.98	15850.56	5.13	101.69	125321866.14	34814.41
328	40.00	3.10	1223989.83	15939.59	5.11	96.00	117504522.85	32642.76
329	-173.50	3.01	741921.44	15724.12	3.96	223.41	165750614.99	46045.52
330	-189.40	1.31	741921.44	15707.53	4.00	194.46	144277339.16	40080.24
331	-192.90	1.36	1865666.29	15701.13	3.86	203.99	380584364.36	105726.34
332	-186.00	4.89	306315.98	15519.31	1.57	702.49	215183984.45	59778.11
333	-190.00	2.82	304102.77	15511.66	1.49	720.94	219241180.93	60905.20
334	-187.30	4.96	427121.84	15518.94	1.69	692.62	295832207.03	82182.19
335	-185.00	2.92	292464.61	15524.14	1.80	665.25	194561570.46	54049.20
336	-183.00	4.99	371591.16	15527.68	1.84	659.88	245204576.03	68117.83
341	-178.80	1.72	577851.33	15535.63	1.79	605.98	350166283.45	97276.19
342	-176.80	5.10	614528.68	15544.15	1.97	635.65	390625803.39	108515.85
343	-176.80	5.10	114498.98	15544.15	1.97	635.65	72781399.69	20218.67
344	-176.80	5.10	500029.70	15544.15	1.97	635.65	317844403.70	88297.18
345	-179.10	4.99	306315.98	15533.79	1.73	669.33	205027934.00	56956.76
346	-177.00	5.04	427121.84	15539.26	1.92	646.39	276085643.35	76696.59
347	-185.40	2.92	304102.77	15520.80	1.59	698.24	212335973.21	58986.93
348	-174.70	5.09	371591.16	15543.56	2.00	625.58	232459986.51	64577.38
349	-180.90	3.02	292464.61	15531.70	1.88	647.86	189476979.36	52636.70
350	-173.50	5.09	604999.29	15720.30	3.78	271.92	164509320.18	45700.69
351	-178.50	3.02	482068.40	15718.79	3.90	234.72	113149958.62	31433.06
352	-180.60	1.31	1865666.29	15713.99	4.02	169.22	315702582.71	87702.18
359	133.10	3.10	8446.14	2948.78	8.82	537.30	4538105.75	1260.69
361	30.00	1.00	7928976.96	125.42	0.44	0.17	1357605.63	377.14
363	30.00	1.00	21156.02	125.42	0.44	0.17	3622.35	1.00

Plugging in data from Table 4-7 into equation 4.70 and 4.71, we get the exergy destruction amount and exergy efficiency for the distillation column section control volume CV307 as 37.91 *MW and* 93.12% respectively.

4.3.5 Exergy analysis for CO$_2$CCU

The CO$_2$CCU section is divided into seven (7) control volumes excluding the cooling water pumps (Figures 3-5 and 3-10). The compressor sections have the highest exergy destruction. Detail exergy equations for the control volume CV101 and CV102 are given below. The results for all the other control volumes, including CV101 and CV102 are analyzed in chapter 5. The generalised form of the equations for these control volumes are given in Table 4-1. Details of the equations for the other control volumes are included in Table 4-9. Following are the exergy analysis equations for the control volume CV101 and CV102 derived from the generic equations in Table 4-1. The generalized balance equation 4.54 and exergy efficiency equation in Table 4-1 take the following form for exergy destruction and exergy efficiency calculation. The exergy analysis data for all the process streams of the CO$_2$CCU are presented in Table 4-8.

$$\dot{I}_{CV101} = \dot{W}_{compressor(185)} + \dot{E}_{101} + \dot{E}_{168} + \dot{E}_{171} + \dot{E}_{173} + \dot{E}_{156} + \dot{E}_{131} + \dot{E}_{158} -$$
$$- \dot{E}_{169} - \dot{E}_{172} - \dot{E}_{174} - \dot{E}_{157} - \dot{E}_{159} - \dot{E}_{112} - \dot{E}_{114} \qquad 4.72$$

$$\psi_{CV101} = \frac{\dot{E}_{169} + \dot{E}_{172} + \dot{E}_{174} + \dot{E}_{157} + \dot{E}_{159} + \dot{E}_{112} + \dot{E}_{114} - (\dot{E}_{101} + \dot{E}_{168} + \dot{E}_{171} + \dot{E}_{173} + \dot{E}_{156} + \dot{E}_{131} + \dot{E}_{158})}{\dot{W}_{compressor(185)}} * 100 \qquad 4.73$$

Plugging in data from Table 4-8 into Equation 4.72 and 4.73, we get the exergy destruction amount and exergy efficiency for the compressor section control volume CV101 as 22.73 *MW and* 68.29% respectively. Similarly for control volume CV102 the equations are,

$$\dot{I}_{CV102} = \dot{W}_{compressor(188)} + \dot{E}_{128} + \dot{E}_{144} + \dot{E}_{176} + \dot{E}_{178} + \dot{E}_{180} - \dot{E}_{149} - \dot{E}_{181} - \dot{E}_{179} - \dot{E}_{177} \qquad 4.74$$

Table 4-8 Stream parameters for exergy analysis for the CO₂CCU

Stream No.	Temperature	Pressure	Flow rate	Specific enthalpy	Specific entropy	Specific exergy	Exergy	Exergy
	°C	bar a	m (kg/hr)	h (kJ/kg)	s (kJ/kg-K)	e (kJ/kg)	$\dot{E}$ (kJ/hr)	$\dot{E}$ (kW)
101	50.00	1.01	805525.24	7856.35	4.63	5.78	4653312.85	1292.69
112	35.00	29.98	961260.61	8266.92	3.48	195.12	187557847.93	52103.57
114	47.80	3.96	46010.34	229.14	3.37	3.72	171119.84	47.54
116	25.00	30.00	960104.99	8263.44	3.44	194.67	186904741.27	51922.14
117	-18.28	29.80	960104.99	8148.35	3.00	209.07	200730779.93	55763.01
121	-18.28	29.80	214909.81	8593.13	3.32	202.52	43523378.23	12090.79
122	-38.20	15.00	214909.81	8572.62	3.35	173.33	37250348.57	10348.15
123	-38.20	15.00	201745.71	8695.27	3.45	168.93	34081693.45	9467.89
124	-38.20	15.00	13164.10	6692.87	1.84	225.87	2973373.43	826.00
125	-37.41	29.70	13164.10	6694.65	1.85	227.02	2988529.60	830.21
127	-27.42	18.80	254387.06	6820.58	2.05	216.71	55129265.70	15314.91
128	2.00	18.60	254387.06	7127.91	3.27	159.54	40585377.45	11274.62
131			201745.71	8751.61	3.67	160.59	32398745.26	9000.37
132	-18.28	29.80	501456.23	8593.13	3.32	202.52	101554549.20	28211.85
133	-50.00	29.60	501456.23	8335.29	2.26	260.24	130499716.54	36252.82
134	-50.00	29.60	127276.45	12553.35	3.65	250.53	31886027.96	8857.94
135	-50.00	29.60	374179.78	6900.53	1.794099	243.7427	91203604.55	25336.36
136	-41.63	29.4	127276.45	12562.43	3.687337	247.2659	31471121.26	8742.677
137	7.00	29.20	127276.45	12611.90	3.88	238.40	30342344.10	8429.10
140	21.26	1.10	127276.45	12638.57	4.75	5.96	758158.14	210.62
141	-46.44	29.4	374179.78	6908.79	1.830916	241.0285	90188008.25	25054.23
142	-55	9.736	374179.78	6908.79	1.847783	235.9991	88306099.73	24531.43
143	-40	9.536	374179.78	7242.97	3.313442	133.1534	49823296.52	13840.91
144	2.00	9.34	374179.78	7282.13	3.47	125.18	46841400.63	13012.54
149	43.00	109.80	628566.84	7100.60	2.70	225.37	141661539.18	39353.58
156	30.03	3.80	1759062.43	125.79	0.44	0.45	798646.13	221.86
157	38.00	3.60	1759062.43	159.09	0.55	1.41	2474017.84	687.28
158	30.03	3.80	2001024.09	125.79	0.44	0.45	908501.09	252.38
159	38.00	3.60	2001024.09	159.09	0.55	1.41	2814322.67	781.82
168	30.03	4.00	323934.22	125.82	0.44	0.47	153615.08	42.67
169	85.00	3.80	323934.22	355.90	1.13	22.59	7319247.77	2033.29
171	30.03	4.00	926957.54	125.82	0.44	0.47	439578.93	122.12
172	60.00	3.80	926957.54	251.09	0.83	8.24	7637060.55	2121.58
173	30.03	4.00	343895.35	125.82	0.44	0.47	163080.99	45.30
174	85.00	3.80	343895.35	355.90	1.13	22.59	7770266.74	2158.58
176	30.03	3.80	210675.51	125.79	0.44	0.45	95650.49	26.57
177	38.00	3.60	210675.51	159.09	0.55	1.41	296302.71	82.31
178	30.03	4.00	151731.23	125.82	0.44	0.47	71953.51	19.99
179	85.00	3.80	151731.23	355.90	1.13	22.59	3428345.67	952.39
180	30.03	3.80	3954060.45	125.79	0.44	0.45	1795214.89	498.71
181	38.00	3.60	3954060.45	159.09	0.55	1.41	5561153.44	1544.89

$$\psi_{CV102} = \frac{\dot{E}_{149} + \dot{E}_{181} + \dot{E}_{179} + \dot{E}_{177} - (\dot{E}_{128} + \dot{E}_{144} + \dot{E}_{176} + \dot{E}_{178} + \dot{E}_{180})}{\dot{W}_{compressor(188)}} * 100 \qquad 4.75$$

Plugging in data from Table 4-8 into Equation 4.74 and 4.75, we get the exergy destruction amount and exergy efficiency for the compressor section control volume CV102 as 10.31 *MW and* 62.38% respectively.

Table 4-9 Exergy balance equations for CO$_2$CCU (Fig B-5)

Unit Operation	Exergy In $\dot{E}$	Exergy Out $\dot{E}$	Exergy Destruction $\dot{i}$	Exergy Efficiency ψ
MP Expand CV103	E137+W162+W163	E140+W155	E137+W162+W163-(E140+W155)	W155*100/(E137+W162+W163-E140)
Pum P101 CV104	E124+W165	E125	E124+W165-E125	(E125-E124)*100/W165
Exp K106 CV 105	E121	E122+W154	E121-(E122+W154)	W154*100/(E121-E122)
LNG 101 CV 106	E136+E123+E127+E143+E116	E117+E144+E128+E137+E131	E136+E123+E127+E143+E116-(E117+E144+E128+E137+E131)	(E117+E144+E128+E137+E131)*100/(E136+E123+E127+E143+E116)
LNG 102 CV 107	E132+E134+E135+E142	E141+E133+E136+E143	E132+E134+E135+E142-(E141+E133+E136+E143)	(E141+E133+E136+E143)*100/E132+E134+E135+E142

In addition to the above exergy equations and details for all four sections of the process model, the exergy analysis often also includes exergy destruction ratios. These ratios along with the exergy performance results of all the other unit operations and efficiency improvement measures are discussed in detail in chapter 5. The real benefit of the exergy analysis becomes evident if follow up corrective and improvement measures are under taken once the exergy analysis is completed.

Chapter 5

Results Analysis and Waste Heat Integration

In this section the results of the exergy analysis are discussed for the base and improved model. Initially, results for the base model are presented and the exergy destruction points are identified where efficiency improvements can be done through waste heat utilization. Based on this findings design changes are suggested and incorporated into the base model to increase the overall efficiency and develop an improved and highly efficient oxy-fuel process model. Finally the results of the improved model are presented in this section.

5.1 Results for the base model

The gross power input to the model is set at 786 MW and the net power output from the model is 521.2 MW. The amount of net power varies depending on various process parameters which influence the auxiliary load and hence determine the net power. As an example, the O_2 purity determines the air intake to the ASU and accordingly the ASU compression load varies which ultimately influences the ASU parasitic power consumption and the overall auxiliary load for the plant. There are few other parameters, but not limited to, that may influence the auxiliary load such as the amount of air leakage in the boiler, amount of flue gas processed in CO_2CCU, product CO_2 purity, CO_2 recovery rate and cooling water supply temperature, etc. The base results presented here used a plant wide cooling water supply temperature of 30°C. A conservative cooling water temperature was selected to make the model applicable to a wide temperature ranges. A different cooling water supply temperature will also have impact on the net power output which is discussed later in the sensitivity analysis section. The performance results of the base model of the integrated oxy-fuel combustion power generation system are presented in Table 5-1. The net HHV efficiency of the plant and the overall cycle exergy efficiency are calculated as 27.75% and 50.09% respectively. The net power output from the plant is 521.2 MW. ASU and the CO_2CCU auxiliary loads are 14.85% and 12.7% of the gross power, respectively. The total exergy loss from the overall plant is 1873 MW. The auxiliary power load on the BOP and the

boiler section is comparatively low, representing only 6.18% of the total gross power. The boiler section alone represents only 1.55% of the gross power.

Table 5-1 Plant Summary Results

PLANT SUMMARY RESULTS	
Gross Power Output (kW)	786,000
Net Power Output (kW)	521,250
Thermal Input, kWt	1,878,000
Net HHV Eff. (%)	27.75
Net HHV HR (kJ/kW-h)	13012
AUXILIARY LOAD SUMMARY	
Boiler and Flue Gas Section (kW) / (% of gross power)	12,160/(1.55%)
ASU (kW) / (% of gross power)	116,730/(14.85%)
BOP (kW) / (% of gross power)	36,390/(4.63%)
CO_2 Capture & Compression (kW) / (% of gross power)	99,850/(12.7%)
Total Auxiliary Loads (kW)	265,130
PLANT PARAMETERS	
Main Steam Flow (kg/s)	613
Final BFW Flow (kg/s)	613
Final BFW Temp (^{o}C)	292
Final BFW Press (kPa)	28850
Hot Reheat Press (kPa)	4522
Hot Reheat Flow (kg/s)	500
Cold Reheat Temp (^{o}C)	357
Cold Reheat Press (kPa)	4900
Cold Reheat Flow (kg/s)	500
Total Fuel Flow (kg/s)	125.61

The auxiliary (parasitic power loss) power load for the ASU, Boiler, BOP and CO_2CCU section as well as the percentage of the auxiliary load with respect to the gross power generation (786 MW) is presented in Figure 5-1.
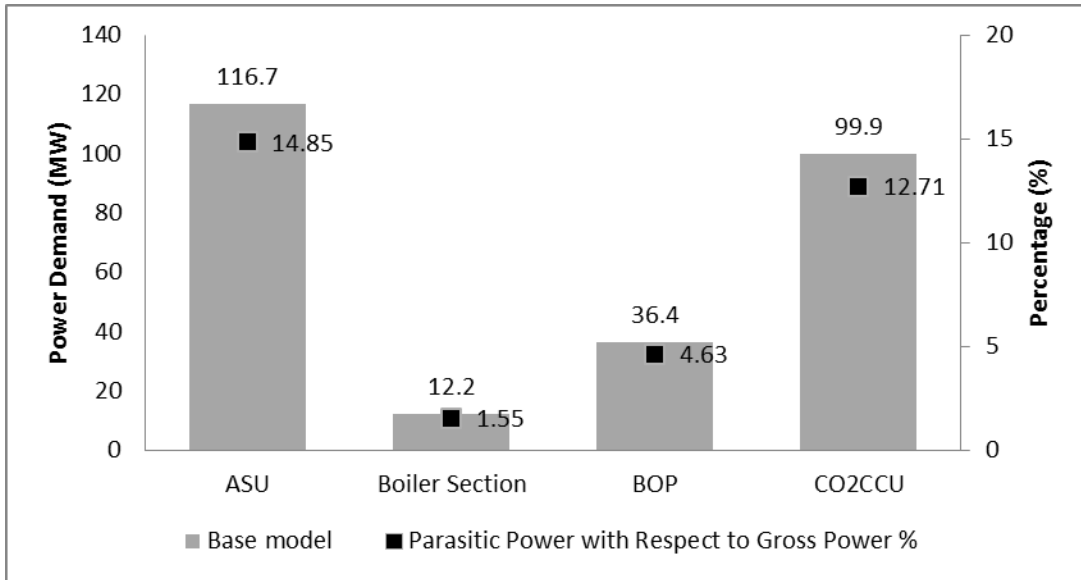
Figure 5-1 Total auxiliary load (parasitic power loss) in plant

5.2 Exergy results for different sections in the base model

Figure 5-2 indicates the overall exergy destruction of the oxy-fuel plant as well as the percentage of the exergy destruction of each section with respect to the total exergy destruction. The boiler and fluegas section has the maximum exergy destruction (1462.2 MW) followed by ASU (216.5 MW) BOP (146.1 MW) and CO_2CCU (47.8 MW). The percentages of exergy destruction with respect to the total exergy destruction are 78.1%, 11.6%, 7.8% and 2.6% respectively for the aforementioned sections. However, it is not sufficient just to know the exergy destruction amount in the control volumes within each section for adopting process improvement measures for a suitable control volume. It might happen that the exergy efficiency of a control volume is significantly high and adding improvement measures are not warranted though it has considerable exergy destruction. So, in order to analyse the exergy data it is important to know both the exergy destruction and exergy efficiency for the control volumes before proposing any improvement actions.

95

Cooling water (CW) pumps throughout the plant have the same exergy efficiency because the CW supply temperature and pressure is constant and the discharge pressure of all the CW pumps are maintained at a user defined value, in this case it is 4 bar.
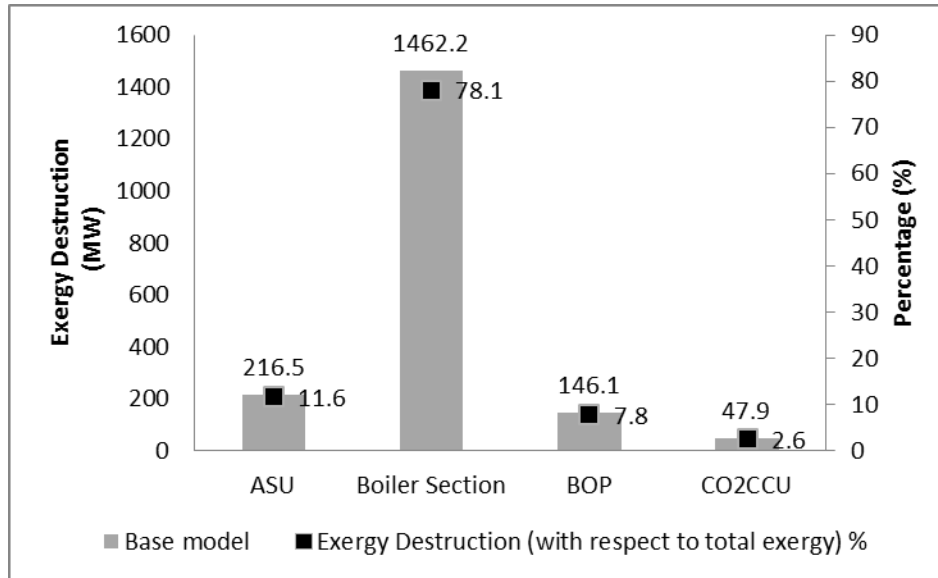
Figure 5-2 Total exergy destruction of the overall process

In the following section, detailed exergy destruction amounts and exergy efficiencies are listed for the separate plant sections.

5.2.1 Exergy results for the boiler and flue gas section

The total exergy destruction amount in the boiler and flue gas section is 1462.2 MW. The exergy destruction amount in different control volumes for this section is presented in Figure 5-3. Most of the exergy is destructed in the combustion chamber which is 1414.9 MW. The second highest destruction point is the PG Cooler1 (23.8 MW) and the rest of the control volumes have less amount of exergy destruction. Figure 5-4 indicates the exergy destruction and exergy efficiency percent for the individual control volumes of the boiler and flue gas section. Most of the exergy destruction (96.8%) happens in the combustion section of the boiler (CV201) with an exergy efficiency of 39.7%. It is worth to explore possibilities to improve the boiler section for the overall improvement of the plant. Combustion is a

significant source of irreversibility and a dramatic reduction of it is quite impossible with conventional approaches. Few known approaches for exergy improvement measures are air preheating for conventional boilers and reducing air to fuel ratio (Bejan et al., 1996).
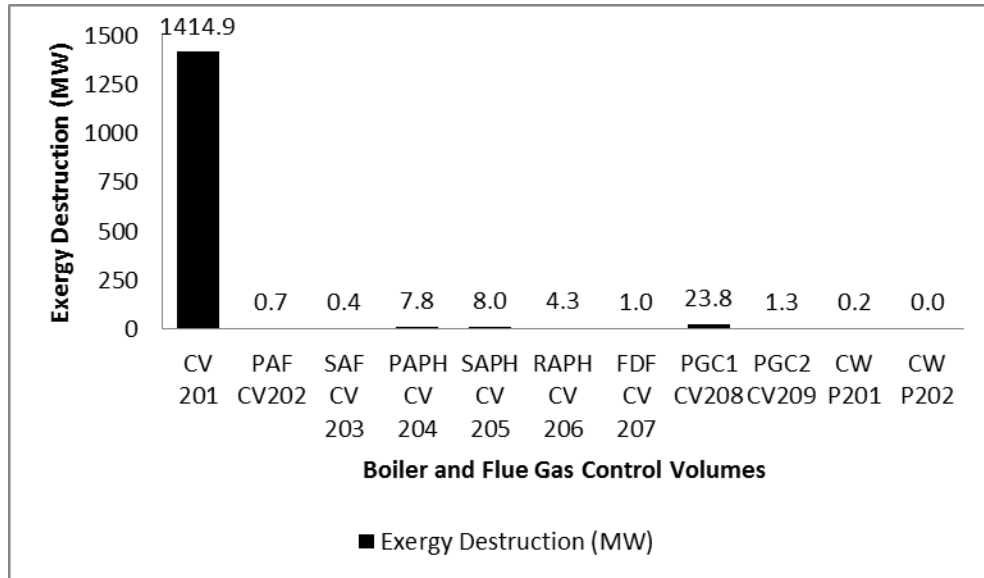
Figure 5-3 Boiler and flue gas section exergy destruction
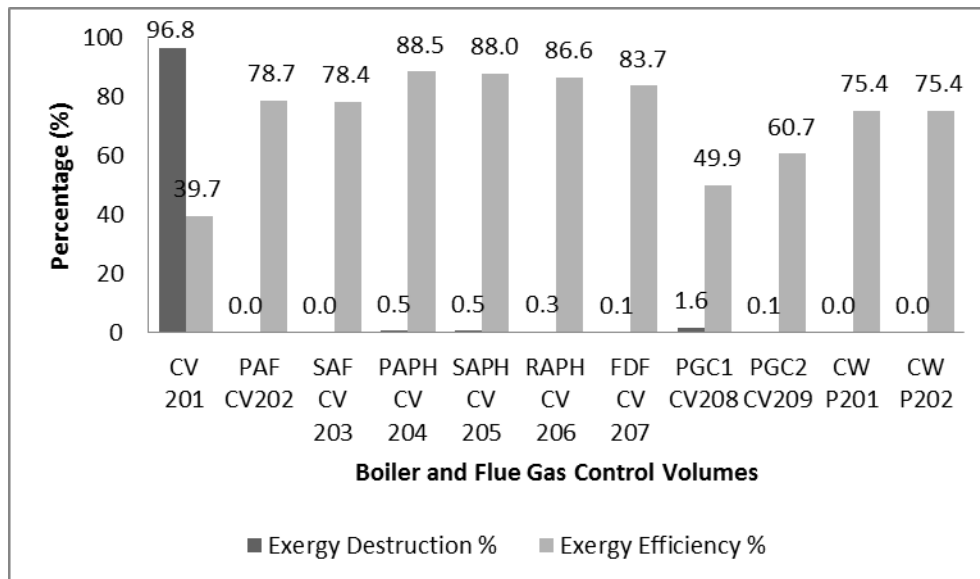
Figure 5-4 Boiler and flue gas section exergy efficiency and exergy destruction percent

Furthermore, materials limitation is one of the major constraints to improve the boiler efficiency from its existing performance level. PG Cooler1 has low exergy efficiency (49.9%) and second highest exergy destruction. It can be looked into for implementing performance improvement measures. The other control volumes have significant high exergy efficiency and low exergy destruction and may not need further improvement measures.

5.2.2 Exergy results for the BOP section

The total exergy destruction amount in the BOP section is 146.1 MW. The exergy destruction amount in different control volumes in the BOP and the percentage of destruction with respect to the total exergy destruction in this section is presented in Figure 5-5.
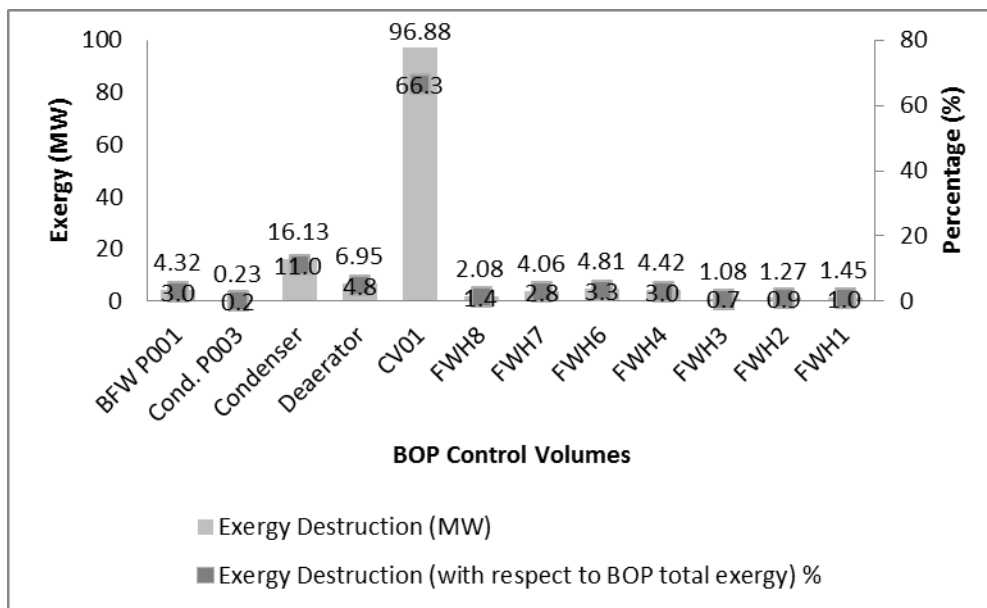
Figure 5-5 BOP exergy destruction

The turbine section has the highest exergy destruction amount which is 96.88 MW followed by the condenser and deaerator with 16.13 MW and 6.95 MW, respectively. The other sections have lower exergy destruction amounts (below 5 MW). Figure 5-6 indicates the exergy destruction and exergy efficiency percentages for the individual control volumes of the BOP section. It can be noted that CV01, Condenser and FWH1 have low exergy

efficiency and can present for improving the efficiency and for reducing the exergy destruction amount. The other control volumes have relatively high exergy efficiency. CV01 is the turbine section where possible improvements are constrained by the turbine design as well as the amount of injection and extraction sterams to and from the turbine section. Extraction steam for heating up of the feed water heaters (FWH) can also be optimized, but, it depends on the overall turbine design. Increasing the individual turbine stage efficiencies will also lead to the overall exergy efficiency improvement of the turbine section.
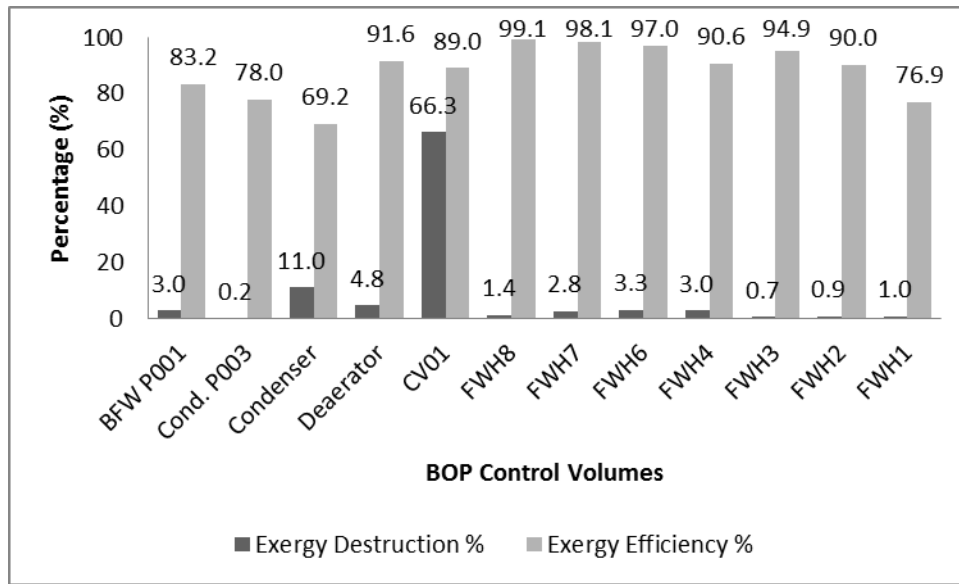
Figure 5-6 BOP section exergy efficiency and exergy destruction percent

The condenser section has little room to improve the overall efficiency unless the condenser pressure is reduced. However it cannot be done in isolation without considering the LP turbine design condition as it is directly connected with the exhaust of the LP turbine section. FWH1 has potential for improvement as the exergy efficiency is relatively low (76.9%) in this exchanger compared to the other control volumes.

5.2.3 Exergy results for the ASU section

The total exergy destruction amount in the ASU section is 216.5 MW. The exergy destruction amount in different control volumes in the ASU and the percentage of destruction with respect to the total exergy destruction for this section are presented in Figure 5-7. Figure

5-8 indicates the exergy destruction and exergy efficiency percent for the individual control volumes of the ASU section.
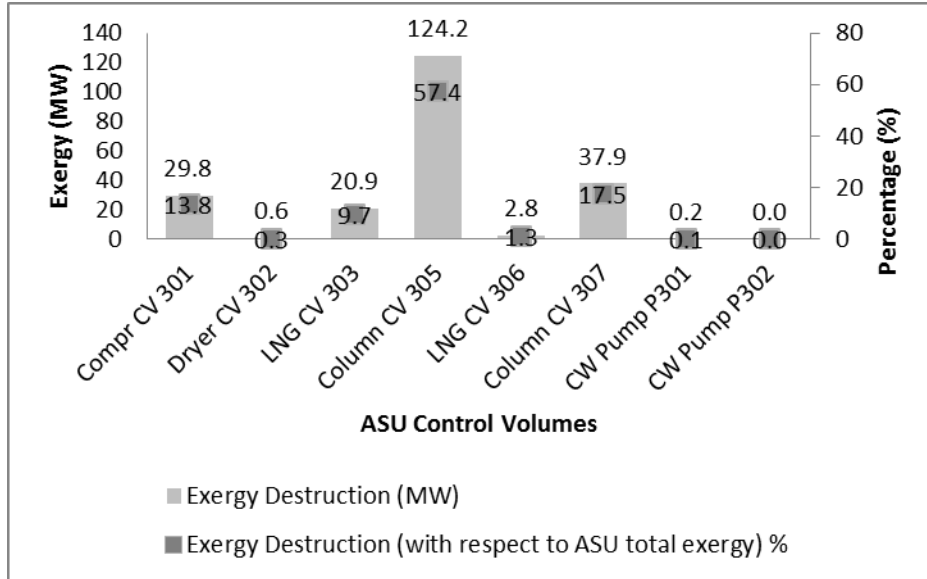
Figure 5-7 ASU Exergy Destruction
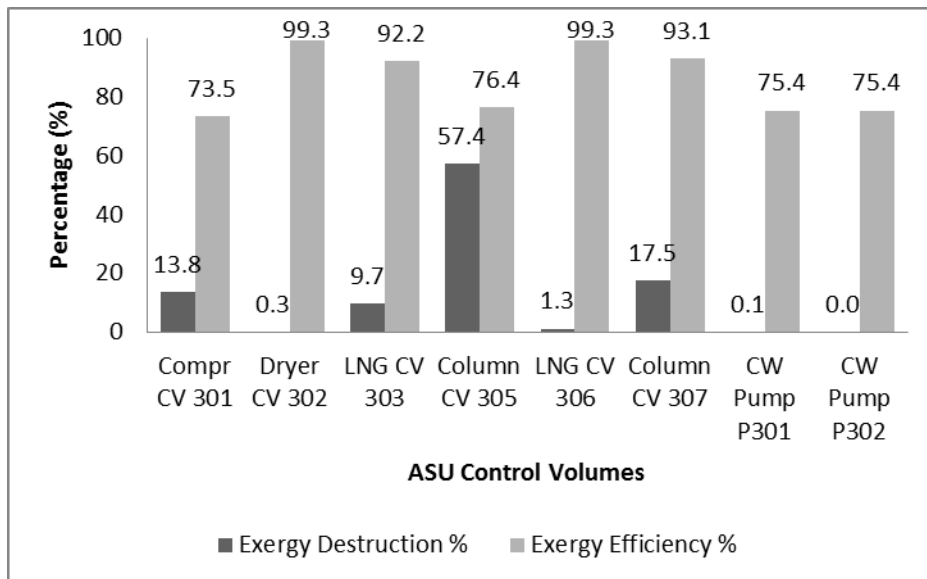
Figure 5-8 ASU section exergy efficiency and exergy destruction percent

The high pressure double column 304/305 (CV305) has the highest exergy destruction (124.2 MW in fig 5-7) with moderate efficiency (76.4% in fig 5-8). However CV307, which include all three columns, shows higher efficiency (93.1%). Control volume CV301 has some potential to look into for further improvement in exergy efficiency (currently 73.5%) and reducing the exergy destruction amount (currently 29.8 MW). The rest of the control volumes have high exergy efficiency and low to moderate exergy destruction amount and have low priority for further improvement measures.

5.2.4 Exergy results for the CO_2CCU section

The total exergy destruction amount in the CO_2CCU section is 47.9 MW. The total exergy destruction amount in different control volumes for this section and the percentage of destruction with respect to the total exergy destruction are presented in Figure 5-9.
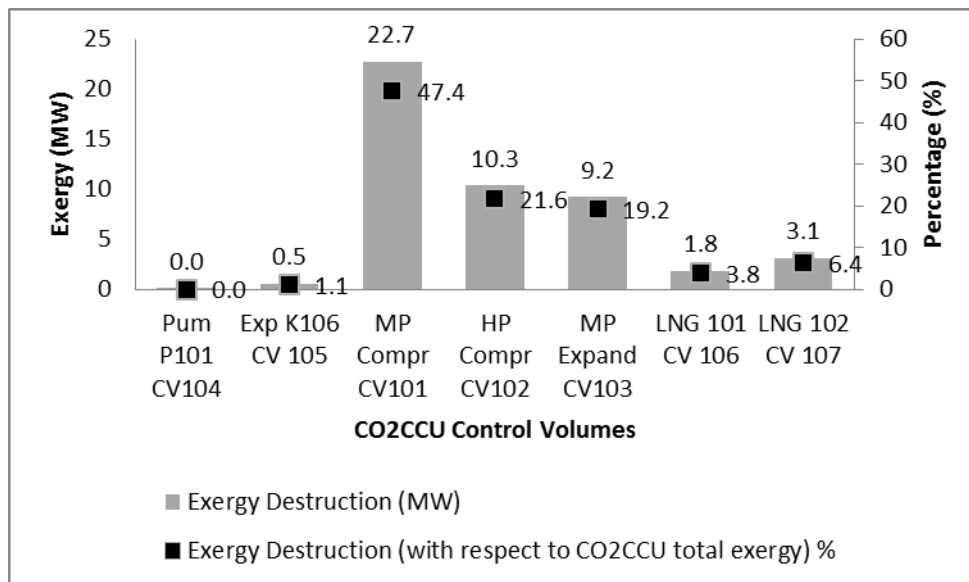
Figure 5-9 CO_2CCU exergy destruction

Figure 5-10 shows the exergy destruction and exergy efficiency results for the individual control volumes of the CO_2CCU section.
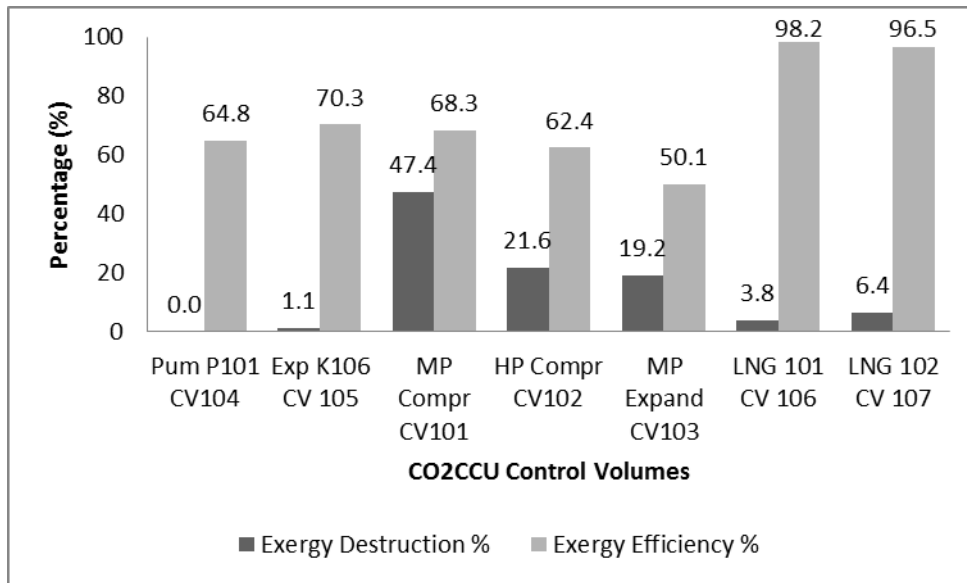
Figure 5-10 CO₂CCU section exergy efficiency and exergy destruction percent

There are potential to improve the efficiency in control volumes CV101, CV102 and CV103 as the exergy destruction is relatively high (22.7 MW, 10.3 MW and 9.2 MW respectively) and the exergy efficiency (68.3%, 62.4% and 50.1% respectively) is relatively low in these sections. The remaining control volumes have less opportunity to improve efficiency as they are already performing at high efficiency level. There are significant challenges in the efficiency improvement in the turbine and compressor section as they are mostly related to mechanical design changes in these sections (e.g. blade material and shape) and hence beyond the scope of this thesis.

5.3 Overall exergy results for the base model

Detailed exergy analysis for the overall plant identifies the exergy destruction amount and the exergy efficiencies of all the control volumes/unit operations. A control volume might have both high exergy efficiency and relatively high exergy destruction amount. However, in a process improvement and design perspective these control volumes will not be suitable candidates as the efficiency improvement will not be an easy task with a unit that has already a relatively high efficiency. Such an example could be CV303 (E301) in the ASU section. The heat exchanger E301 has very good exergy efficiency (92.2%) but, with a considerable

exergy loss of 20.91 MW. As mentioned earlier, in order to reduce exergy losses in a heat exchanger, one needs to increase the heat transfer area which then makes it unfeasible from an engineering design perspective. Similarly, the distillation column control volume CV307 has a good exergy efficiency (93.1%) but with a significant exergy destruction (37.9 MW). There is little incentive to try to improve the exergy efficiency of this control volume as the distillation column would require an infinite number of stages to reach equilibrium and hence reduce the exergy destruction amount. Again it will be an inappropriate approach to reduce exergy destruction from an engineering design and economic perspective. However if a control volume has low exergy efficiency, irrespective of the amount of exergy destruction, it will be a suitable candidate for incorporating exergy improvement measures. These criteria necessitate the grouping or ordering of the control volumes in ascending order with respect to the exergy efficiency. Detailed exergy analysis in the overall plant identifies all the unit operations and control volumes with respect to their exergy destruction and exergy efficiency. These are ranked in ascending order, according to the exergy efficiency, and are presented in Table 5-2 for the base model.

Table 5-2 Exergy efficiency, destruction and ranking of the control volumes

BOP			PC Boiler			CO$_2$CCU			ASU			Ranking
Exergy			Exergy			Exergy			Exergy			
Control Volume	Efficiency %	Destruction MW	Control Volume	Efficiency %	Destruction MW	Control Volume	Efficiency %	Destruction MW	Control Volume	Efficiency %	Destruction MW	
Condenser	69.2	16.134	CV208	49.9	23.807	CV103	50.1	9.129	CV301	73.5	29.782	1
FWH1	76.9	1.454	CV209	60.7	1.294	CV102	62.4	10.272	CV305	76.4	124.247	2
ConP003	78.0	0.232	CV201	65.7	1414.914	CV104	64.9	0.002	CV303	92.2	20.911	3
BFWP001	83.2	4.315	CV203	78.4	0.423	CV101	68.3	22.730	CV307	93.1	37.906	4
CV01	89.0	96.882	CV202	78.7	0.694	CV105	70.3	0.515	CV302	99.3	0.623	5
FWH2	90.0	1.269	CV207	83.7	0.985	CV107	96.5	3.016	CV306	99.3	2.846	6
FWH4	90.6	4.420	CV206	86.6	4.280	CV106	98.2	1.751				7
Deaerator	91.6	6.952	CV205	88.0	7.998							8
FWH3	94.9	1.085	CV204	88.5	7.758							9
FWH6	97.0	4.812										10
FWH7	98.1	4.064										11
FWH8	99.1	2.080										12

This ranking table is also the main output result from the exergy analysis undertaken on the overall process. Once the ranking table is developed the next step is to consider the 1st row of control volumes for their efficiency improvement as they have the lowest exergy efficiency. Efficiency improvement measures are then considered based on acceptable engineering

design practice and their applicability to industrial use. If a control volume is found to be not suitable for the efficiency improvement due to major design changes, then the next control volume will be the candidate for the efficiency improvement measures. The selection of the control volumes will continue in the same fashion for each control volume. The next step is to utilize waste heat, available from other sources within the plant, in the selected control volumes through process integration and increase the efficiency of these control volumes. This is done in most cases by reducing the temperature difference between the two streams of an exchanger as the exergy destruction associated with any heat exchanger can be reduced by lowering the temperature difference between its streams. Once this is done, a new ranking table will be established and again the control volumes in the first row of the new table with a different set of control volumes will be the next candidate for efficiency improvement measures. This iteration process may continue until a satisfactory improvement is achieved in the overall process. The integration of the waste heat into the plant in each iteration step will produce an improved process design of the overall plant. The graphical representation of the iteration steps is presented in Fig 5-11
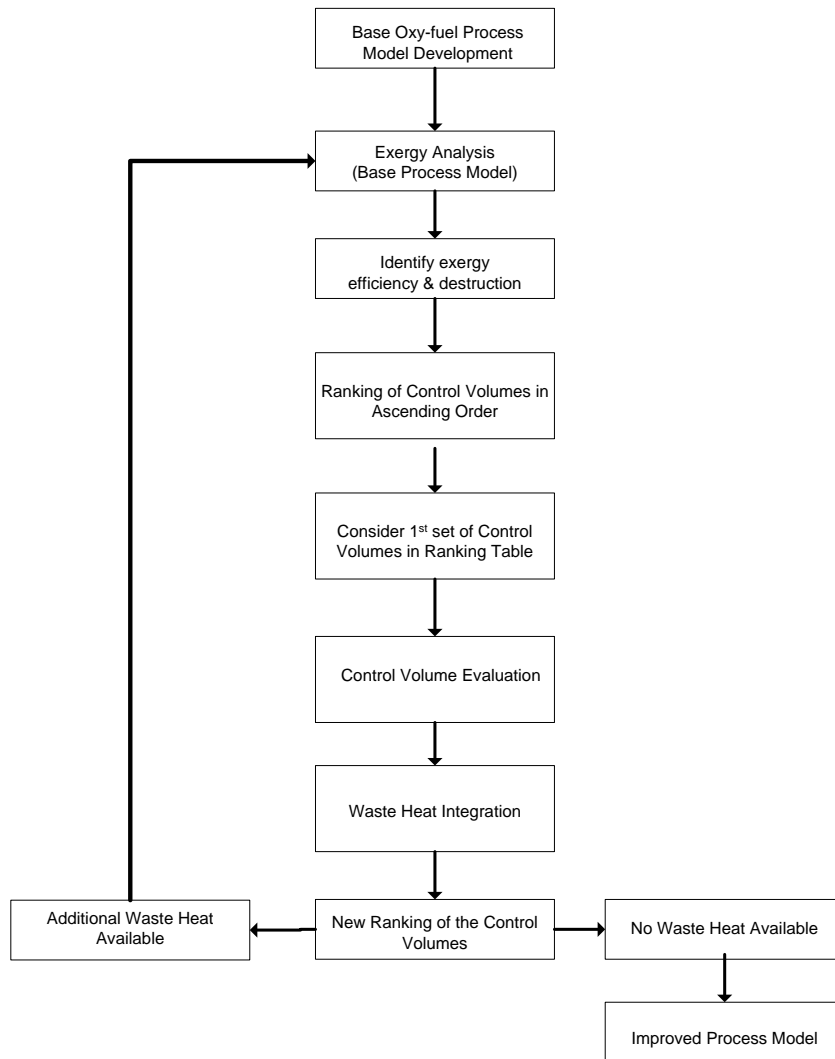
Figure 5-11 Exergy evaluation and process integration approach

5.3.1 Decision making based on the ranking table

Process improvement measures were undertaken based on the identification and ranking made in Table 5-2 for different unit operations in the base oxy-fuel model. Based on the ranking, the control volumes in the first row have been selected for incorporating exergy efficiency improvement measures. These control volumes are marked in shaded area in Table 5-2. It is important to note that the degrees of freedom for selecting more than one control volume for efficiency improvement in a particular section are limited by the availability of waste heat and their utilization potential. Waste heat made available through cooling water

circuit and utilization of this waste heat to more than one control volume depends on the heat content and the cooling water flow rate. Additionally, depending on the availability of waste heat, it is worth to consider any control volume which has exergy efficiency of less than 90% with coupled exergy destruction greater than 5 MW. These limits can be redefined depending on particular design of a power plant.

In the BOP section, the first control volume in the ranking table is the turbine exhaust steam condenser. It has high exergy loss (16.13 MW) and low efficiency (69.2%). However, no significant attempt was made to increase the condenser efficiency as it is directly related to the performance of the turbine and its design. Hence the next control volume (FWH1) was considered for efficiency improvement. It has an exergy efficiency of 76.9% in the base model. As seen later, the increased efficiency value in the improved model is 93.6%. The next two control volumes are condenser pump and BFW pump. The efficiency improvements for these pumps are dependent on the design efficiency for the pumps and hence no improvements are proposed. Following these, the remaining control volumes have relatively high (near 90% or above) efficiency. No additional improvement measures were undertaken for these control volumes as these are all ranked low in the ranking table. The efficiency improvement for these control volumes can be investigated further by manipulating the extraction steam to these individual feed water heaters. However, this might result in a new turbine design.

In the boiler and flue gas section, the first control volume in the ranking table is the process gas cooler 1(PG Cooler 1) which is CV208. The efficiency of CV208 is the lowest (49.9%) and the exergy destruction amount is 23.8 MW. The efficiency of this exchanger was improved and as seen later, the increased efficiency for this in the improved model is 61.4%.The next control volume is CV209 which indirectly participated in the efficiency improvement by generating waste heat in this control volume and supplying it to CV208. The next potential control volume for efficiency improvement is the combustion boiler (CV201). It has its own inherent losses that require fundamental improvement of the boiler design for any efficiency improvement and hence not considered here. The remaining control volumes have either low exergy destruction amount or high exergy efficiency (close to 90%). Further

investigation can be done on these control volumes by manipulating the process stream parameters (flow, pressure, temperature). However, this might result in a new design for the boiler and flue gas section, which is out of the scope of this work.

In the CO_2CCU section, the first control volume in the ranking table is the impurities exhaust system through the expander K107 represented by the control volume CV 103. The exergy efficiency and exergy destruction in CV103 are 50.1% and 9.13 MW respectively. As seen later, the increased efficiency number in the improved model is 58.1%. The next control volume is CV102. As mentioned earlier, the degrees of freedom to choose the control volumes for efficiency improvement are dependent on the availability of waste heat. As seen later, all the available waste heats are utilized for control volume CV103 and hence, the remaining control volumes are not investigated further.

Most of the heat generated in the ASU section, more specifically generated through the air compression, is further utilized in other sections of the overall plant and hence no significant improvement is possible with the ASU control volume CV301 which is the first item in the ranking table. The items in the ranking table with ascending order are distillation columns and plate and fin exchangers. Significant improvement in these control volumes is difficult for thermodynamic reasons as explained in the previous section. So no improvement measures are considered at this point for the ASU section.

The other unit operations and the control volumes in the overall plant might come up for further improvement measures after the first round of integration is completed and a new ranking table is established. As explained in the next section, the process integration has contributed to a net power gain of 11.15 MW (2.14% increase, based on net power) in the overall plant. The improved model is derived from the base model upon implementing the process improvement measures after exergy analysis and waste heat utilization. The details of these are explained in the following sections.

5.4 Waste heat utilization and improved plant configuration

The waste heat in this power generation system is mainly generated from different heat exchangers. This heat energy is transported by the cooling water system. With the completion of the exergy analysis, the potential locations for improvements are identified for

waste heat utilization. Based on the preliminary evaluation and the ranking, improvement measures are introduced for the control volumes presented in Table 5-2 for the shaded ones. The improved integration measures are shown in the Figures 5-22, 5-23, 5-24, and 5-25 with solid blue lines for the four separate section of the model.

5.4.1 Waste heat integration approach

The waste heat integration approach was considered from a realistic industrial perspective and implemented in the simulation. The intention was to finalize a process design for seamless transition of the process model into detailed engineering design for actual industrial application with fewer changes in the model. In general, the compressors in ASU and CO_2CCU section produced lots of waste heat due to the compression of the air and process gas streams. These heats are usually taken out from the inter stage coolers in the compression section. The usual industrial practice to remove this heat is by the cooling water loop in the plant. In this current study these waste heat are utilized by process integration and required only minor design changes in the overall process model. It is understood that gas to gas heat exchange is probably not an efficient approach for heat transfer/utilization and probably not economically viable due to the exchanger size and cost. In that context, this study introduced heat integration through partially circulating closed cooling water (PCCW), closed cooling water (CCW) or open cooling water (OCW) loops where applicable. In all cases, heat was carried away by the cooling water from the high temperature area and was transferred to the low temperature area. In PCCW or CCW case the process is partially or totally cyclic in nature and has a lower cooling tower load to cool down the rest of the CW as it passes multiple exchangers to utilize waste heat. In these cases heat is transferred from a low temperature area to a high temperature area by CW circulation as shown in Figure 5-12 (a, b and c). Apart from waste heat utilization, two significant additional benefits with the introduction of PCCW and CCW loop is lower fresh water intake for the overall cooling water loop and thereby reducing the pump power consumption in the overall plant.
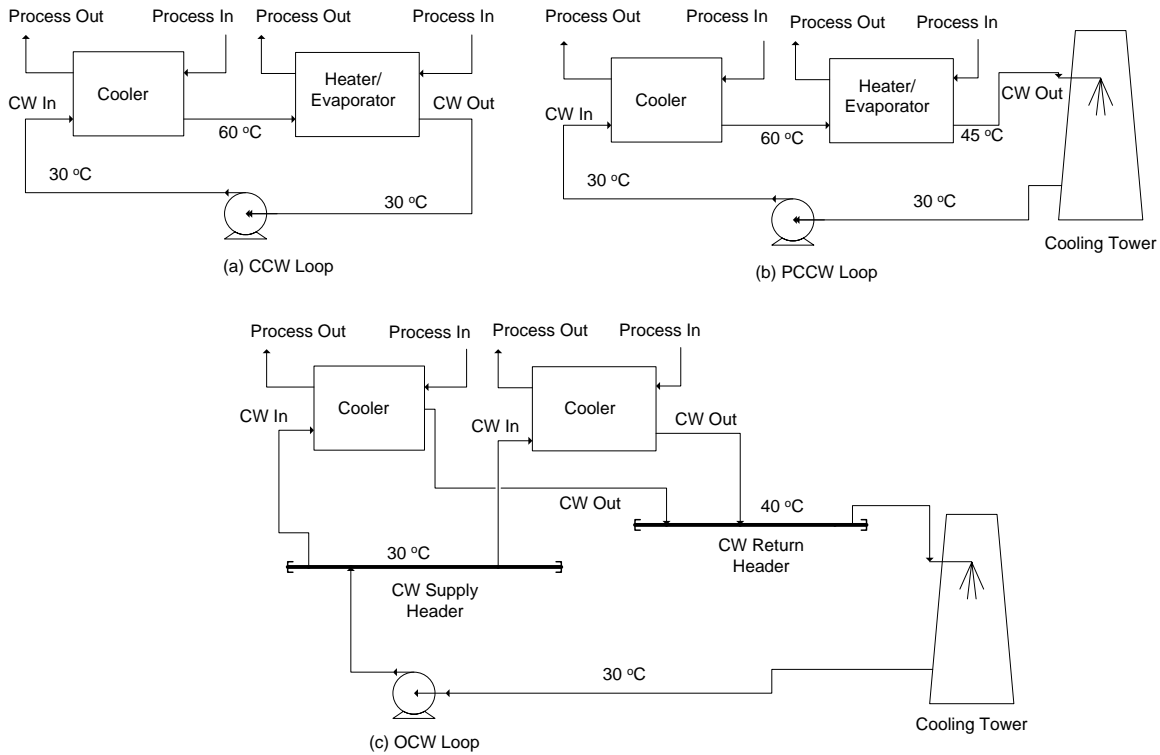
Figure 5-12 Different cooling water loops (PCCW, CCW, and OCW)

However, in the case of OCW it always requires a conventional cooling tower with higher load to bring back the total CW supply temperature to its initial state as all the cooling is done by the cooling tower (Figure 5-12c). The OCW loops are generally used in all the existing power plants. In the current study only PCCW and a smaller OCW loop are considered. In these model configurations the cooling water supply temperature is maintained at 30°C. The cooling water return temperatures at different locations are maintained at 38/60/85°C depending on the process conditions and waste heat utilization potential within the plant modules. These return temperatures are user defined and can be changed as needed with a single change in the input/output block in the main flow sheet. Also in this study, the process stream parameters, except the CW loops, at different sections in the overall plant remain constant in both the base and improved models. These process parameters were kept constant as a specific plant design would require certain predefined process parameters. Hence, only the cooling water temperatures and flow rates were varied to observe the impact

on exergy efficiency and the overall net power output. Subsequently, efficiency improvement in the overall plant in terms of the net power gain, compared to the base case, was achieved by utilizing the available waste heat. A change in other plant process parameters can easily be implemented in this integrated model. However, this has not been considered for this study as it will change the design of the overall plant. Appropriate PCCW loop is introduced in each plant to reduce the fresh CW intake in the coolers which increases the overall net power efficiency as well as exergy efficiency.

5.4.2 Waste heat integration through cooling water loop

5.4.2.1 Integration approach-1

In this configuration the waste heat is utilized by PCCW loop connecting individual plant sections through multiple heat exchangers in the overall plant. Figure 5-13 represents a composite curve for breakdown of heat integration within multiple heat exchangers of such kind and their thermal gain. In this case the external overall integration is between 3 exchangers in ASU, Boiler and CO_2CCU section via CW stream 162.1. After completing the in-plant PCCW loop integration within the CO_2CCU, a sizeable amount of waste heat was still available which was carried away by stream 162.1. Stream 162.1 was first used to preheat the CO_2 vent stream 137 (Figure 5-25), following that it was reused to preheat BFW stream 3 through the proposed new feed water heater FWH9 (Figure 5-23) and finally oxygen stream 323 in the ASU is preheated with the same CW stream in exchanger E308 (Figure 5-24).

Figure 5-13 Diagram

3A 47.3 °C | 3 42.2 °C

137 7 °C | 324 40 °C

137.1 80.1 °C — E113 (CO2CCU) — 162.1 85 °C

162.2 82.35 °C — FWH9 (BOP) — 162.3 72 °C

324 40 °C — E308 (ASU) — 323 15.5 °C | 162.4 68.3 °C

162.1 85 °C 137.1 80.1 °C 162.2 82.35 °C 162.3 72 °C 162.4 68.3 °C

3A 47.3 °C 3 42.2 °C 324 40 °C 323 15.5 °C

137 7 °C

CO2CCU 2.54 MW | BOP 9.89 MW | ASU 3.6 MW
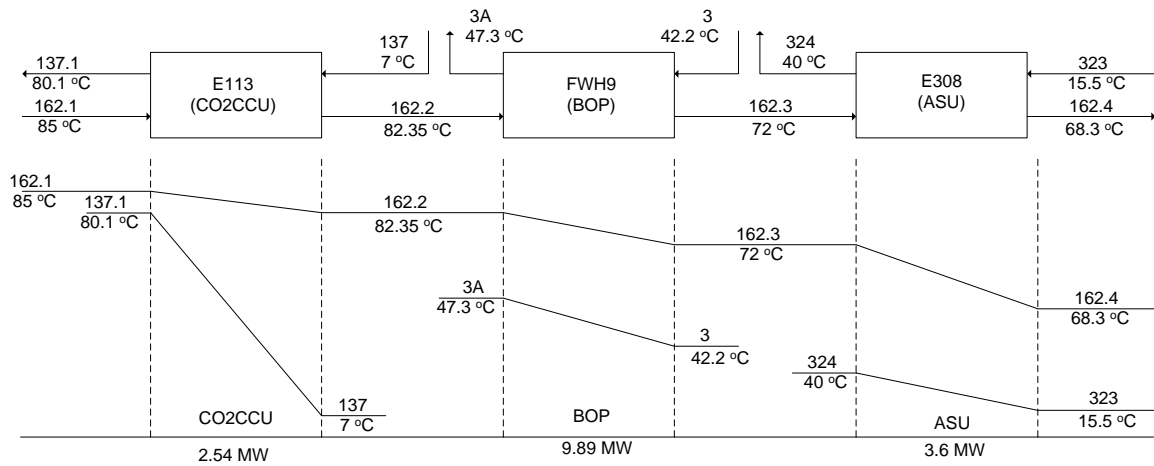
Figure 5-13 Multi exchanger waste heat integration between CO₂CCU, BOP and ASU

The amount of waste heat utilized in E113 is 2.54 MW. The performance curves for the two new exchangers (FWH9 and E113) are given below in Figures 5-14 and 5-15.

FWH9

Temperature (C) vs Heat Flow (kW)

Stream 3A
Stream 162.2
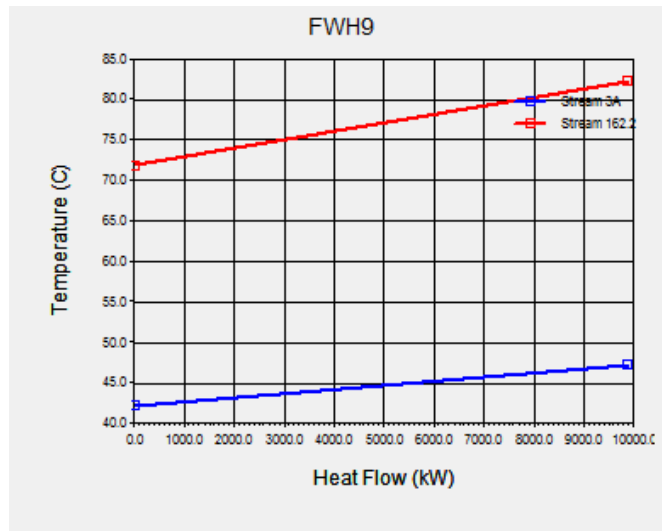
Figure 5-14 Performance curve for heat exchanger (FWH9)

The net energy savings by oxygen preheating is 3.6 MW. The same amount of electrical energy is required to preheat the oxygen stream for the base model in absence of any steam heating system. Hence, this waste heat integration offers a net gain in power of 7.2 MW for

the ASU section compared to the base case. However with this plant wide integration, a total of 16.03 MW waste heat is utilized compared to no waste heat utilization in the base case.
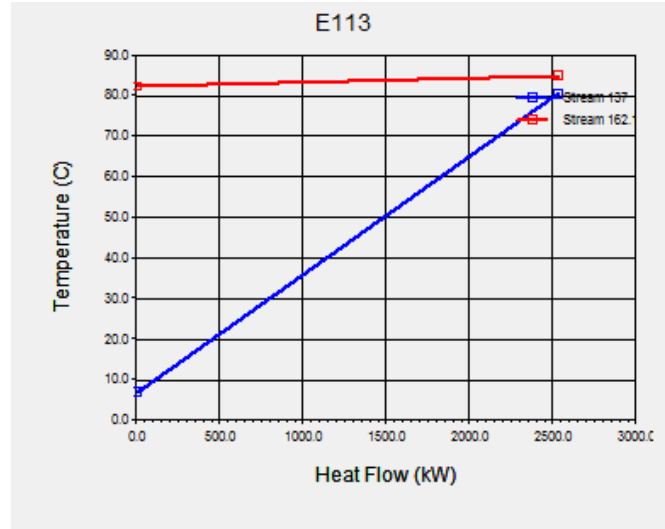
Figure 5-15 Performance curve for heat exchanger (E113)

A conservative approach is taken for preheating the BFW in the BOP section by keeping stream 4's temperature (Figure 5-23) constant while introducing the proposed new exchanger FWH9 for waste heat utilization upstream of FWH1. The temperature of stream 4 (Figure 5-23) was kept constant at 61°C to maintain the design parameters for the rest of the BOP loop constant. With this approach the size of the FWH1 was reduced by approximately the same amount of waste heat utilized (9.89 MW) in FWH9. The reduced size of the FWH1 in the integrated model is 26.71 MW compared to 36.14 MW in the base model. The extraction steam from the LP turbine for BFW preheating FWH1 is also subsequently reduced by 14850 kg/hr due to this size reduction. In addition, the reduction of extraction steam from the LP turbine increased the electrical output of the LP turbine by approximately 700 kW.

5.4.2.2 Integration approach-2

The second external overall integration is implemented by another PCCW loop and it is done between two existing exchangers, one in the ASU section and the other in the Boiler section via CW stream 305. Stream 305 carries away waste heat from E305 in the ASU

section but still remains at a lower temperature (38°C) with a significant mass flow rate, which is combined with stream 274 (38°C) from P202 and then utilized to cool down PG Cooler1 in the boiler section. This integration, as shown in Figures 5-22, 5-24 and 5-16, reduces the pumping load on the pump P201 by approximately 686 kW compared to the base model. With this integration, the exergy efficiency of the PG Cooler 1 also goes up significantly, from 49.87% to 61.41%, as the fresh low temperature CW intake is decreased to the exchanger.
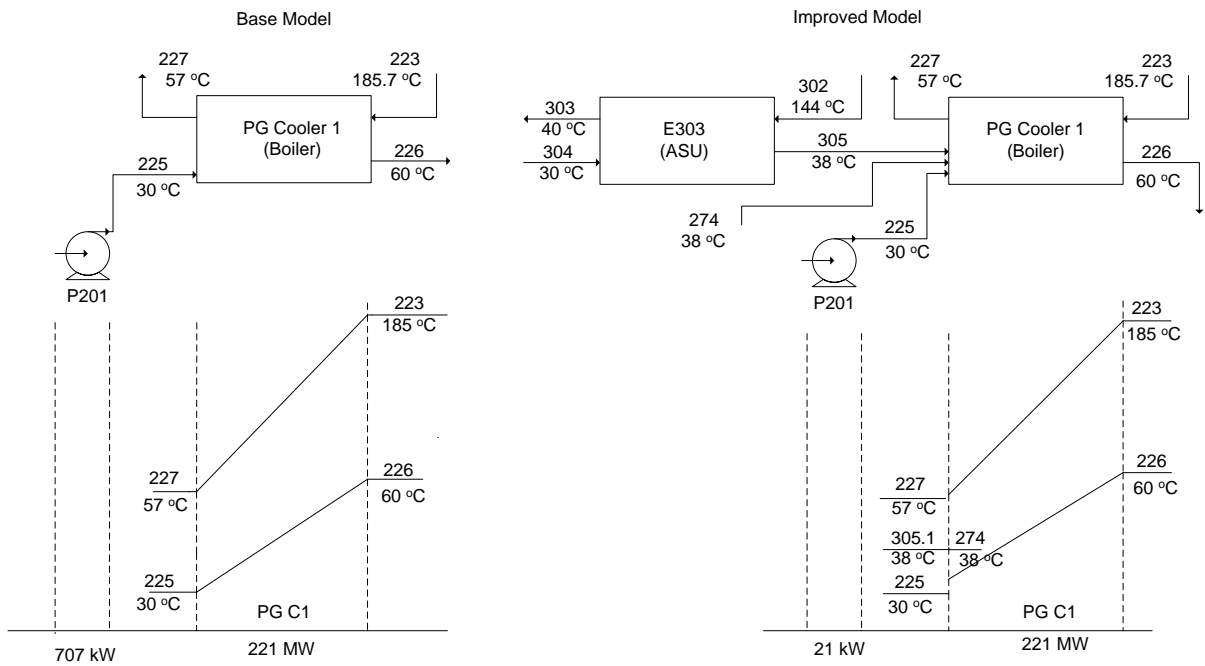
Figure 5-16 Multi exchanger waste heat integration between ASU and boiler

The performance curves for the PG Cooler 1 for both base and improved models are given in Figures 5-17 and 5-18. It can be noticed that the amount of heat exchange remains the same, however it takes place at an elevated temperature as the fresh cooling water intake is reduced. The exergy performance of PG Cooler 1 in the improved model improves significantly by 11.5 percentage points.
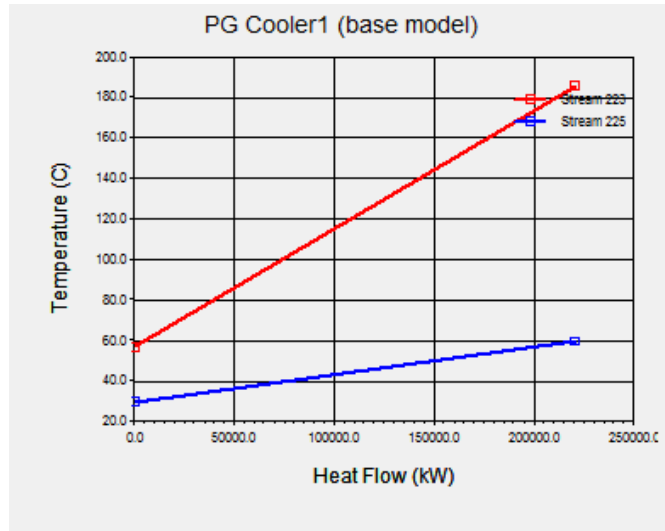
Figure 5-17 Performance curve for PG Cooler1 (base model)
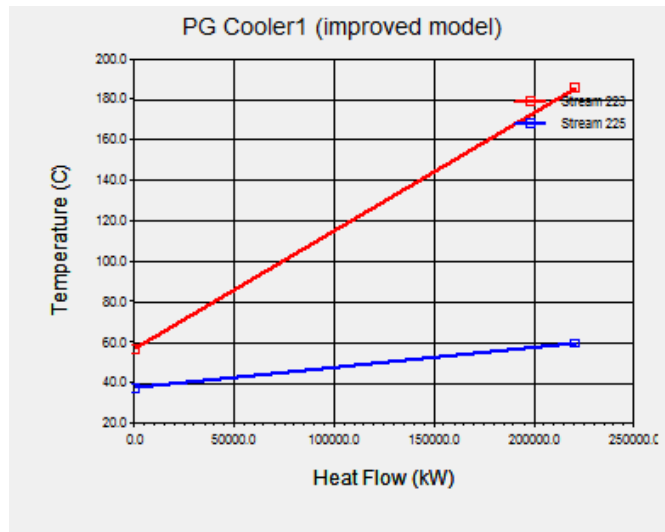
Figure 5-18 Performance curve for PG Cooler1 (improved model)

5.4.2.3 Integration approach-3

In this configuration, in addition to the heat integration shown in Figures 5-13 and 5-16, a few exchangers in CO_2CCU section have been integrated. An internal PCCW loop integration between exchangers E102 and E104 saves CW pump P102 electrical energy by

about 101.4 kw, as shown in Figures 5-19 and 5-25. The reduced power consumption is due to the low demand of fresh cooling water intake to the system.
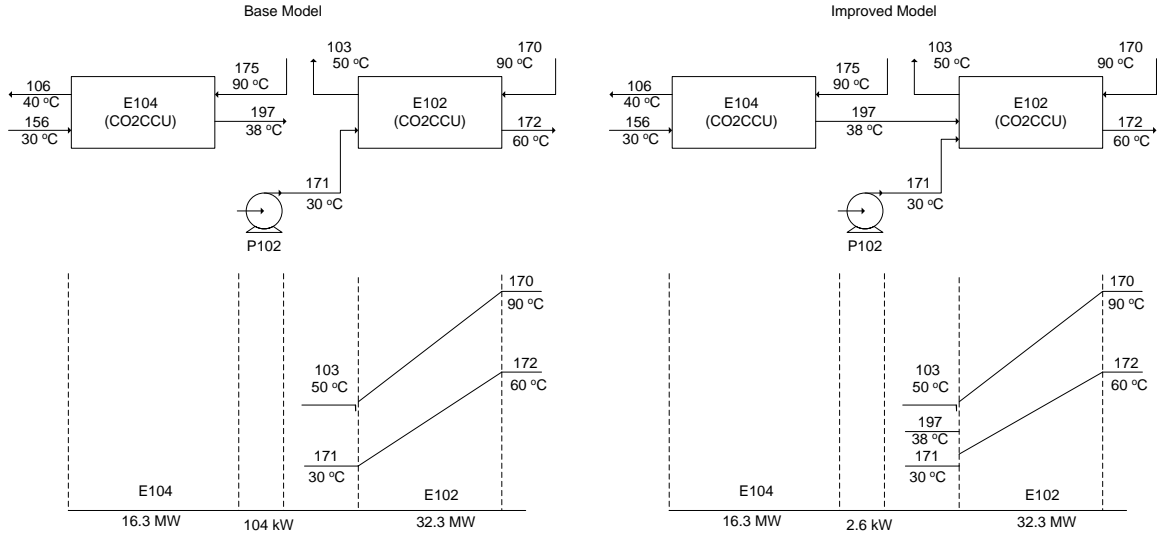
Figure 5-19 Waste heat integration in CO$_2$CCU section

5.4.2.4 Integration approach-4

In this configuration waste heat integration through a PCCW loop between E101, E103, E109 and the proposed new exchanger E113 is shown in Figures 5-20 and 5-25 which saves 2.54 MW.
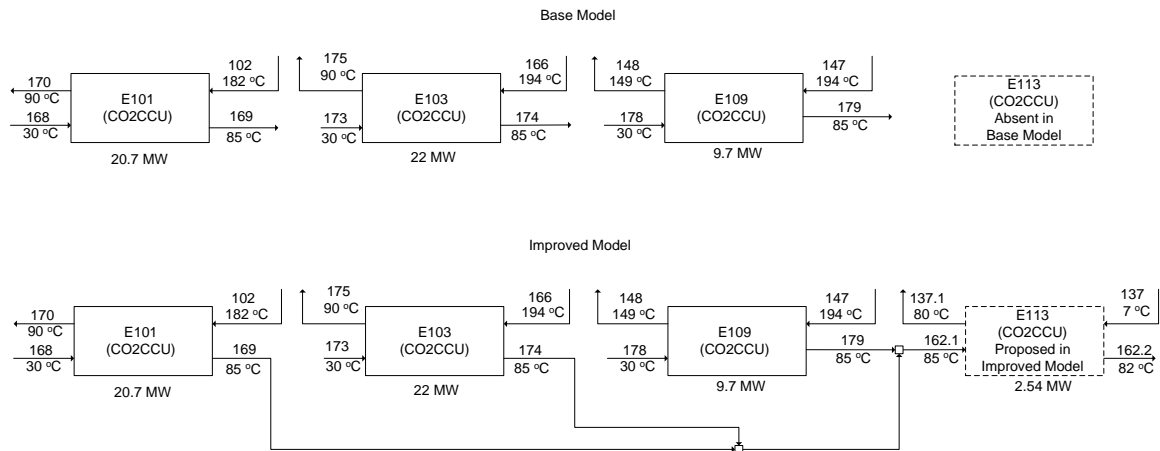
Figure 5-20 Waste heat integration in CO$_2$CCU section

115

In total, these internal integration reduces parasitic power demand for the CO_2CCU from 99.85 MW to 97.25 MW. This represents a total savings of 2.64 MW for this particular case. With these exchanger integrations, the exergy efficiency of the control volume CV103 goes up from 50.1% to 58.06%. A minor improvement was also noticed in CV101 where the efficiency improved from 68.29% to 68.81% due to process integration. This improvement happens in the CO_2CCU section as the fresh low temperature CW intake is decreased to these exchangers by an amount of 915,000 kg/hr.

5.4.3 Waste heat utilization from N_2 stream in ASU

In the ASU section, no internal integration is proposed. N_2 stream from ASU, in this particular study, is vented to the atmosphere. However, in actual practice, part of it can be used in plant utilities or coal drying and the rest of the N_2 can be sold outside as a by-product. The capital gain from the N_2 sell is not included in the current study as no economic analysis is being done in this study. In this particular ASU model, N_2 temperature is maintained high (74°C) which is suitable for coal drying. A lower N_2 temperature (user defined) can be easily implemented by manipulating stream 312 CW outlet temperature (Figures 3-4 and 5-24) to a lower value (e.g. 38°C) which is currently set at 85°C in this case study. This is an additional automated feature in the ASU model which can be user defined. The available heat from N_2 stream, if cooled to ambient temperature (25°C), is 26.97 MW which can be used for coal drying or any other plant use. However, this is not included in the energy savings calculation as mentioned earlier.

5.5 Development of the improved process models

The process improvements are made in the overall oxy-fuel model by design changes in the process flow sheet and waste heat integration as explained in the previous section. The design changes are made based on the ranking table (Table 5-2). Addition of new unit operations and material and energy streams are made as appropriate, and finally an improved oxy-fuel power generation system model is developed. The location of the new unit operations (heat exchanger in this case) and the material and energy stream are dictated by the ranking table. The HYSYS main process flow sheet user interface for the improved

model is shown in Figure 5-21. In comparison to the base model (Figure 3-6); this improved model has additional process stream lines interconnecting the ASU, Boiler, BOP and CO$_2$CCU sections. These additional stream lines, highlighted in blue colour, are the interconnected waste heat streams that are introduced in the improved model for heat integration.

N2		
Temperature	74.99	C
Pressure	1.200	bar
Mass Flow	1.866e+006	kg/h
Mole Frac N2	0.9849	
Mole Frac Ar	0.0039	
Mole Frac O2	0.0111	

Heat Available		
Heat Flow	2.700e+004	kW

Air		
Temperature	9.000	C
Pressure	1.012	bar
Mass Flow	2.460e+006	kg/h

Oxygen		
Temperature	40.09	C
Pressure	1.012	bar
Mass Flow	5.779e+005	kg/h
Mole Frac O2	0.9402	
Mole Frac Ar	0.0290	
Mole Frac N2	0.0308	

Fuel Coal		
Temperature	25.00	C
Pressure	1.012	bar
Mass Flow	4.522e+005	kg/h

HP Throttle Steam		
Temperature	592.4	C
Pressure	242.3	bar
Mass Flow	2.206e+006	kg/h

| To Atmosphere		
Temperature	21.27	C
Pressure	1.100	bar
Mass Flow	1.273e+005	kg/h
Mole Frac CO2	0.2882	
Mole Frac O2	0.1674	
Mole Frac N2	0.4391	
Mole Frac Ar	0.1053	
Mole Frac SO2	0.0000	
Mole Frac NO	0.0000	
Mole Frac NO2	0.0000	

CO2CCU Result		
Recovery Rate	92.55	%
Energ Comp-Ex kWhr/kg	0.1586	

CO2CCU Inlet		
Temperature	50.00	C
Pressure	1.007	bar
Mass Flow	8.054e+005	kg/h
Mole Frac CO2	0.7179	
Mole Frac O2	0.0367	
Mole Frac N2	0.0911	
Mole Frac Ar	0.0251	
Mole Frac SO2	0.0033	
Mole Frac NO	0.0000	
Mole Frac NO2	0.0000	

CO2 to Pipeline		
Temperature	43.00	C
Pressure	109.8	bar
Mass Flow	6.286e+005	kg/h
Mole Frac CO2 %	0.9578	
Mole Frac O2 %	0.0101	
Mole Frac N2 %	0.0183	
Mole Frac Ar %	0.0091	
Mole Frac SO2	0.0047	
Mole Frac NO	0.0000	
Mole Frac NO2	0.0000	

Waste Heat Integration streams ▬▬▬

Figure 5-21 Improved integrated oxy-fuel process model in HYSYS with waste heat integration streams highlighted.

The improved process model for the boiler and flue gas section is presented in Figure 5-22. The performance of the PG Cooler1 in the boiler and flue gas section is improved by reducing the fresh cooling water intake (reduced by 6,148,000 kg/hr) to the exchanger through process integration between PG Cooler 2 (boiler section) and the heat exchanger E303 (compressed air cooler in ASU) by stream 274 and 305.1, respectively as shown in Figure 5-22. The differences between the base and the improved boiler models can be seen when comparing Figures 3-2 and 5-22. The differences are the blue inter connected cooling water lines. This integration increases waste heat utilization and also increases the efficiency of the PG Cooler 1. Furthermore, this integration is highly desirable as it reduces huge amount of fresh cooling water intake and subsequently reduce the load on the cooling water

demand. The reduction of cooling water demand might resolve one of the key site specific design challenges where water shortage is an acute issue for some specific locations.
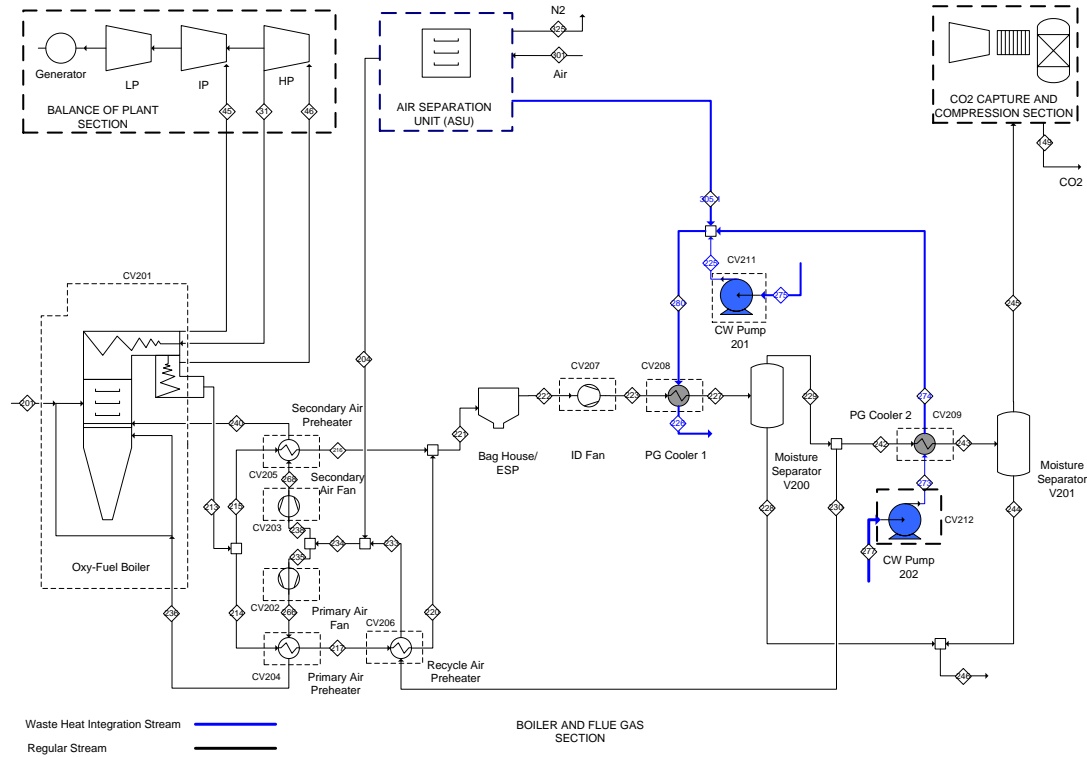
Figure 5-22 Improved boiler and flue gas section process model withwaste heat integration streams highlighted.

The improved process model for the BOP section is shown in Figure 5-23. The performance of the FWH1 and the exergy efficiency in the BOP section is improved by increasing the boiler feed water intake temperature to FWH1 by 5°C from 42°C (stream 3) to 47°C (stream 3A). This is done by process integration between exchanger E113 (CO$_2$CCU section) and installing a new exchanger (FWH9) in the BOP section through the process stream 162.2, as shown in Figure 5-23. This integration also reduces extraction steam (stream 27) by 14,850 kg/hr from the LP turbine for heating up of boiler feed water in FWH1 and ultimately improves the LP turbine power generation by 0.7 MW. The differences between the base BOP model and the improved model can be seen when comparing Figures 3-3 and 5-23. The

118

differences are the blue inter connected cooling water lines. This integration also increases waste heat utilization and reduces the exergy destruction.
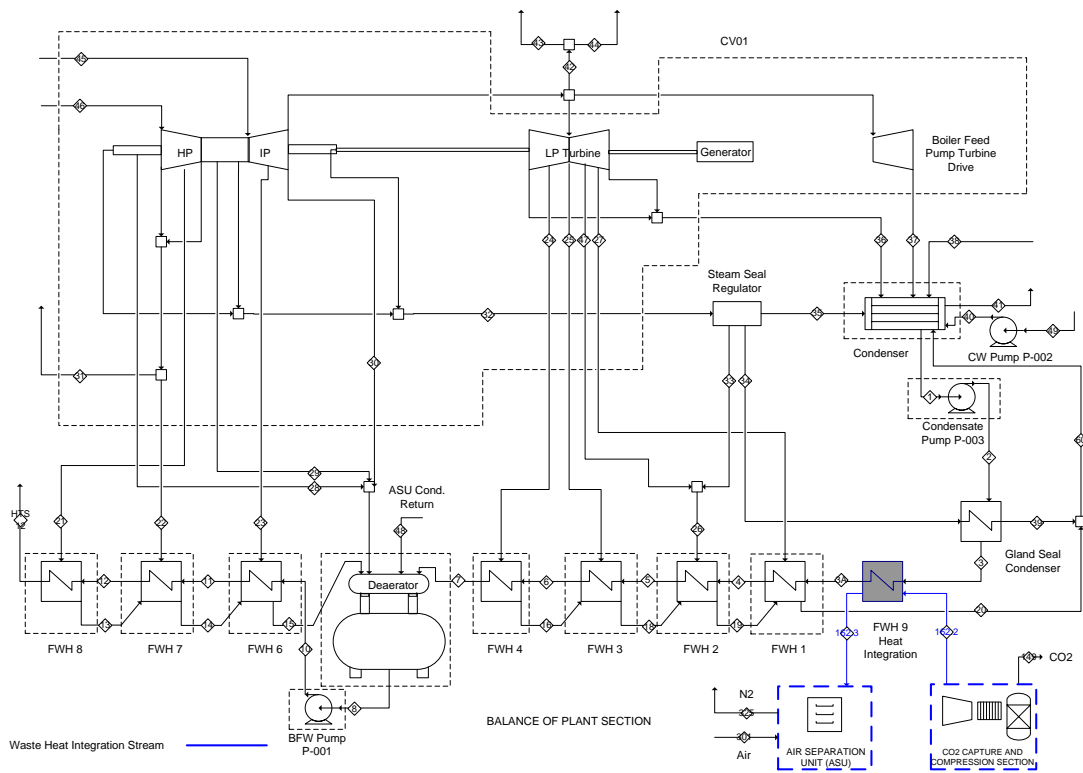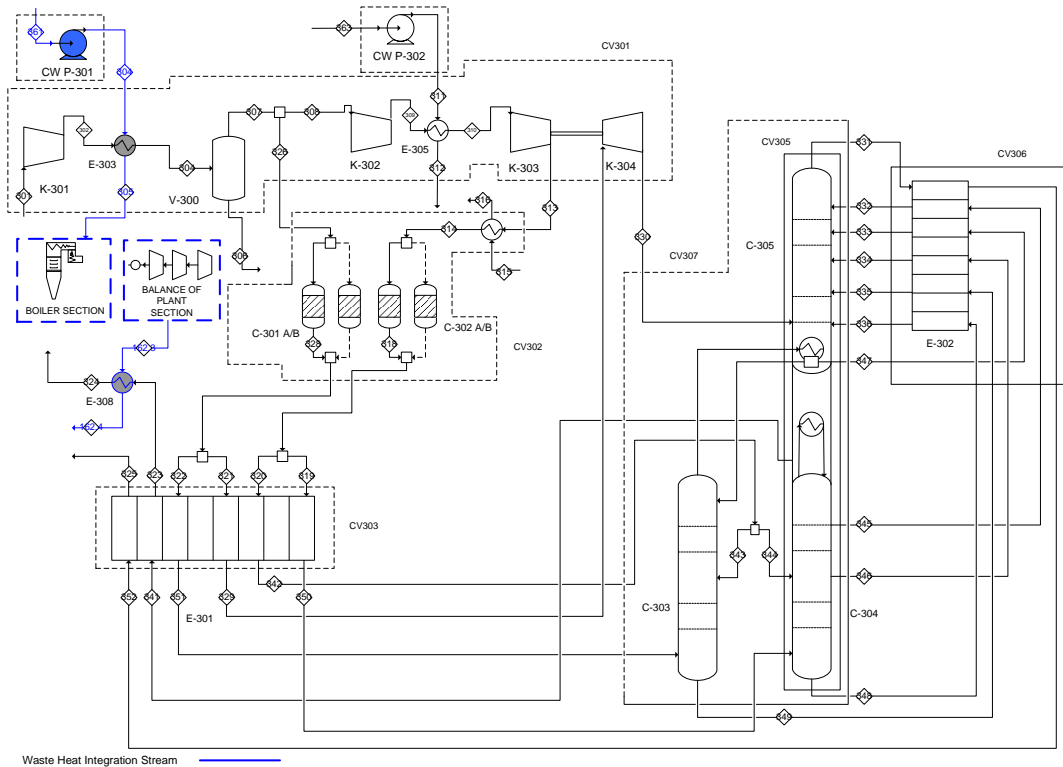

Figure 5-23 Improved BOPsection process model withwaste heat integration streams highlighted

The improved process model for the ASU section is presented in Figure 5-24. The exergy efficiency of the ASU control volumes do not change in this process integration and in the improved model. The main reason for this is because in one case, in exchanger E308, electric heating is replaced by waste heat so the process parameters remain same. However, 3.6 MW waste heat is utilized. In another case waste heat from E303 is utilized in PG Cooler1 in the boiler and flue gas section through stream 305. Essentially no process parameters in the ASU are being affected with this process integration compared to the base and the integrated model. The differences between the base ASU and the improved model can be observed

comparing Figures 3-4 and 5-24. The differences are the blue inter connected cooling water lines. This integration also increases waste heat utilization.

Figure 5-24 Improved ASU section process model with waste heat integration streams highlighted

The improved process model for the CO_2CCU section is presented in Figure 5-25. The exergy efficiency of CV103 improves significantly in the CO_2CCU section as the process stream (137) temperature inlet to CV103 is increased by installing a new exchanger E113 and utilizing waste heat generated from CV101 in the same section. With this process integration the inlet temperature in the base model (stream 137) increases from 7°C to 81°C - (stream 137.1) in the improved model and subsequently reduces the heating demand by approximately 2.54 MW for heater E106 in CV103. This waste heat utilization is achieved by integrating the compressor inter stage cooling water loops in the CO_2CCU section, as shown in Figure 5-25. The cooling water stream (162.2) further integrates the BOP section and

creates significant positive impact on the overall process as described above in the BOP section. The differences between the base CO_2CCU model and the improved model can be observed comparing Figures 3-5 and 5-25. The differences are the blue inter connected cooling water lines. This integration increases waste heat utilization and reduces the exergy destruction in the CO_2CCU section.
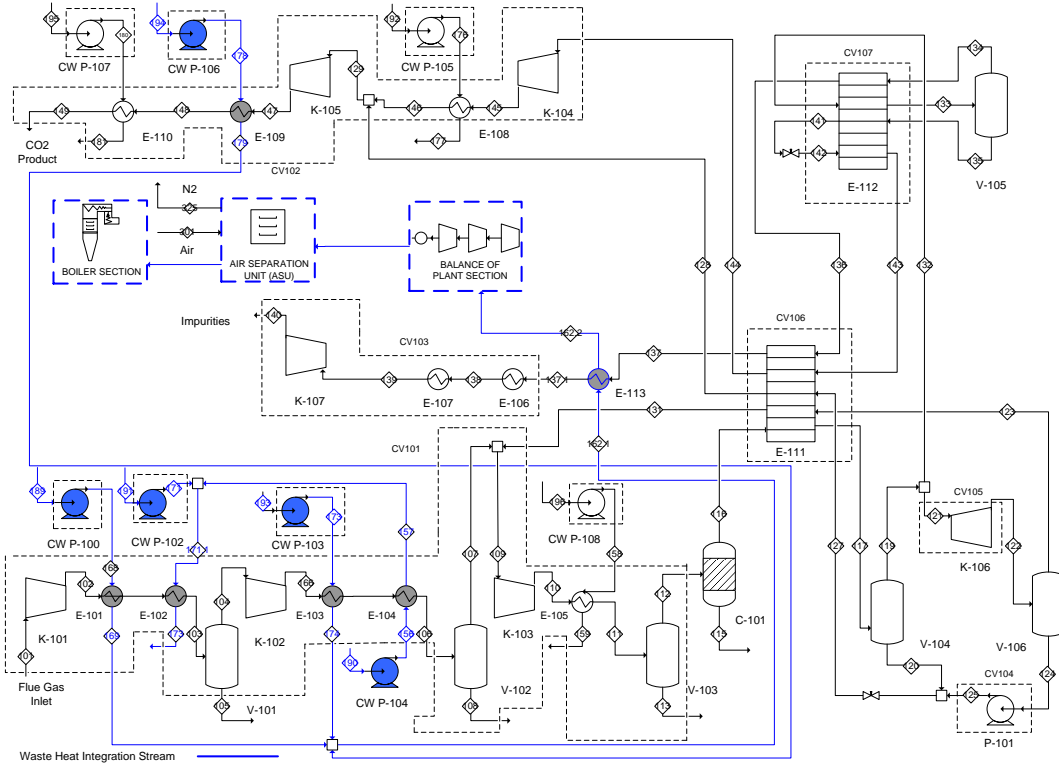
Figure 5-25 Improved CO₂CCU section process model with waste heat integration streams highlighted

5.6 Model comparison and summary results

The overall exergy efficiencies for the base and improved models are presented in Table 5-3. The ranking column was kept the same as the original Table 5-2 to highlight the differences. Based on the ranking in Table 5-2, process improvement actions were undertaken around the first set of control volumes to improve their efficiency. The exergy efficiency of the FWH1 in the BOP section is increased significantly to 93.6% from 76.9%.

The condenser efficiency also slightly increased from 69.2% to 69.3 % due to the other improvement measures adopted in the overall model. The efficiency increase drops the ranking of FWH1 in the ranking table below the deaerator. In the Boiler section, the exergy efficiency of CV208 increases from 49.9% to 61.4% and it's ranking drop down one level, below CV209, in the ranking table. The first item for the boiler section in the table (Table 5-3) now becomes CV209. In the CO_2CCU section the exergy efficiency of the control volume CV103 increases from 50.1% to 58.1%. However, no ranking change happens in this section. So the focus in the CO_2CCU will still remain on the CV103 for any further improvement.

Table 5-3 Exergy efficiency and ranking of the control volumes (base and improved model)

BOP			PC Boiler			CO_2CCU			ASU			
Exergy Efficiency %			Exergy Efficiency %			Exergy Efficiency %			Exergy Efficiency %			Ranking
Control Volume	Base Model	Improved Model	Control Volume	Base Model	Improved Model	Control Volume	Base Model	Improved Model	Control Volume	Base Model	Improved Model	
Condenser	69.2	69.3	CV208	49.9	61.4	CV103	50.1	58.1	CV301	73.5	73.5	1
FWH1	76.9	93.6	CV209	60.7	60.7	CV102	62.4	62.4	CV305	76.4	76.4	2
ConP003	78.0	78.0	CV201	65.7	65.7	CV104	64.9	64.6	CV303	92.2	92.2	3
BFWP001	83.2	83.2	CV203	78.4	78.4	CV101	68.3	68.8	CV307	93.1	93.1	4
CV01	89.0	89.0	CV202	78.7	78.7	CV105	70.3	70.3	CV302	99.3	99.3	5
FWH2	90.0	90.1	CV207	83.7	83.7	CV107	96.5	96.5	CV306	99.3	99.3	6
FWH4	90.6	90.6	CV206	86.6	86.7	CV106	98.2	98.2				7
Deaerator	91.6	91.6	CV205	88.0	88.0							8
FWH3	94.9	94.9	CV204	88.5	88.5							9
FWH6	97.0	97.0										10
FWH7	98.1	98.1										11
FWH8	99.1	99.1										12

Table 5-3 also shows at a glance where attention is needed in the overall plant. A new ranking table is prepared based on the exergy analysis for the improved model and presented in Table 5-4. The renewed focus for the next round of process improvement measure, if undertaken, will be for the first row of control volumes as indicated in this new table. This iterative process may continue as shown in Figure 5-11 till the overall system reaches to its maximum efficiency and does not show any further improvement.

Table 5-4 New ranking table for the improved model

BOP		PC Boiler		CO$_2$CCU		ASU		
Exergy Efficiency %		Exergy Efficiency %		Exergy Efficiency %		Exergy Efficiency %		Ranking
Control Volume	Improved Model	Control Volume	Improved Model	Control Volume	Improved Model	Control Volume	Improved Model	
Condenser	69.3	CV209	60.7	CV103	58.1	CV301	73.5	1
ConP003	78.0	CV208	61.4	CV102	62.4	CV305	76.4	2
BFWP001	83.2	CV201	65.7	CV104	64.6	CV303	92.2	3
CV01	89.0	CV203	78.4	CV101	68.8	CV307	93.1	4
FWH2	90.1	CV202	78.7	CV105	70.3	CV302	99.3	5
FWH4	90.6	CV207	83.7	CV107	96.5	CV306	99.3	6
Deaerator	91.6	CV206	86.7	CV106	98.2			7
FWH1	93.6	CV205	88.0					8
FWH3	94.9	CV204	88.5					9
FWH6	97.0							10
FWH7	98.1							11
FWH8	99.1							12

The overall exergy destruction and the parasitic power demand for the individual sections of the overall plant are presented in the following Figures 5-26 and 5-27.
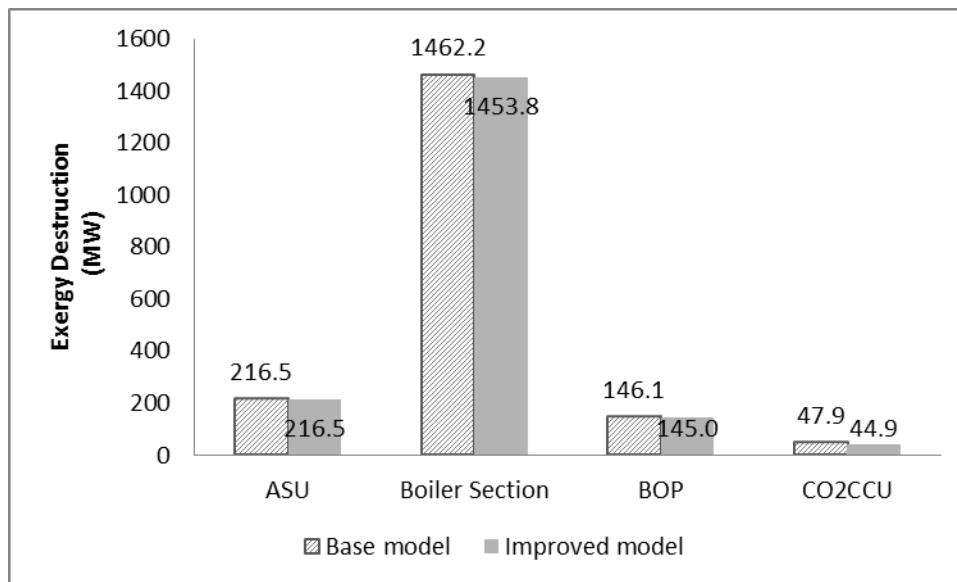
Figure 5-26 Overall exergy loss in the plant (base and improved model)

The total exergy loss is 1873 MW and 1863 MW respectively for the base and improved model and the breakdown for individual sections can be seen in Figure 5-26.
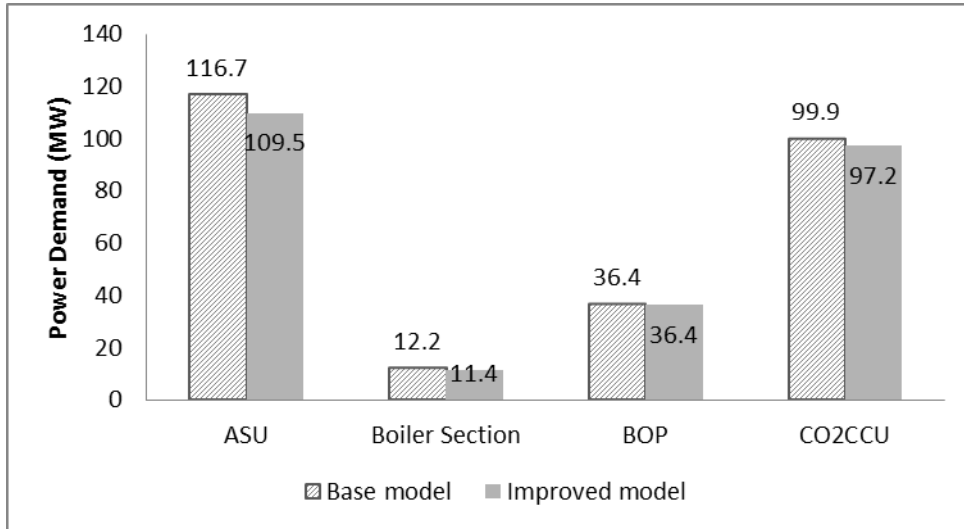
Figure 5-27 Overall auxiliary load in the plant (base and improved model)

The overall cooling water demand in the plant also reduced significantly in the improved model due to the waste heat utilization approach through the cooling water loop, as seen in Figure 5.28.
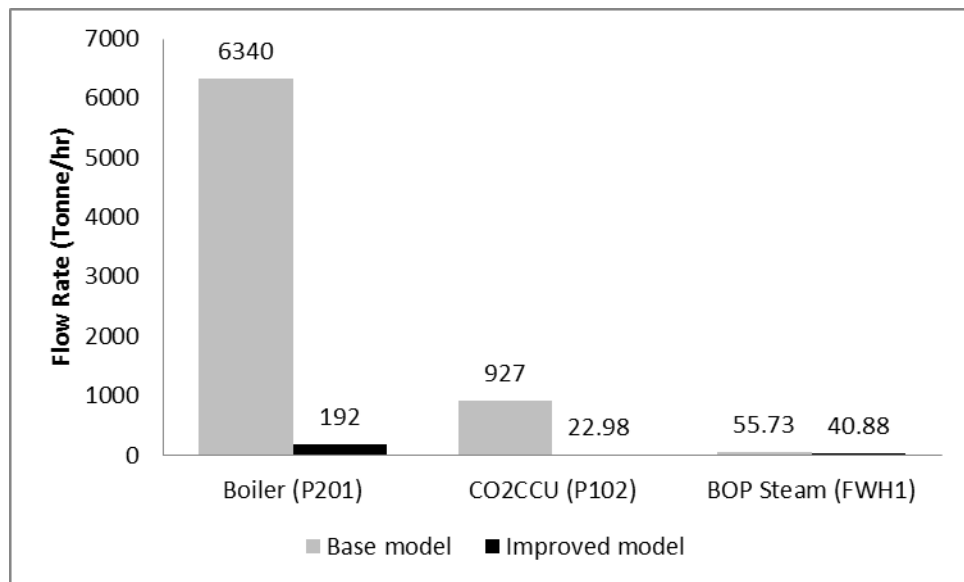
Figure 5-28 Cooling water demand and steam reduction in the improved model

Figure 5-28 shows the reduction of cooling water and extraction steam flow to the pumps and feed water heater in Boiler, CO_2CCU and BOP sections. The demand for cooling water in pump P201 in the Boiler section is reduced from 6340 tonnes/hr to 192 tonnes/hr (96.97% reduction). The cooling water demand in pump P102 in the CO_2CCU section is reduced from 927 tonnes/hr to 22.98 tonnes/hr (97.5% reduction). A few other exchangers also have reduced demand in cooling water in the CO_2CCU section. Altogether, 915 tonnes/hr of cooling water is reduced in the CO_2CCU section. The amount of extraction steam to feed water heater FWH1 is also reduced to 40.88 tonnes/hr from 55.73 tonnes/hr (26.65% reduction). These are significant reduction in cooling water and extraction steam flow rates which also reduces the plant capital as well as operating cost.

A summary result of few important parameters for the base and the integrated model is presented in Table 5-5.

Table 5-5 Summary results for the overall plant (base and improved model)

PLANT SUMMARY RESULTS	BASE MODEL	IMPROVED MODEL
Gross Power Output (kW)	786,300	787,000
Net Power Output (kW)	521,250	532,400
Fuel Thermal Input, kWt	1,878,000	1,878,000
Net HHV Eff. (%)	27.75	28.35
Total Exergy Destruction (kW)	1,873,000	1,863,000
Cycle Exergy Efficiency (%)	50.09	50.36
Cooling Water Temperatuer (^{o}C)	30	30
CO_2 Capture (%)	92.54	92,55
CO_2 Purity (%)	95.77	95.78
AUXILIARY LOAD SUMMARY		
Boiler and Flue Gas Section (kW)	12,160	11,480
ASU (kW)	116,730	109,500
BOP (kW)	36,390	36,360
CO_2 Capture & Compression (kW)	99,850	97,190
Total Auxiliary Loads (kW)	265,130	254,600

The total auxiliary loads for the base and improved models are 265.2 MW and 254.6 MW and the breakdown for the individual sections can be seen in Figure 5-27. It can be noticed that all the auxiliary plant loads in the improved model have come down due to the waste heat utilization. The total net plant HHV efficiency gain for the improved model is 0.6 percentage point. However the net power increase is 2.14% to 532.4 MW. The overall cycle exergy efficiency is calculated to be 50.36% in the improved model compared to 50.09% in the base model. The N_2 stream from the ASU has about 26.97 MW of waste heat potential which is not included in the overall calculation. This will improve the plant efficiency further if it is used for coal drying in actual practice.

5.6.1 Pipeline ready CO_2 product stream

The major benefit of the oxy-fuel power plant with CO_2 capture system is that it produces a nearly pure CO_2 product stream for reuse in process industries as raw material, or in enhanced oil recovery (EOR), or pipeline transportation and storage. The CO_2 is captured in the CO_2CCU section of the oxy-fuel plant. The CO_2 product purity remains very high (>95% by mole), as well as the recovery rate of CO_2 (> 92%). The CO_2 recovery rate is defined by the following equation with respect to Figure 5-25:

$$CO_{2\ recovery(\%)} = \frac{mass\ of\ CO_2\ in\ stream\ 149}{mass\ of\ CO_2\ in\ stream\ 101}\ X\ 100 \qquad\qquad 5.1$$

The compression energy consumption for CO_2 capture is also reduced by 3.9 kW-hr/ tonne of CO_2 captured in the improved model. The energy consumption in the improved model is 0.1586 kW-hr/kg of CO_2 captured. The amount in the base model is 0.1625 kW-hr/kg of CO_2 captured. The specification of the CO_2 product stream is given below in Table 5-6.

Table 5-6 CO$_2$ pipe line product flow specification

CO$_2$ to Pipeline		
Parameters	Unit	Value
Temperature	^{o}C	43
Pressure	bar absolute	109.8
Flow rate	kg/hr	628,600
CO$_2$ Recovery Rate	%	92.55
Compression Energy	kW-hr/kg CO$_2$	0.1586
Composition		
CO$_2$	mole %	95.78
O$_2$	mole %	1.01
N$_2$	mole %	1.83
Ar	mole %	0.91
SO$_2$	mole %	0.46
NO$_2$	mole %	0.01

5.7 List of new items added for design change in the improved model

Exergy analysis showed the pathway to incorporate necessary improvement measures in the oxy-fuel plant by introducing new unit operations or material and energy streams. Following are the overall list of additional unit operations and the process streams in the improved process model presented in Table 5-7 for the current study.

Table 5-7 Additional items in the improved model

Additional Items in the Improved Model			Total Gain	
Plant Section	Unit Operation	Material Stream	HHV efficiency	Net Power
	Name	Number	(percentage point)	%
Boiler Section		274, 280, 305.1		
BOP	FWH9	162.2, 162.3		
ASU		162.3, 162.4, 305	0.6~1.15	2.14~4.12
CO$_2$CCU	E113	162.1, 162.2, 179		

It can be noticed that with addition of only two new exchangers and nine process streams, the efficiency of the power generation system increased significantly for HHV up to 1.15

percentage point and for net power gain of up to 4.12%. The increased efficiency numbers can be achieved with process sensitivity analysis, as explained in the following section.

5.8 Process sensitivity

There are several parameters that influence the overall power output or the exergy destruction amount. These parameters can be changed to investigate their impact on the overall process. A single change in the parameter value generates an updated set of data in the model. The major process parameters that can be considered for the sensitivity analysis include:

- cooling water temperature (supply and return)
- cooling water pressure
- condenser pressure in the BOP section
- flue gas processing/CO_2 recovery rate in CO_2CCU
- environment reference temperature
- O_2 preheating to Boiler
- N_2 temperature from ASU
- O_2 purity from ASU
- fuel composition
- air leakage into the boiler
- boiler temperature
- flue gas recycle ratio to the boiler
- amount of moisture content in the recycle flue gas in the boiler
- excess O_2 percent in the boiler
- CO_2 product purity from CO_2CCU
- Turbine, pump and compressor efficiencies

The sensitivity analysis has not been carried out for all these parameters. Only the first eight in the list were considered and the results are presented here. Sensitivity analysis on the other parameters requires major changes in the process design which generates a new set of data of its own. Hence no analysis was done. However, the effects of these othere parameters are

128

explained qualitatively in detail in section 5.8.9. The sensitivity analysis is done for the improved model only.

5.8.1 Process sensitivity on cooling water supply temperature

The variation in cooling water supply temperature influences the overall plant net power generation and the exergy loss. This analysis is done at a constant supply pressure of 4 bar (abs) for the cooling water loop. A decrease in cooling water supply temperature from 30°C to 15°C increases the net power from 532.4 MW to 539 MW as shown in Figure 5-29. The exergy destruction increases with decreasing cooling water temperature. The exergy destruction increases from 1863 MW to 1896 MW with an exergy efficiency penalty of 0.87 percentage point. The efficiency decrease from 50.35% to 49.48% is due to the low temperature of the cooling water stream. This follows the usual phenomenon of exergy efficiency reduction when the temperature differences between the hot and cold streams are increased. However, the overall effect is a net gain of 7 MW power in the overall plant.
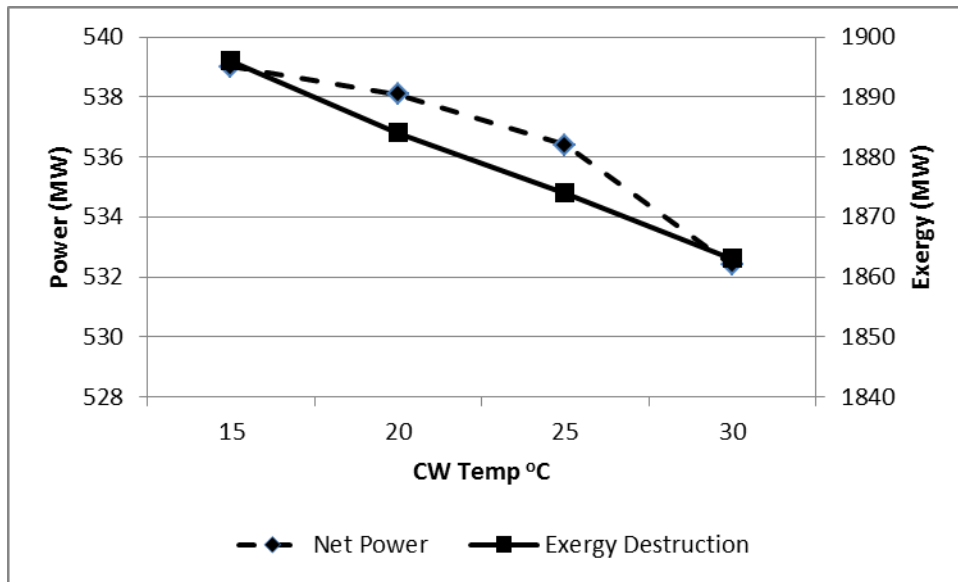
Figure 5-29 Net power generation and exergy destruction at different cooling water temperatures, but atconstant cooling water pressure (improved model)

The impact on the net plant efficiency and the exergy efficiencies with respect to the cooling water temperature at constant pressure (4bara) is shown in Figure 5-30. The total HHV efficiency gain for the plant is 0.36 percentage point when reducing the cooling water temperature from 30°C down to 15°Cwith HHV efficiency increasing from 28.34% to 28.70%. The exergy efficiency drops from 50.35% to 49.48%. The maximum net power gain is 3.46% at a temperature of 15°C compared to the base net power of 521 MW. Reduction of cooling water temperature reduces the overall fresh water intake demand to the cooling water loop by 6091 tonnes/hr, which is a very significant amount.
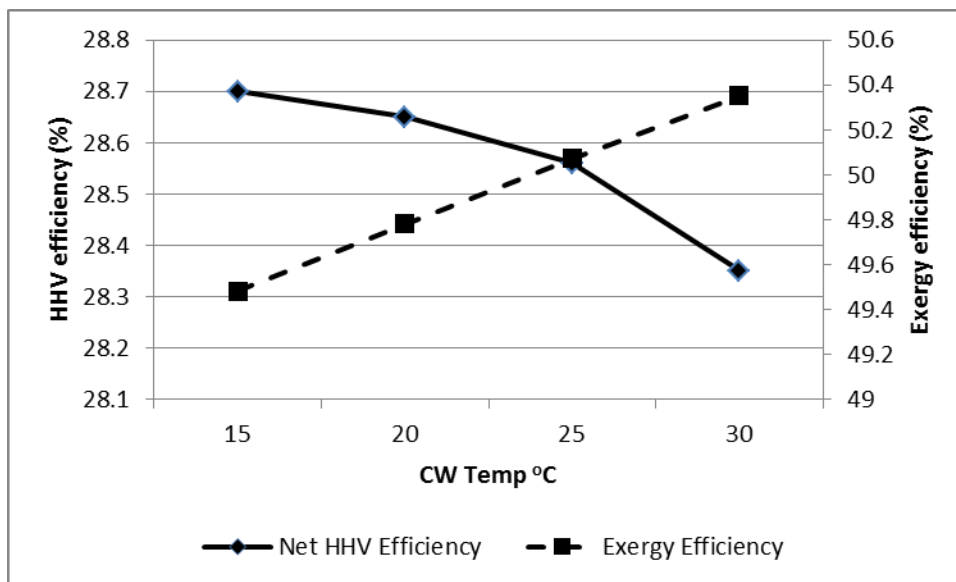
Figure 5-30 Net efficiency gain at different cooling water temperatures, but at constant cooling water pressure (improved model)

In general, reducing the cooling water temperature should increase the plant efficiency as the density of the process streams goes up which in turn increases the efficiency of the fans and blowers. This results in comparatively low energy consumption for the rotating equipment. However this scenario is not included here as the process streams were kept constant for this particular process design. Table 5-8 indicates the comparative summary results for the base and improved model with respect to different cooling water temperatures.

5.8.2 Process sensitivity on cooling water supply pressure

Similar to the cooling water supply temperature, the variation in cooling water supply pressure also influences the overall plant net power generation and the exergy loss. This analysis is done at a constant supply temperature of 30℃ for the cooling water loop. A decrease in cooling water supply pressure from 4 bara to 2 bara increases the net power from 532.4 MW to 539.8 MW, as shown in Figure 5-31. The exergy destruction slightly decreases and the change is 1.3 MW only when decreasing cooling water pressure. Exergy destruction decreases from 1863 MW to 1861.7 MW (0.07% reduction). However, the overall effect is a net gain of 7.4 MW power in the overall plant.
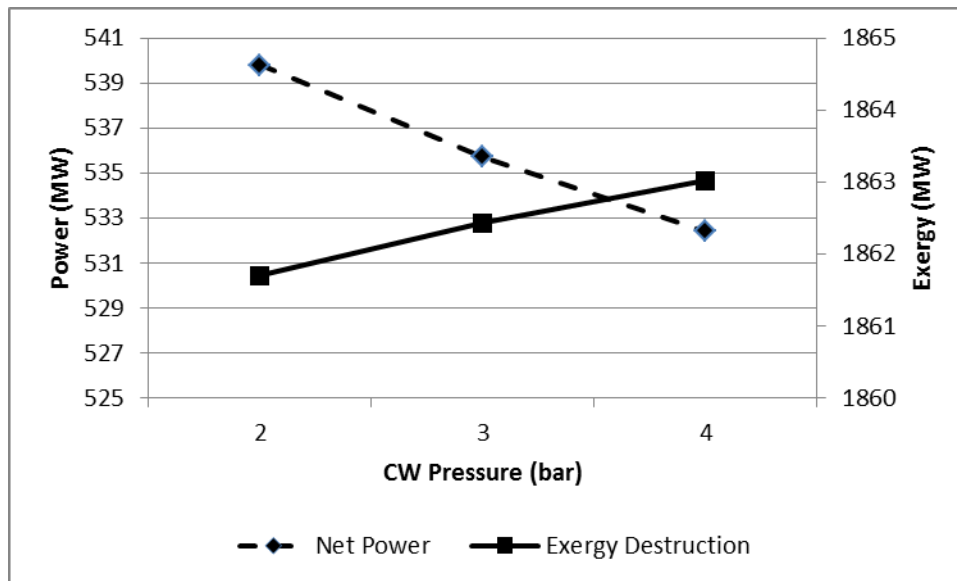
Figure 5-31 Net power generation and exergy destruction at different cooling water pressure, but at constant cooling water temperature (improved model)

The power gain is mainly because of the low power demand for the cooling water pumps as the supply pressure is low. No effort was made to do a sensitivity analysis for cooling water temperature below 15°C and a supply pressure below 2 bara as these values are beyond the realistic numbers in actual industrial practice. Pressure is usually maintained approximately at 4 bar in the cooling water headers in industries (DOE 2008). The impact on the net plant efficiency with respect to the cooling water pressure at constant temperature of 30°C is

shown in Figure 5-32. The total HHV efficiency gain for the plant is 0.4 percentage point when decreasing the cooling water pressure from 4 bara down to 2 bara (HHV efficiency increases from 28.34 up to 28.74%) The maximum net power gain is 3.60% at a pressure of 2 bara compared to the base net power of 521 MW.
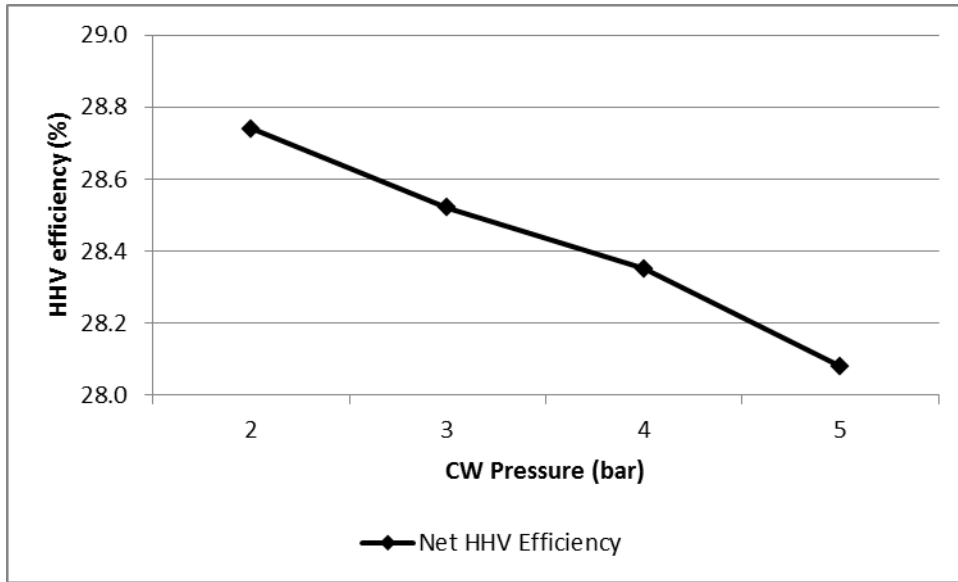
Figure 5-32 Net efficiency gain at constant cooling water temperature (improved model)

Table 5-8 Summary result based on different cooling water temperatures and Pressures

PLANT SUMMARY RESULTS	BASE MODEL	IMPROVED MODEL			
		Constant Cooling Water Pressure			
Cooling Water Temperatuer (^{o}C)	30	30	25	20	15
Cooling Water Pressure (bar a)	4	4	4	4	4
Gross Power Output (kW)	786,300	787,000	787,000	787,000	787,000
Net Power Output (kW)	521,110	532,400	536,400	538,100	539,000
Thermal Input, kWt	1,878,000	1,878,000	1,878,000	1,878,000	1,878,000
Net HHV Eff. (%)	27.75	28.35	28.56	28.65	28.7
Total Exergy Destruction (kW)	1,870,000	1,863,000	1,874,000	1,884,000	1,895,000
CO_2 Capture (%)	92.54	92,55	92,55	92,55	92,55
CO_2 Purity (%)	95.77	95.78	95.78	95.78	95.78
AUXILIARY LOAD SUMMARY					
Boiler and Flue Gas Section (kW)	12,160	11,480	11,630	11,660	11,650
ASU (kW)	116,730	109,500	109,200	109,100	109,000
BOP (kW)	36,390	36,360	32,650	31,010	30,080
CO_2 Capture & Compression (kW)	99,850	97,190	97,110	97,150	97,220
Total Auxiliary Loads (kW)	265,200	254,600	250,600	248,900	248,000
		Constant Cooling Water Temeprature			
Cooling Water Pressure (bar a)	4	4	3	2	-
Cooling Water inlet Temperatuer (^{o}C)	30	30	30	30	-
Gross Power Output (kW)	786,300	787,000	787,000	787,000	-
Net Power Output (kW)	521,110	532,400	537,700	539,800	-
Thermal Input, kWt	1,878,000	1,878,000	1,878,000	1,878,000	-
Net HHV Eff. (%)	27.75	28.35	28.52	28.74	-
Total Exergy Destruction (kW)	1,870,000	1,863,000	1,862,000	1,861,000	-
CO_2 Capture (%)	92.54	92.55	92.55	92.55	-
CO_2 Purity (%)	95.77	95.78	95.78	95.78	-
AUXILIARY LOAD SUMMARY					-
Boiler and Flue Gas Section (kW)	12,160	11,480	11,430	11,350	-
ASU (kW)	116,730	109,500	10,930	10,900	-
BOP (kW)	36,390	36,360	33,610	30,180	-
CO_2 Capture & Compression (kW)	99,850	97,190	96,920	96,600	-
Total Auxiliary Loads (kW)	265,200	254,600	251,300	247,100	-

5.8.3 Impact of condenser pressure

The LP turbine exhaust steam condenser at the BOP section plays an important role in the overall LP section design and the power output from the turbine and generator section. A lower pressure is always favourable for more electricity output from the LP stage. Figure 5-33 shows the impact of condenser pressure in the BOP section over the net power generation.
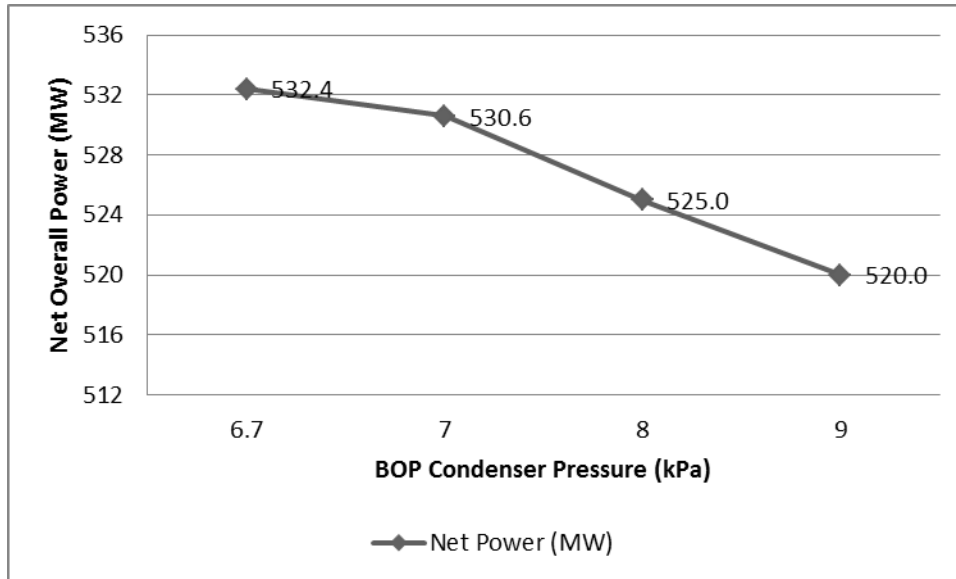
Figure 5-33 Impact of condenser pressure on net power (improved model)

The net power decreases from 532.4 MW to 520 MW with the increase of condenser pressure from 6.7 kPa to 9 kPa only. Condenser pressure cannot be changed drastically as it is directly related to turbine design and the performance of the overall BOP section.

5.8.4 Impact of percentage of boiler flue gas processed in CO_2CCU

Electricity demand in power grid varies during the peak and off peak hours in each day. During peak hours the demand remains very high for a limited time, and additional power can be produced by temporary reducing the percentage of CO_2 captured/processd by sending less gas to the CO_2CCU from the boiler and flue gas section. This will reduce the power consumption by the CO_2CCU and free up additional power to the grid. .In the current study all the analysis in the base and improved model has been done for a 100% processing of flue

gas. However, Figure 5-34 shows the net power generation with the change in percentage of flue gas processing in the CO_2CCU and the amount of freed up electricity to the grid. If the total flue gas amount from boiler to CO_2CCU is decreased from 100% to 40% then the net power generation increases from 532.4 MW to 590.7 MW. It frees up an additional 58.3 MW of electricity to the grid for consumption during the peak hours.
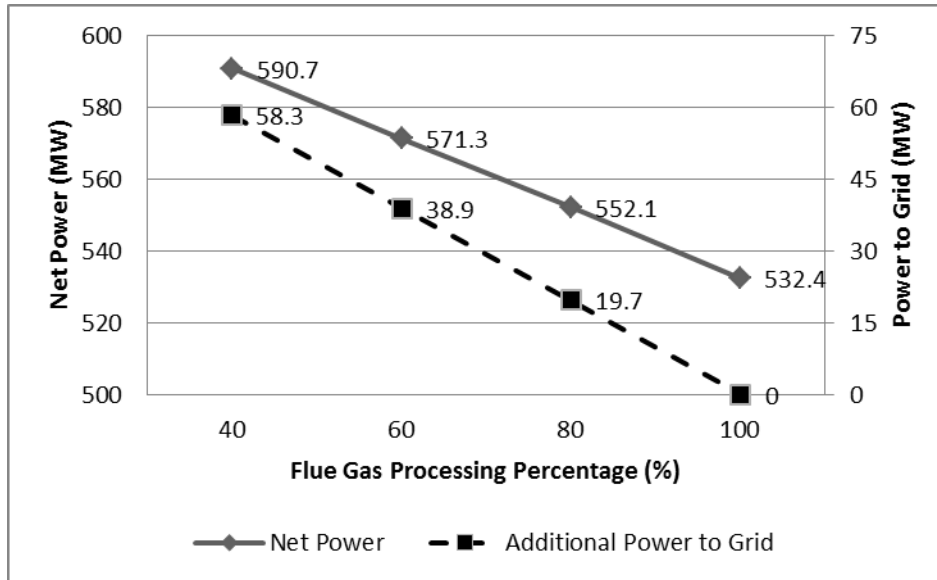
Figure 5-34 Impact of flue gas processing on net power generation and additional power to grid (improved model)

5.8.5 Impact of reference environment temperature

Reference temperature has a large impact on the exergy analysis. Exergy values of different unit operations and process streams vary when changing the reference temperature. Figures 5-35 shows the impact of exergy reference environment temperature on the exergy destruction for the ASU, BOP and CO_2CCU section. The reference environment temperature is changed from 15°C to 35°Cand accordingly the exergy destruction amount increased for all the subsections. The exergy destruction amount for the boiler section varies from 1431 MW to 1483 MW (52 MW increase, i.e. 3.64% increase) for the improved process model. Similarly for BOP it varies from 141 MW to 149MW (8MW increase, i.e. 5.74% increase),

for ASU it varies from 209 MW to 224 MW (15 MW increase, i.e. 7.29% increase) and for CO_2CCU it varies from 43 MW to 47 MW (4 MW increase, i.e. 9.28% increase).
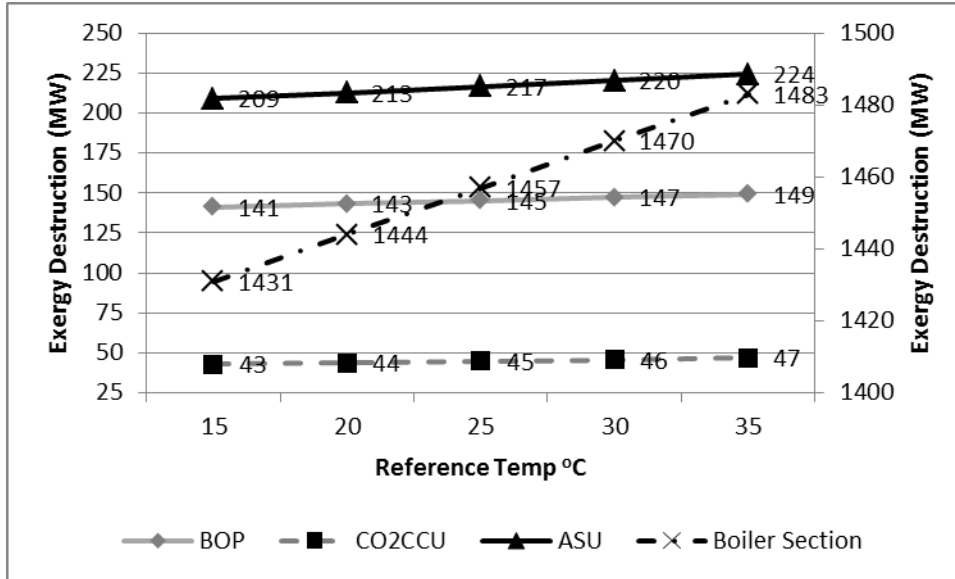
Figure 5-35 Exergy destruction at various reference temperature (improved model)

The change in total cycle exergy efficiency with respect to the environment temperature is shown in Figure 5-36. Cycle efficiency decreases from 51.4% to 49.3% when the reference temperature increases from 15°C to 35°C only.
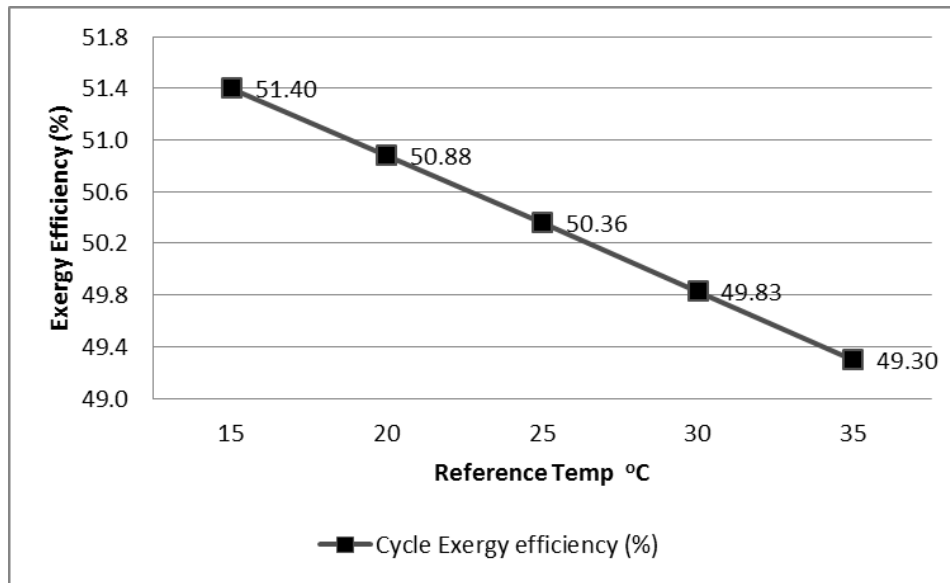
Figure 5-36 Cycle efficiency at various reference temperature (improved model)

5.8.6 O_2 preheating temperature to Boiler

The O_2 preheating temperature before feeding into the boiler in the base and improved model was used as 40°C. However the new stream 162.3 (Figure 5-24) from the BOP section has a potential to increase the O_2 temperature up to 60°C in exchanger E308 in the ASU section. O_2 preheat temperature is dictated by the atomic oxygen composition in the fuel and by O_2 supply line to the burner. As O_2 is mixed in the primary and secondary air lines, more investigation is needed to verify the limit of O_2 temperature with respect to the spontaneous combustion of fuel in the pipeline as the primary air is used to carry solid fuel in the boiler. With the change in O_2 preheat temperature from 40 to 60°C, the net power can be increased by 2.5 MW. It increases from 532.4 MW to 534.9 MW as shown in Figure 5-37.
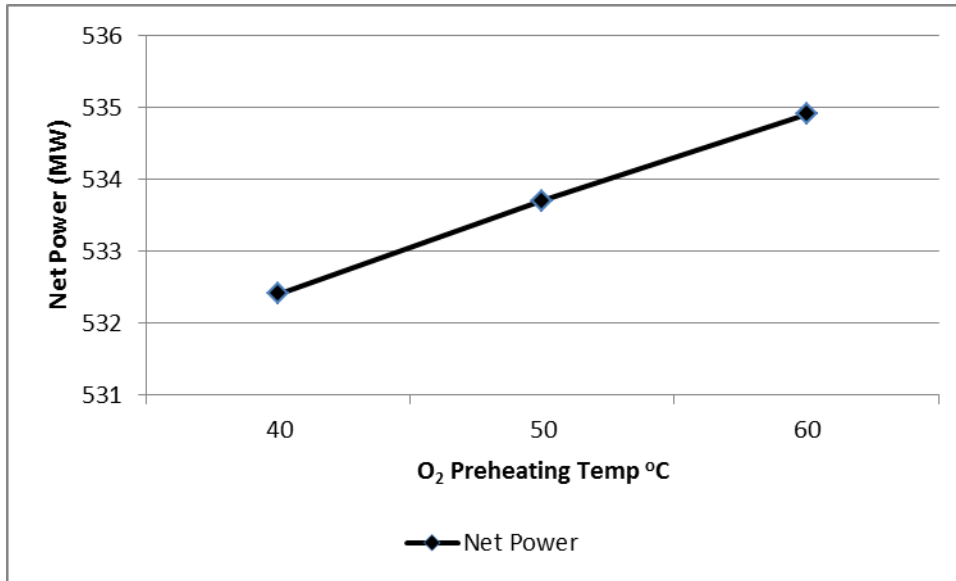
Figure 5-37 O_2 preheating and net power gain (improved model)

5.8.7 N_2 exit temperature from ASU

The temperature of the N_2 stream coming out from the ASU section can be varied at different temperature level as needed. The N_2 temperature variation can be achieved by maintaining the cooling water (312) outlet temperature from the heat exchanger E305 (in Figure 5-24) at different values within a range of 40°C to 85°C. This translates into a N_2 temperature variation of 37°C to 75°C. A higher N_2 temperature will have the potential to use it for coal drying. However, maintaining a high N_2 temperature reduces the purity of O_2 stream slightly by a little over one percentage point. The purity of O_2 drops from 95.48% to 94.02% by mole. However, the available heat potential for coal drying would then increase from 6.36 MW to 27 MW. The effect of N_2 temperature on the available heat potential for coal drying and the O_2 purity is shown in Figure 5-38.
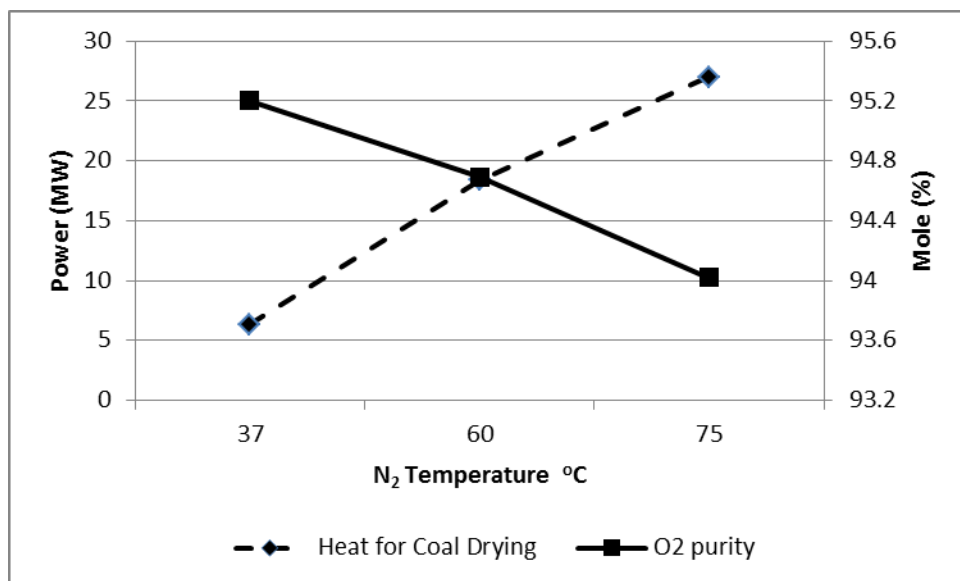
Figure 5-38 O_2 purity and available heat for coal drying as a function of N_2 exit temperature (improved model)

The effect of temperature variation on the exergy destruction and net power is very minimum, as shown in Figure 5-39. The change in exergy destruction is from 1863 MW to 1865 MW (2 MW decrease, i.e. 0.1% decrease) when the temperature is reduced from 75°C to 37°C. Similarly, the net power gain is only 0.5 MW (0.094% increase in net power). The net power increases from 532.4 MW to 532.9 MW. The minor increase in net power is because of the lower power consumption by the CW P-302 due to reduced cooling water flowrate at low cooling water temperature. CW P-302 pump supplies cooling water to E305. The effect of this power consumption is insignificant up to 60°C, however, some impact is seen above 60°C as seen in Figure 5-39. If the sensitivity calculation for N_2 stream would have been done using a cooling water supply temperature of 15°C instead of 30°C, as used in this case, then the O_2 purity would have gone up to 95.48%. However, the available heat for coal drying would drop by 1.4 MW in this scenario. So it is clear that the temperature of the N_2 stream will be determined based on the need of a particular plant design. All these results show the process sensitivity of the integrated plant to different parameters. Several other process sensitivity analysis can be done as needed.
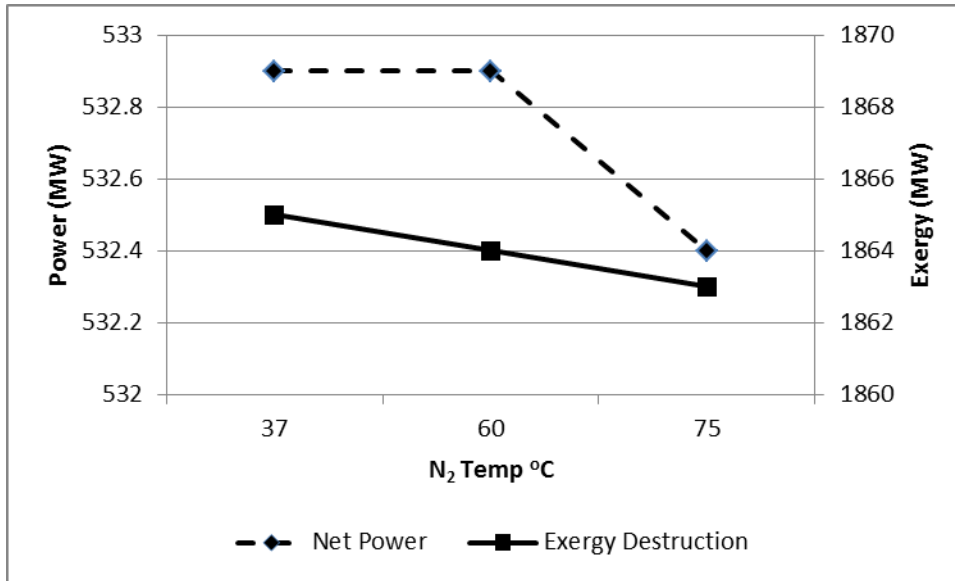
Figure 5-39 Net power and exergy destruction as a function of N$_2$ exit temperature (improved model)

The variation of N$_2$ temperature from 37°C to 75°C also influences the CO$_2$ product purity and CO$_2$ recovery rate in the CO$_2$CCU section. The change in O$_2$ purity changes the overall composition of the flue gas in the boiler section which in turn changes the inlet gas composition to CO$_2$CCU. The effect on CO$_2$ product purity from CO$_2$CCU is insignificant (only a decrease of 0.02 percentage point by mole) and the purity remains almost constant. The reason is that CO$_2$CCU produces high purity CO$_2$ irrespective of the inlet gas composition, however, the recovery rate varies. The CO$_2$ recovery rate drops by 1.05 percentage point from 93.6% to 92.55%. Figure 5-40 shows the impact of changing N$_2$ temperature on CO$_2$ product purity and recovery rate.
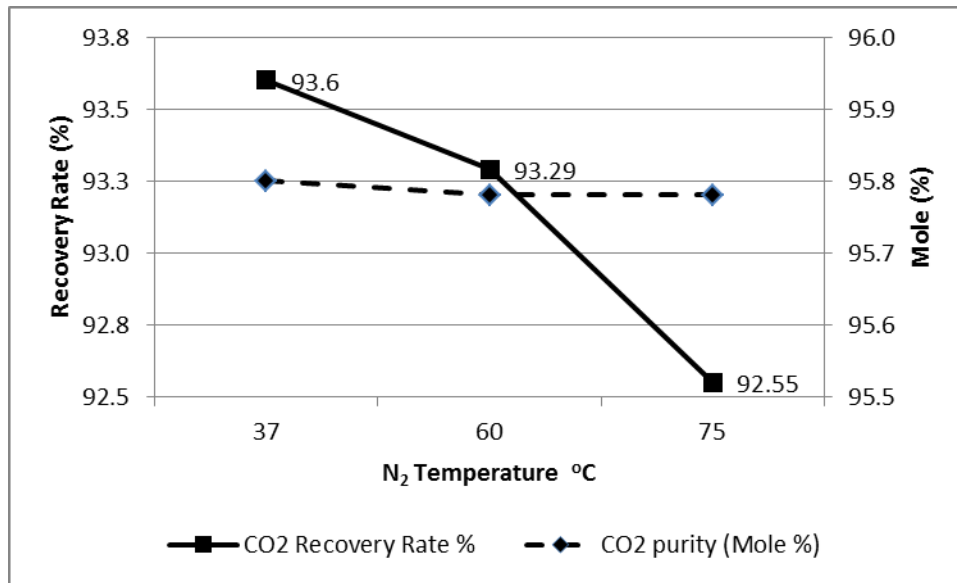
Figure 5-40 CO$_2$ purity and recovery rate from CO2CCU as a function of N$_2$ exit temperature (improved model)

5.8.8 Preferred sensitivity case

There are unlimited potential in this process model to explore the sensitivity of different parameters on the plant performance. However, a set of preferred and achievable parameters in the improved model was selected to manipulate and investigate the impact on the performance of the overall process design. The parameters include maintaining cooling water inlet temperature at 15°C, setting cooling water discharge pressure at 4 bar and maintaining O$_2$ preheating temperature at 60°C. To be consistant with the improved model, the N$_2$ temperature from the ASU was maintained at 75°C. With this new set of operating parameters, the net power increased to 541.5 MW (from 532.4 MW for the improved model). and the net power compared to the base model (521 MW) increased by 3.94%, The overall efficiency (HHV basis) compared to the base model increased by 1.08 percentage point, from 27.75% to 28.83% (0. 5 percentage point compared to the improved model). However, if the N$_2$ temperature is reduced to 28°C, the HHV efficiency will increase to 28.9% and net power will increase to 542.7 MW. In this case the CO$_2$ recovery rate will go up to 93.37% in the CO$_2$CCU section. The CO2 purity will increase to 95.81 and the energy penalty for CO$_2$

141

capture will also reduce to 0.156 kw-hr/kg CO_2 captured. In summary this investigation indicates that the plant HHV efficiency can be increased up to 1.15 percentage point through a systematic exergy analysis and process improvement measures.

5.8.9 Other parameters for sensitivity analysis

Fuel composition will have much more effect on the overall plant performance and sensitivity. It will change all the gas composition and flow rates in different plant sections. It will also change the energy consumption of the rotating devices. It will also influence the heat transfer properties in the heat exchangers. All these changes will result in a new set of data for the model. Hence, no effort was made to do a fuel sensitivity analysis as it would require a presentation of almost the same amount of data as presented in this study.

Air leakage into the boiler will affect the ASU size. However the impurities will increase in the overall system and the effect of which will be a higher energy penalty in the CO_2CCU section for CO_2 capture. The boiler temperature was kept constant in this study. However a change in boiler temperature can be achieved by varying the flue gas recycle ratio. The exergy destruction amount within the boiler section will be affected with this scenario. However the other sections will not be much affected as the flow rates out of the boiler section will remain the same. Only the flow in the recycle loop will change in this case. Flue gas recycle ratio and the boiler temperature are interconnected.

The moisture content in the recycle flue gas has an impact on the boiler temperature and its performance. A dry recycle would require more recycle flue gas to achieve a same temperature range in the boiler in case of a wet recycle. Heat of vaporization plays an important role in these two different cases. Also the primary and secondary air fan power consumption will be affected.

In all combustion boilers, excess O_2 is maintained for complete combustion of fuels and restrict the carbon monoxide (CO) generation. Excess O_2 usually does not have a big impact on the boiler heat transfer performance and the overall flow rate of the flue gas system. However, it is important with respect to the ASU size for an oxy-fuel plant.

CO_2 product purity is an important factor in terms of end user requirement. A high purity CO_2 is desirable for various end uses. The presence of impurities affects the CO_2 capture

system while processing the flue gas. A higher impurity causes more energy penalty, specifically in the compression system, in the overall process. CO_2 purity can be varied by temperature changes in the CO_2CCU section.

The turbine, pump and compressor efficiencies influence the temperature and pressure of the process streams. It is not suggested to change the efficiency arbitrarily. In this current study, the turbine adiabatic efficiencies were maintained in between 72% and 99% based on the published literature. No effort was made to change the efficiency as it requires detailed turbine knowledge and turbine system development studies. For the pumps the adiabatic efficiencies were maintained in between 75% and 80%. The adiabatic efficiencies for the compressors were maintained in between 80% and 87%. No effort was made to chage the compressor efficiencies as it is again depends on the compressor design. In general, it might give us a lot less auxiliary power load if we would use very high efficiency numbers in the compressors and pumps; however, the intention was to keep the model as realistic as possible.

Chapter 6
Conclusions and Recommendations

6.1 Conclusions

The main goal of this study was to improve the performance of an oxy-fuel power generation system through a systematic method involving exergy analysis. There are different areas in a power generation system where efficiency improvement can be done. However, in order to do that it requires the quantification of heat loss from different unit operations/control volumes and identify the right unit operation/control volume to adopt the improvement measures for waste heat utilization. To achieve this goal a systemic thermodynamic method based on exergy analysis was developed and utilized to generate an efficient and flexible integrated process model of an oxy-fuel power generation system with air separation and CO_2 capture and compression modules.

The systematic approach included a base process model development, followed by implementation of exergy analysis equations in all process streams, calculation of the exergy destruction and exergy efficiency for various unit operations /control volumes in the plant and finally ranking the unit operations/control volumes in ascending order of exergy destruction for the four different plant sections, specifically boiler, BOP, ASU and CO_2CCU. In the the next step, evaluation of the first set of unit operations/control volumes with lowest exergy efficiency were completed.   The following step was to include the process improvement measures in the first set of unit operations/control volumes in order to reduce the exergy destruction. The final outcome of this stepped approach was the development of an improved oxy-fuel process design associated with an improved process model. After adopting the improvement measures a new ranking table was established again. The first set of unit operations/control volumes in this new ranking table again becomes the potential candidate for next round of exergy improvement actions. This cycle of improvement measures can continue until any design or engineering constraint becomes an impediment for the process improvement.

The method was applied to a 786 MW gross oxyfuel power plant, which was initially modelled and developed in HYSYS process simulation software package (referred to as base model). The ranking table determined the specific unit operation/control volume where improvement measures were needed. The first set of improvement actions were undertaken for three unit operations/control volumes i.e. FWH1 (Feed Water Heater1), CV208 (Process Gas Cooler1) and CV103 (expander K107) in the BOP, boiler and CO_2CCU section respectively. Significant exergy efficiency improvements were acheived for these control volumes through waste heat utilization.

The input parameters in the process model were set at very conservative values to develop robust base and improved process model. As an example the cooling water inlet temperature throughout the plant was set at 30°C which is a very conservative number. However, this temperature selection makes the process model robust and does not impose any temperature constraint for site selection if implemented in a location where the cooling water temperature is high.

The HHV efficiency for the base model was 27.75% and the cycle exergy efficiency was 50.09%. The net power available from this model was 521 MW. The auxiliary power load for different sections of the base power plant was 265.2 MW and total exergy destruction amounted to 1873 MW. Significant efficiency gain was achieved after implementing process improvement measures by utilizing the available waste heat in the plant. Ultimately an improved process model for oxy-fuel power generation system with higher efficiency was developed.

The HHV efficiency for the improved model was 28.35% and the cycle exergy efficiency was 50.35%. The net power available from this model was 532.4 MW while the auxiliary power load for different sections was reduced to 254.6 MW. The total exergy destruction amount was also reduced to 1863 MW compared to 1873 MW in the base model. The net HHV efficiency gain was 0.6 percentage point. The gain in net power to the electrical grid was 11.4 MW which translates into a net power gain of 2.14 % compared to the base net power. The gain in cycle exergy efficiency was 0.26 percentage point. These efficiency

improvement measures were accomplished by utilizing waste heat available in the plant. The waste heat utilization was done through cooling water loops.

The unique property of this model is its flexibility in accepting a wide range of process parameters to study their impact on the overall integrated oxy-fuel power generation system. This integrated model is an effective tool and platform to conduct research and perform studies on combustion, emission control, and CO_2 capture processes for energy efficiency improvement of the oxy-fuel power generation plants. This process model is flexible and fully automated. Several sensitivity studies can be carried out by changing different process parameters and the results are generated automatically.

A set of sensitivity analysis was carried out on the improved model. It was found that cooling water temperature and pressure have a big impact on the plant efficiency. The sensitivity analysis indicates that if the cooling water temperature is reduced to 15°C or the cooling water supply pressure is reduced to 2 bar, then the HHV efficiency becomes 28.7% and 28.74%, respectively, which results in efficiency gain of 0.36% and 0.4% percentage point compared to the improved model which was 28.34%. In a best case sensitivity analysis with changing few other parameters (CW temperature, CW pressure, N_2 temperature and O_2 preheating) it was found that the plant HHV efficiency could be increased to 28.9% which is an increase of 1.15 percentage point. The net power gain will be 4.12% with these changes in the plant (power increase from 521.25 MW to 542.7 MW). The improved model also reduces the overall cooling water demand by -6091 tonnes/hr (5.16% reduction). This reduction will translate into a smaller cooling water loop and low capacity cooling water pumps. The ultimate effect of which is efficiency improvement, as noted already, and the overall capital and operating cost reduction.

In summary, the exergy based process improvement approach helped develop an efficient oxy-fuel process model from a based inefficient process model. The efficiency improvement was accomplished through a plant wide waste heat utilization approach as dictated by the exergy analysis.

6.2 Recommendations

The following are the recommendations for future work:

1) Optimization of the improved model:

The improved model can be optimized by incorporating process optimization functions in the model for the overall oxy-fuel plant including the four major sections. The optimization can be done on the performance of various unit operations in the model. The localized objective functions of the optimization blocks could be for the boiler section, e.g. maximize steam production, minimize pump and power consumption, etc. The objective functions for the BOP section could be, for example, minimizing the extraction steam for BFW preheating, minimizing condenser pressure, maximizing turbine power, etc. The objective functions for the ASU section could be minimizing air compressor power, maximizing O_2 purity, maximizing O_2 flow rate, etc. The objective for the CO_2CCU could be: maximizing CO_2 recovery and CO_2 product purity, minimizing compression power, etc. In general, the global optimization focus should be minimization of losses or energy penalty and maximization of energy efficiency in the plant.

2) Introduction of the costing tool in the model:

Cost analysis is a necessary feature for any process to demonstrate its economic feasibility. Various cost functions can be implemented in each section of the plant. In order to do that, a different costing tool in HYSYS could be used for cost calculation. Also custom cost data and cost functions can be implemented as needed. This model can be transformed into a techno-economic model including the optimization tool and can serve as a base for the techno-economic studies.

3) Introduction of the chemical exergy equations:

The chemical exergy values for the base and improved models for different streams were not included in the exergy calculation. Only the fuel chemical exergy was included. The physical exergy was the dominant form of exergy values for different process streams. It was dominant because no chemical changes were happening in most of the process streams

in the overall process. However, the chemical exergy equations can be incorporated in the model to see its impact on the overall calculation. One disadvantage could be that the model becomes slower in terms of converging time as more equations are introduced in the model.

4) <u>Dynamic modelling of the oxy-fuel process:</u>

A dynamic mode is needed for a process to understand the behaviour of different control loops with respect to process input changes. This is also very helpful from plant operation perspective before implementing a complex integrated industrial process for commercial application. A dynamic model can be developed for the improved process model. It can provide the insight on the process dynamics of the integrated oxy-fuel plant with CO_2 capture. The dynamic model will be useful for the understanding of different control structure and their interaction in this highly integrated plant. Many different perturbations could be studied to see their impact on the four different sections of the plant and on the overall plant efficiency.

5) <u>Transition to air and oxy-fired scenario:</u>

Most of the oxyfired plants will initially start and run with air combustion mode. Once the combustion is established then the switchover will take place between the air and oxy-fired case. A detailed study can be performed on the transition between the airfired and oxyfired study with this model. However a significant adjustments and addition are needed to make the model suitable for air fired case with a sovent based CO_2 capture. Such study will require the use of the dynamic model mentioned in the previous recommendation.

6) <u>Part load and full load study:</u>

The power plant does not always run on full load. The load variation depends on the electricity demand from the power grid. It may vary with the seasons e.g. winter or summer and it may also vary with day and night. It may even vary from 50% to 100% during the peak and off peak hours of a particular day. So the load variation is a normal phenomenon for a power plant operation. However, the load variation for an integrated oxy-fuel power plant is a complex scenario as different subsections of the integrated plant (e.g. ASU, CO_2 Capture

Unit, BOP etc) need to be optimized at part load condition to minimize the losses. It requires an in depth analysis to determine the impact of part load condition and subsequently optimize the parameters for the part load scenario. Specifically, the load variation has more to do with respect to the ASU design and operation. The losses during a part load condition with respect to the operability of the ASU should be investigated. A detailed study on the part load scenarios can be done with this improved integrated model.

Process Model Validation for BOP

The comparison data for the BOP model between DOE report and the HYSYS model are shown here in Table A-1. The BOP model from the DOE report is presented in Figure A-1 (DOE, 2008). The discrepancies between the two models were observed to be very minimum and negligible. A few selective major process streams marked in dotted circle in Figure A-1 were considerd for the comparison and preseted in the following table.
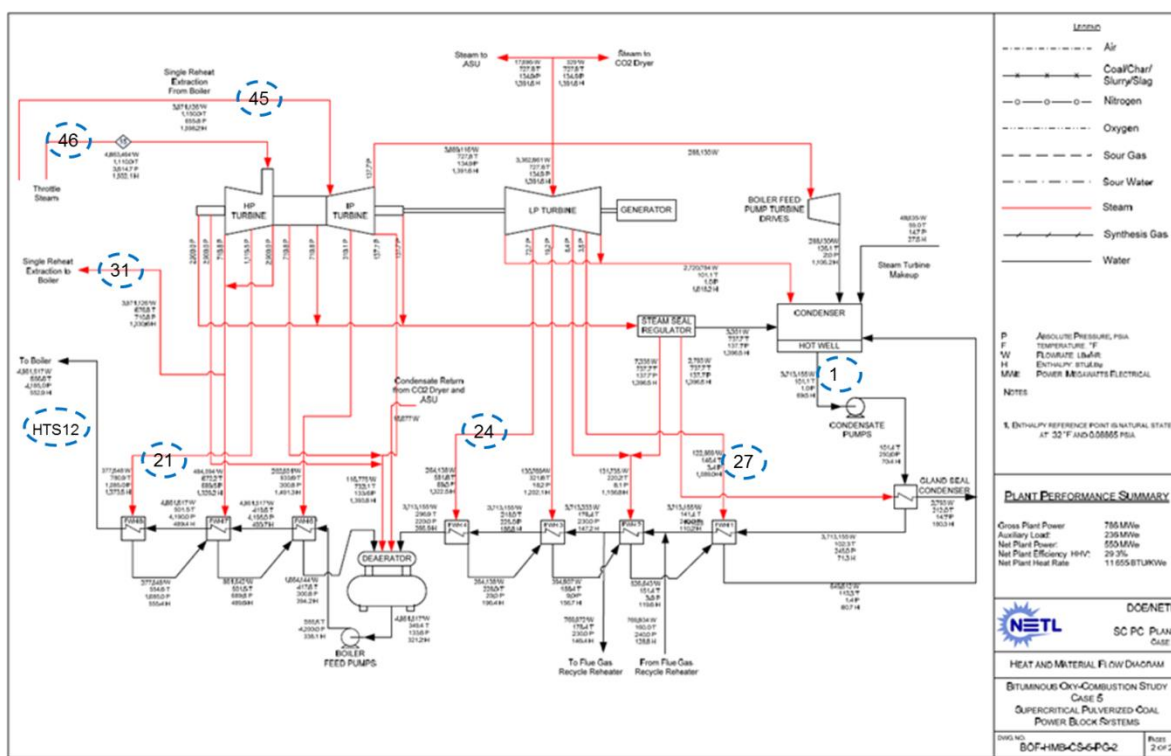
Figure A-1 DOE report: BOP process flow diagram

Table A-1 Model validation for BOP: DOE report (figure A-1) and current thesis (figure 3-3)

	DOE Report: Selected Process Parameters for BOP							
Stream No#	Throttle Steam (15)	Single reheat extraction to boiler	Single reheat extraction from boiler	BFW to condenstae pump	BFW to Boiler	27	24	21
Composition (mol%)								
N_2	-	-	-	-	-	-	-	-
Ar	-	-	-	-	-	-	-	-
O_2	-	-	-	-	-	-	-	-
Water	1	1	1	1	1	1	1	1
CO_2	-	-	-	-	-	-	-	-
Flow (kg/hr)	2,206,033	1,801,275	1,801,275	1,684,261	2,205,150	55,732	119,811	171,253
Pressure bar (a)	239.1	48.35	44.61	0.068	284.7	0.23	4.69	73.8
Temperature ^{o}C	599	358	621	38.38	291.4	63.56	305	416
	Current Thesis Model Validation: Selected Process Parameters for BOP							
Stream No#	46	31	45	1	HTS12	27	24	21
Composition (mol%)								
N_2	-	-	-	-	-	-	-	-
Ar	-	-	-	-	-	-	-	-
O_2	-	-	-	-	-	-	-	-
Water	1	1	1	1	1	1	1	1
CO_2	-	-	-	-	-	-	-	-
Flow (kg/hr)	2,206,000	1,801,000	1,801,000	1,685,000	2,205,000	55,730	119,800	171,300
Pressure bar (a)	242.3	49.01	45.22	0.069	288.5	0.234	4.75	74.81
Temperature ^{o}C	592.5	357.2	621.1	38.39	291.6	63.56	304.9	409.8
Relative error for flow (%)	0.001	0.015	0.015	-0.044	0.007	0.004	0.009	-0.027
Relative error for pressure (%)	-1.338	-1.365	-1.367	-1.471	-1.335	-1.739	-1.279	-1.369
Relative error for temperature (%)	1.085	0.223	-0.016	-0.026	-0.069	0.000	0.033	1.490

Appendix B

Thermal Exergy Calculation

For any reversible process with ideal gas as the system (B.1), the first law of thermodynamics states that

$$dQ = C_v dT + pdV \qquad \text{B1.1}$$
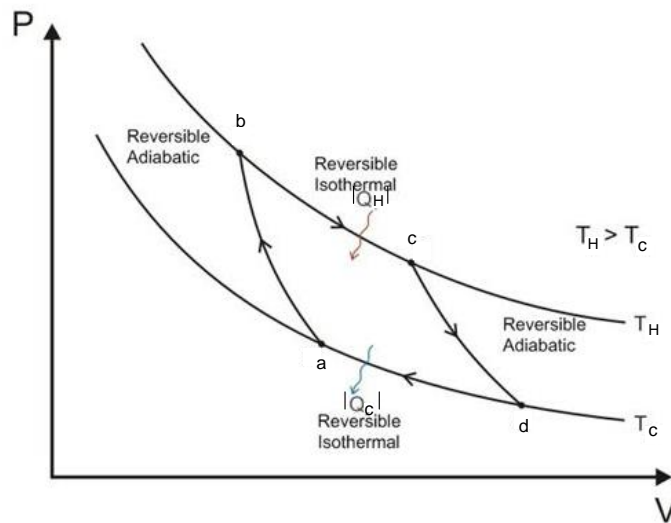
Figure B-1 PV diagram for ideal gas

For the isothermal step b to c : P= RT/V where T (or T_H) is the high temperature step and T_0 (or T_C) is the low temperature step. For the isothermal expansion (b to c) with absorbing heat $|Q|$ (or $|Q_H|$), integration of Equation B1.1 gives

$$|Q| = \int_{V_b}^{V_c} PdV = RT \ln \frac{V_c}{V_b} \qquad \text{B1.2}$$

Similarly for the isothermal step (d to a) with rejection of heat $|Q_0|$ (or $|Q_C|$), integrating Equation B1.1 gives

$$|Q_0| = \int_{V_d}^{V_a} PdV = RT_0 \ln \frac{V_d}{V_a} \qquad\qquad\qquad \text{B1.3}$$

Where $P = RT_0/V$, from Equation B1.2 and B1.3 we get

$$\frac{|Q|}{|Q_0|} = \frac{T}{T_0} \frac{\ln \dfrac{V_c}{V_b}}{\ln \dfrac{V_d}{V_a}} \qquad\qquad\qquad \text{B1.4}$$

For the adiabatic process, Equation B1.1 can be written as

$$- C_V \, dT = PdV = \frac{RT}{V} dV$$

or

$$-\frac{C_V}{R} \frac{dT}{T} = \frac{dV}{V} \qquad\qquad\qquad \text{B1.5}$$

For the adiabatic compression (a to b) with temperature rise from T_0 to T, integrating equation B1.5 gives

$$\int_{T_C}^{T_H} \frac{C_V}{R} \frac{dT}{T} = \ln \frac{V_a}{V_b} \qquad\qquad\qquad \text{B1.6}$$

Similarly for adiabatic expansion (c to d) with temperature decrease until T_0 we get

$$\int_{T_C}^{T_H} \frac{C_V}{R} \frac{dT}{T} = \ln \frac{V_d}{V_c} \qquad\qquad\qquad \text{B1.7}$$

From Equation B1.6 and B1.7 we get

$$\ln\frac{V_a}{V_b} = \ln\frac{V_d}{V_c}$$

This can also be written as

$$\ln\frac{V_c}{V_b} = \ln\frac{V_d}{V_a} \qquad\qquad\qquad \text{B1.8}$$

So Equation B1.4 can be written as

$$\frac{|Q|}{|Q_0|} = \frac{T}{T_0} \qquad\qquad\qquad \text{B1.9}$$

After substitution, from Equation 4.3 and B1.9 we get

$$W_{rev} = Q[1 - T_o/T] \qquad\qquad\qquad \text{B1.10}$$

Sample HYSYS Diagrams with Stream Numbers
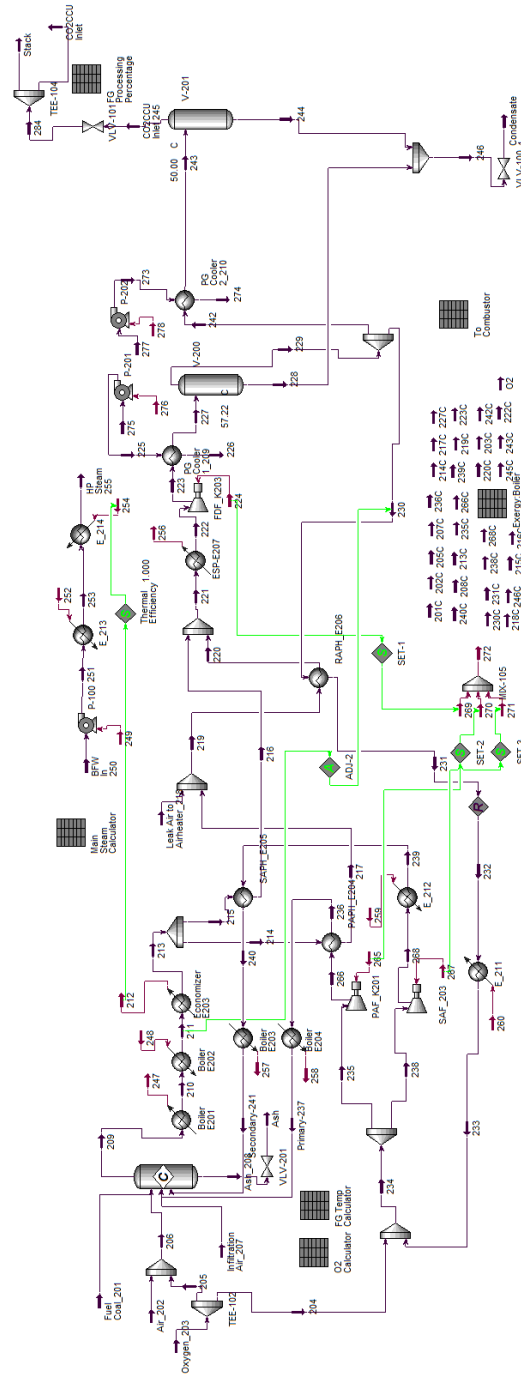
Figure C-1 Boiler and flue gas section process stream numbers for exergy analysis

155

Figure C-2 BOP section process stream numbers for exergy analysis

156

Figure C-3 ASU section process stream numbers for exergy analysis
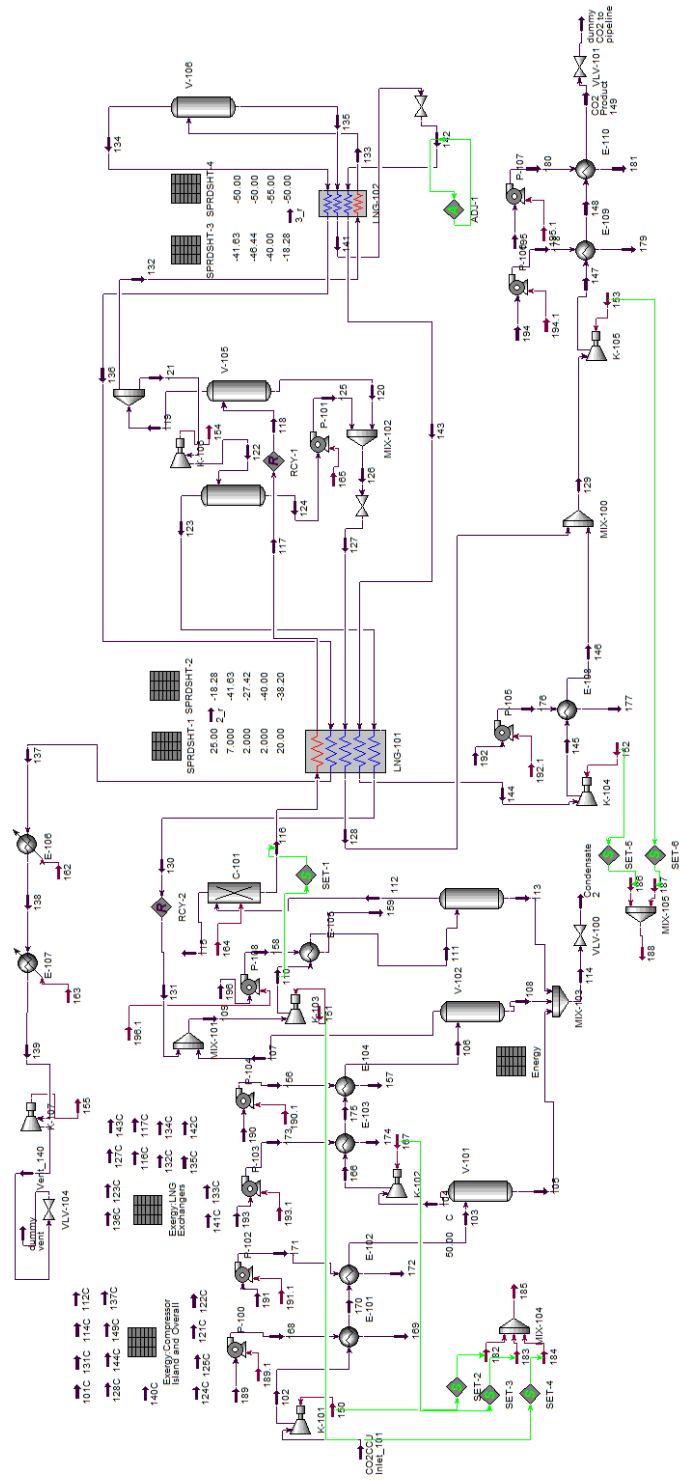
Figure C-4 CO₂CCU section process stream numbers for exergy analysis

Bibliography

Acır, A., Bilginsoy, A. K., and Coskun, H. 2012. Investigation of varying dead state temperatures on energy and exergy efficiencies in thermal power plant. Journal of the Energy Institute.

Aljundi I.H., 2009. Energy and Exergy Analysis of a steam Power Plant in Jordan, Applied Thermal Engineering, 29: (2009) 324-328

Ameri M., Ahmadi P., and Khanmohammadi S, 2008. Exsergy analysis of a 420 MW Combined Cycle Power Plant, International Journal of Energy Research, 32 (2008):175-183.

Adams, D., Davison, J., 2007. Capturing CO_2. IEA Greenhouse Gas R&D Programme.

American Society for Testing and Materials (ASTM), 2014a. ASTM G128 Standard Guide for Control of Hazards and Risks in Oxygen Enriched Systems.

American Society for Testing and Materials (ASTM), 2014b. ASTM G88 Standard Guide for Designing Systems for Oxygen Service

Bejan A., Tsatsaronis G., Moran M., 1996. Thermal Design and Optimization, John Wiley and Sons, USA.

BERR, 2007. Technology Options for the Canadian Market, Report No. COAL R309, BERR/Pub, URN 07/1251.

CALLIDE, 2014. Callide Oxy-fuel project, Retrieved April 10, 2014. http://www.callideoxyfuel.com/What/CallideOxyfuelProject.aspx

Canadian Electricity Association (CEA), 2012, Statistics Canada Survey 2151, 2012, Retrieved April 07, 2014.

 (http://www.electricity.ca/media/Electricity101/Electricity101.pdf)

Cengel, Y.A., and Boles, M.A., 2006. Thermodynamics-An Engineering Approach. Fifth Edition. McGraw Hill.

Cornelissen, R.L., Hirs, G.G., 1998. Exergy Analysis of Cryogenic Air Separation.Energy Conversion and Management. 39:16-18, 1821-1826.

Chansomwong, A., Zanganeh, K., Shafeen, A., Douglas, P., Croiset, E., and Ricardez, L., 2013a. Dynamic modelling of a CO_2 capture and purification unit for an oxy-coal-fired power plant. International Journal of Greenhouse Gas Control (in press).

Chansomwong, A., Zanganeh, K., Shafeen, A., Douglas, P., Croiset, E., and Ricardez, L., 2013b. Dynamic simulation and control of a CO_2 compression and purification process for oxy-coal-fired power plants. Proceedings of the 3rd IEA GHG Oxyfuel Combustion Conference, Spain.

Chansomwong, A., Zanganeh, K., Shafeen, A., Douglas, P., Croiset, E., Ricardez, L., 2011. A decentralized control structure for a CO_2 compression, capture and purification process: An Uncertain Relative Gain Array Approach. Proceeding of the 18th IFAC World Congress, IFAC, Milano, Italy.

Dincer, I., and Rosen, M.A., 2007. Exergy-Energy, Environment and Sustainable Development. Elsevier.

DOE, 2004. An Integrated Modeling Framework for Carbon Management Technologies, DE-FC26-00NT40935, Volume 1: Amine-Based CO2 Capture and Storage Systems for Fossil Fuel Power Plant.

DOE, 2008. Pulverized Coal Oxy combustion Power Plants, DOE/NETL-2007/1291, Volume 1: Bituminous Coal to Electricity, Final Report.

Earth System Research Laboratory (ESRL), 2014. Global Monitoring Division, National Oceanic & Atmospheric Administration. U.S. Department of Commerce. Retrieved April 10, 2014 (http://www.esrl.noaa.gov/gmd/ccgg/trends/weekly.html)

Eiserman W., Johnson P., and Conger W.L., 1980. Estimating Thermodynamic Properties of Coal, Char, Tar, and Ash, Fuel Proc. Tech., Vol.3, pp.39-53

Fu, C., Gundersen, T., 2013. Exergy Analysis and Heat Integration of a Coal-Based Oxy-combustion Power Plant. Energy Fuels, 27: 7138-7149.

Fu, C., Gundersen, T., 2012. Using Exergy Analysis to Reduce Power Consumption in Air Separation Units for Oxy-combustion Processes. Energy 44: 60-68.

Gale, J., and Freund, P., 2000. Greenhouse Gas Abatement in Energy Intensive Industries. Proceedings of the 5th Int'l Conference on Greenhouse Gas Control Technologies (GHGT5). Australia.

Ganapathy, T., Alagumurthy, N., Gakkhar, R.P., Murugesan, K., 2009. Exergy Analysis of Operating Lignite Fired Thermal Power Plant. Engineering Science and Technology Review. 2(1) 123-130.

Goloubev, D., 2012. Oxygen Production for Oxy-Fuel Power Plants Status of Development. Linde Engineering. 2nd International Workshop on Oxyfuel FBC Technology, Germany.

Gupta, M., Shafeen, A., Hashi, M., Zanganeh, K.E., and Rose, D., 2007. A Novel Process Integration Approach for Zero Emission Oxy-fuel Power Plants Using Low Rank Coals. 24th International Pittsburgh Coal Conference. Johannesburg.

Hack, H., Lupion, M., Otero, P., López, C., Muñoz, F., Hotta, A., Kuivalainen, R., Alvarez, J., 2011. Update on the Operation of the CIUDEN Oxy-CFB Boiler Demonstration Project. Proceedings of POWER-GEN International Conference, Las Vegas, USA.

Hagi, H., Nemer, N., Moullec, L.Y., Bouallou, C., 2013. Pathway for advanced architectures of oxy-pulverized coal power plants: minimization of the global system exergy losses. GHGT-11, Energy Procedia 37 (2013) 1331-1340.

HYSYS, 2014. Documentation: Aspen HYSYS Simulation basis. AspenTech, USA.

International Energy Agency (IEA), 2011a. CO_2 Emissions from Fuel Combustion Report, ISBN 978-92-64-10283-5. Paris: IEA.

International Energy Agency (IEA), 2011b. World Energy Outlook 2011, ISBN: 978-92-64-12413-4 Paris: IEA.

International Energy Agency (IEA), 2005. Oxy Combustion Processes for CO_2 Capture from Power Plant, IEA Report Number 2005/9.

International Energy Agency (IEA), 2006. CO_2 Capture in low Rank Coal Power Plants, Technical Study, IEA Report Number: 2006/1.

Intergovernmental Panel on Climate Change (IPCC), 2005. IPCC Special Report on Carbon Dioxide Capture and Storage. Available at (www.cambridge.org/9780521863360).

Kanniche, M., Gros-Bonnivard, R., Jaud, P., Valle-Marcos, J., Amann, J.M., Bouallou, C., 2010. Pre-combustion, post-combustion and oxy-combustion in thermal power plant for CO_2 capture. Applied Thermal Engineering. 30, 53-62.

Kreutz, T. G., Williams, R.H., Socolow, R.H., Chiesa, P., and Lozza, G. 2002. Production of Hydrogen and Electricity from Coal with CO_2 Capture. Proceedings of the 6th International Conference on Greenhouse Gas Control Technologies (GHGT6). Japan.

Levasseur, A.A., Chapman, P. J., Nsakala, N., Kluger, F., 2009. Alstom's Oxy-Firing Technology Development and Demonstration - Near Term CO_2 Solutions. The 34th International Technical Conference on Coal Utilization & Fuel Systems, Clearwater, USA.

Modesto, M., Nebra, S.A., 2009. Exergoeconomic analysis of the Power Generation System Using Blast Furnace and Coke Oven Gas in a Brazilian Steel Mill. Applied Thermal Engineering, 29 (2009) 2127-2136.

National Energy Board (NEB), 2013a, Canadian Energy Dynamics, 2013, Energy market Assessment.

National Energy Board (NEB), 2013b, Canada's Energy Future, Energy Supply and Demand Projections to 2035.

National Fire Protection Association (NFPA), 2014. NFPA 53 Recommended Practice on Materials, Equipment and Systems Used in Oxygen-Enriched Atmospheres

Peng D., Robinson D.B., 1970. A new Two-Constant Equation of State. 4th Interantional Heat Transfer Conference, Paris, Heat Transfer 1970, volume VI, paper B.7.b.

Rubin, E.S., Mantripragada, H., Marks, A., Versteeg, P., Kitchin, J., 2012. The outlook for improved carbon capture technology. Prog. Energ. Combust. 38, 630-671.

Saidur, R., Ahamed J.U., and Masjuki H.H., 2010. Energy, Exergy and Economic Analysis of Industrial boilers, Energy Policy 38(2010) 2188-2197.

Norio Sato, 2004. Chemical Energy and Exergy-An Introduction to Chemical Thermodynamics for Engineers, Elsevier.

Szargut, J., Morris, D.R., Steward, F.R., 1988. Exergy Analysis of Thermal, Chemical and Metallurgical Processes.

Santos, S., 2013. Current status to the development of oxy-fuel combustion technology. Retrieved April 15, 2014.

http://www.vtt.fi/files/sites/flexiburncfb/workshop2013/Stanley_Santos_Development_of_Oxyfuel.pdf

Shafeen, A., Zanganeh, K., Douglas, P., and Croiset, E., 2013a. Process Model Development and Simulation of an Integrated Oxy-fuel Power Generation System with CO_2 Capture. Proceedings of the OPTIMIZE 2013 conference, Boston, USA.

Shafeen, A., Zanganeh, K., Douglas, P., and Croiset, E., 2013b. Energy Management and Efficiency Improvement for Oxy-fuel Power Generation Systems with CO_2 Capture: An Exergy-based Approach. Proceedings of the 3rd IEA GHG Oxyfuel Combustion Conference, Spain.

Shafeen A., and Zanganeh K.E., 2010. Experimental Assessment of Lead Chamber Reactions in an Integrated CO_2 Capture and Compression Unit (CO_2CCU) for Oxy-fuel Plants. The 35th International Technical Conference on Coal Utilization & Fuel Systems, Clearwater, USA.

Smith, J.M., and Van Ness H.C., 1987. Introduction to Chemical Engineering Thermodynamics. Fourth Edition. McGraw Hill.

Sengupta, S., Datta, A., Duttagupta, D., 2007. Exergy Analysis of a Coal-based 210 MW Thermal Power Plant. International Journal of Energy Research. 31: 14-28.

Steam/its generation and use. 2005. Babcock & Wilcox. 41 ed. pp 1106.

Strömberg, L., Lindgren1 G., Jacoby J., Giering R., Anheden M., Brchhardt W., Altmann H., Kluger F., Stamatelopoulos G.N,. 2009. First Test Results from Vattenfall's 30 MWth Oxyfuel Pilot Plant in Schwarze Pumpe. The 34th International Technical Conference on Coal Utilization & Fuel Systems, Clearwater, USA.

Stryjek, R., Vera, J.H., 1986. PRSV: An Improved Peng-Robinson Equation of State for Pure Components and Mixtures, The Canadian Journal of Chemical Engineering, v64.

Van der Ham, L., 2011. Improving the Second law efficiency of a cryogenic air separation unit. PhD dissertation. Norwegian University of Science and Technology (NTNU-Trondheim). ISBN 978-82-471-3217-3

Vattenfall, 2014. Oxy-fuel Demonstration project. Retrieved April 15, 2014. http://www.vattenfall.com/en/ccs/schwarze-pumpe.htm

Vosough, A., Noghrehabadi, A., Ghalambaz, M., Vosough, S., 2011. Exergy Concept and its Characteristics. Journal of Multidisciplinary Science and Engineering. 2(4).

Wall T, and Yu J., 2009. Coal-Fired Oxyfuel Technology Status and Progress to Deployment. The 34th International Technical Conference on Coal Utilization & Fuel Systems, Clearwater, USA.

Wall T., Stranger R., and Santos S., 2011. The current state of oxy-fuel technology: demonstrations and technical barriers. 2nd Oxyfuel Combustion Conference, Queensland, Australia.

White, V., Torrente-Murciano, L., Sturgeon, D., and Chadwick, D., 2008. Purification of Oxyfuel-Derived CO_2. Proceedings of the 9th International Conference on Greenhouse Gas Control Technologies. Washington D.C., USA.

Wilfrid W, 1924. Manufacture of Sulphuric Acid (Chamber-Process). Gurney and Jackson, London, UK.

World Intellectual Property organization-WIPO, 2014, Auto-refrigerated Gas Separation System for Carbon Dioxide Capture and Compression. WO/2011/127552, PCT/CA2010/000572, CA2769687A1, EP2478312A1, US20120137728, Retrieved April 07, 2014, (http://patentscope.wipo.int/search/en/result.jsf)

Yilmazoglu, M.Z., Amirabedin, E., 2011. Second Law and Sensitivity Analysis of a Combined Cycle Power Plant in Turkey. Thermal Science and Technology. 31,2,41-50.

Zanganeh K.E., Shafeen A., and Salvador C., Beigzadeh A., and Abbassi M., 2010. CO_2 Processing and Multi-pollutant Control for Oxy-fuel Combustion Systems Using an Advanced CO_2 Capture and Compression Unit (CO_2CCU). Proceedings of the 10th International Conference on Greenhouse Gas Control Technologies (GHGT-10). Amsterdam, The Netherlands.

Zanganeh K.E., Shafeen A., and Salvador C., 2009a. On the Performance of an Advanced Pilot-Scale CO_2 Capture and Compression Unit (CO_2CCU). 1st International Oxyfuel Combustion Conference, Cottbus, Germany.

Zanganeh K.E., Shafeen A., and Salvador C., 2009b. Experimental results from a pilot-scale CO_2 Capture and Compression Unit (CO_2CCU). The 34th International Technical Conference on Coal Utilization & Fuel Systems, Clearwater, USA.

Zanganeh K.E., Shafeen A., and Salvador C., 2008a. CO_2 Capture and Development of an Advanced Pilot-Scale Cryogenic Separation and Compression Unit. Proceedings of the 9th International Conference on Greenhouse Gas Control Technologies (GHGT-9). Washington D.C., USA.

Zanganeh K.E., Shafeen A., and Salvador C., 2008b. Development of an Integrated CO_2 Capture and Compression Unit (CO_2CCU) for Oxy-Fuel Power Plants. The 33rd International Technical Conference on Coal Utilization & Fuel Systems. Clearwater, USA.

Zanganeh K.E., Shafeen A., Gupta M., Ogedengbe E., and Mitrovic M., 2008c. Gas Turbine Integrated High-Efficiency Oxy-Fuel Combustion Process with CO_2 Capture. ASME Turbo Expo, Berlin Germany.

Zanganeh K.E., Shafeen A., Gupta M., and Salvador C., 2006. Comparative Performance Evaluation of CO_2 Capture and Compression Processes for Advanced Oxy-Fuel Power Plants. 31st International Conference on Coal Utilization and Fuel Systems. Clearwater, Florida. USA.

Zanganeh K.E., Shafeen A., Salvador C., and Mitrovic M., 2007a. Oxy-Fuel Technology: Its Current State and Opportunities for Greenhouse Gas Mitigation and Pollution Prevention. AICHE Annual Meeting/Conference. USA.

Zanganeh K.E., Shafeen A., Mitrovic M., and Salvador C., 2007b. Oxy-Bitumen Combustion with CO_2 Capture and Storage for In-Situ Recovery Process: Towards Carbon Neutrality. 32nd International Conference on Coal Utilization and Fuel Systems. Clearwater, Florida, USA.

Zanganeh K.E., and Shafeen A., 2007c. A novel process integration, optimization and design approach for large-scale implementation of oxy-fired coal power plants with CO_2 capture. International Journal of Greenhouse Gas Control 1 (1), pp. 47-54.